SMART MATERIALS:

FUNCTIONAL DESIGN OF THERMAL TEXTILES

TONG JIAHUI

PhD

The Hong Kong Polytechnic University

2018

The Hong Kong Polytechnic University

Institute of Textile and Clothing

SMART MATERIALS:
FUNCTIONAL DESIGN OF THERMAL TEXTILES

TONG JIAHUI

A thesis submitted in partial fulfillment of the

requirements for the degree of Doctor of Philosophy

June 2017

CERTIFICATE OF ORIGINALITY

I hereby declare that this thesis is my own work and that, to the best of my knowledge and belief, it reproduces no material previously published or written, nor material that has been accepted for the award of any other degree or diploma, except where due acknowledgement has been made in the text.

TONG JIAHUI

ABSTRACT

Recently, thermal textiles have become increasingly popular because they possess advantageous characteristics that could enable them to be widely applied in fields such as body warming, physical therapy, and drug delivery. The thermal function of thermal textiles is achieved by the embedded conductive yarns. Compared with conventional thermal devices, thermal textiles offer physical flexibility and comfort in addition to thermal functions. Temperature control is one of the most important aspects of thermal textiles. Thus this study aims to explore the thermal behavior of thermal textiles and achieve precise temperature control. Specifically, this study aims to explore the factors that are relevant to the thermal behavior, such as the electrical resistance, thermal conductivity and surrounding environment.

In the first stage of the study, the electrical resistance change of thermal fabrics was investigated. The results showed that the resistance of thermal fabrics will decrease when the temperature increases. The research results attributed this property to the morphologic change of conducting yarns during heating. Accordingly, a theoretical model was proposed to simulate the heating process.

In the second stage of the study, the thermal behavior of thermal fabrics of different sizes was studied. A modified and generalized model was developed to simulate the thermal behavior of thermal fabrics of different sizes. In the model, different parameters including electrical resistance, thermal conductivity, fabric size and interaction between them were studied. The research results presented deviation from simulation due to two reasons: limitation of quality control in textile industry

and morphologic change of textile materials.

In the third stage of the study, the influence of airflow on thermal fabrics was valuated. The results show that airflow can greatly influence the heating process and a proportional relationship was found between the thermal conductivity and airflow rate. The airflow direction has a limited influence on the heating process. A quantitative model was established to simulate and predict the thermal behavior of thermal fabrics in a windy environment.

In the final stage of the study, the heat process was investigated when the thermal fabric was covered by other fabrics. The results shows that there is a linear relationship between the thermal resistance of the system and the number of cover layers. The thermal resistance brought from multiple-cover layers can be estimated by simply adding up the thermal resistance of each piece of cover layer. Furthermore, the thermal conductivity measured by a thermal conductivity meter is different from the implied thermal conductivity in the heating process.

Both internal parameters and external factors that can influence the heating process have been explored in this research. This study serves as a pilot study to complement research on the thermal behavior of conductive thermal textiles and thermal control of thermal textiles. It provides guidance for precise temperature control for different situations.

Keywords: *Conductive Yarns, Resistance, Thermal Conductivity, Temperature Control, Thermal Fabrics, Thermal Textiles*

PUBLICATIONS ARISING FROM THE THESIS

REFEREED JOURNAL PUBLICATIONS:

Tong JH, Ding F, Tao XM, et al. Temperature effect on the conductivity of knitted fabrics embedded with conducting yarns. *Textile Research Journal* 2014; 84:1849-1857.

Tong JH, Liu S, Yang CX, et al. Modelling of package-free flexible conductive fabric with thermal regulation where temperature can be customized. *Textile Research Journal* 2015; 85:590-600.

Tong JH, Zhao YF, Yang CX, et al. Comparison of airflow environmental effects on thermal fabrics. *Textile Research Journal* 2016; accepted.

Tong JH, Li L. "Thermal Regulation of Electrically Conducting Fabrics". *Handbook of Smart Textiles 2015*

AWARDS:

LI Li, Wan Kam Man, Tong Jiahui, Zhao Yuanfang, etc. Inventions Geneva: Salon International Des Inventions. 4 April 2014.

ACKNOWLEDGEMENTS

I would be happy to take this opportunity to express my big thanks to the following people for their encouragement and support all the way in my research study.

Firstly, I would like to express my heartfelt thanks to my supervisor Dr. Lilly Li, Prof. Tao Xiaoming, Prof. Yan Feng and Dr. Ding Feng for their sustained guidance and valuable advice throughout my study. Without their patience and encouragement, I wouldn't accomplish my study.

Then I would also like to thank all my colleagues in my study period. They gave a lot of valuable advice and support to my research. Every time I communicated with them, I can learn a lot from them. Special thanks to my colleagues Ms. Liu Su and Ms. Zhao Yuanfang, who helped me prepare high-quality fabrics for my research study.

Finally, I would like to thank my parents and friends who have been supporting me all the way during my study.

CONTENTS

LIST OF FIGURES

LIST OF TABLES

CHAPTER ONE
INTRODUCTION

1.1 Background of the study

Wearable electronics are smart material devices that can be worn on the body and feature practical functions. Compared with the conventional existing electronic techniques, generally, the functional components and interconnections in wearable electronics are intrinsic to the main device component and thus are less visible; this intrinsic nature makes the wearable electronics behave as a piece of clothing rather than an electronic device. Furthermore, wearable electronics also offer physical flexibility and comfort, which cannot be achieved with the the conventional electronic devices. Wearable electronics, in most situations, are fabricated on a textile base and thus combine the strengths of the functions of electronics and good properties of textiles.

The textile industry is an established industry that has been developing for a considerably long time. This industry started to experience a bottleneck period and drew little attention for years. Fortunately, the development of various high-performance materials and technology has added much vitality to the textile industry and functional textile materials, especially wearable electronic textiles, have invigorated the industry in recent years.

Currently, there are a variety of wearable electronics that provide different types of functions and are used for different purposes. Fabrics together with sensors can be used for specific health issue monitoring in personalized healthcare, fitness tracking as a sports tracker, sensing temperature for better thermal control and so on. Wearable electronic textiles can also have an active functionality such as power generation or storage. For example, a textile triboelectric nanogenerator-cloth and a flexible lithium-ion battery belt can be integrated into a self-charging power unit

(Xiong Pu, et al. 2015).

Most recently, thermal textiles, as wearable electronics, have become increasingly popular because they possess advantageous good characteristics that could be widely applied in fields such as body warming, physical therapy, and drug delivery (Paradiso R., Belloc C., et al. 2005; Lymberis A., Rossi D.D., 2004;). Compared with conventional thermal devices, thermal textiles offer physical flexibility and comfort in addition to thermal functions and organically combines the strength of both conventional thermal devices and textiles. Due to the recent development of wearable electronic textiles and smart materials, conductive fabrics and electrically- heated thermal textiles have been extensively studied and applied in many fields. Various electrically-heated thermal textiles have recently appeared in fashion shows and on the clothing market.

Generally, thermal textiles are also conductive textiles because thermal textiles contain conductive materials to perform their heating function. Conductive properties can be imparted to thermal textiles by coating or distributing conductive elements into the textiles to make the textiles conductive at the fabric level. Thermal textiles can also be made with conductive yarns fabricated into the construction of the textile bases. The conductive yarns can be metal-coated yarn, pure metal yarn or conductive polymer based yarn (Bohwon Kim, Vladan Koncar, Claude Dufour, 2006). Because of the rapid growth in material technology, carbon nanotubes are sometimes used to produce electrically conductive yarn (Behabtu Natnael, et al. 2013; Liu F, et al. 2015). Thermal textiles embedded with conductive yarns can be more flexible when fabricating than thermal textiles with conductive materials coated at the fabric level because different conductive yarns and different fabric structures can be selected based on requirements. Among the various types of conductive yarn, silver-coated yarns are the most selected for thermal textiles due to their advantages over other types of conductive yarn. In

general, silver-coated yarns are composed of a non-conductive substrate such as nylon and a conductive silver layer coated on the surface. Thus, by combing the strength of both of these materials, silver-coated yarns show good flexibility and great conductivity. Furthermore, silver coated yarns show an effective antibacterial ability (P C MacKeen, S Person, et al. 1987). Thus my research is focused on thermal textiles embedded with conductive silver coated yarns.

Thermal control is one of the most important aspects of thermal fabrics. When a thermal textile generates heat during the heating process, controlling the temperature precisely is significant for applications in different fields. To determine how to control the temperature of a thermal textile, different parameters of the thermal textiles that are related to the heating process should be studied and fully understand. One of the most essential parameters of a thermal textile, electrical resistance, was studied in the first stage of our research and the factors that may affect the resistance of thermal textiles were fully considered. Some resistive network models have already been established for conductive textiles in different structures and the resistance change variation with external strain has been explored in previous research. However, how temperature influences the resistance of thermal textiles during heating has never been studied. There is a lack of knowledge about the influence of temperature on the resistance of thermal textiles or silver-coated yarns, and temperature control of a thermal fabric can be difficult to achieve, because the electric power applied to the textile depends on the resistance of the textile according to Ohm's law. Another important parameter of a thermal textile is its thermal conductivity or thermal resistance, which relates to the thermal textiles' ability to conduct heat. Thermal textiles with low thermal conductivity or high thermal resistance have better ability to retain heat and save electric power. In addition to these parameters, the external environmental factors that may influence the heating process of thermal textiles should also be fully considered. These environmental factors include air flow, layers covering the

thermal textiles and so on. Research on these environmental factors has never been conducted.

Thermal control is a complicated topic, and cannot be accomplished before much more work is carried out. Selection of high-quality and stable silver-coated yarns is the very first stage of such work. Circuit breaks can easily occur in thermal textiles made of low-quality silver-coated yarns during heating. Thus, a selection standard for silver-coated yarns is necessary in order to obtain high-quality thermal textiles. Precise thermal control cannot be achieved without high-quality thermal textiles. Then, a theoretical model that considers electrical resistance, thermal conductivity, and environmental factors should be established to accurately simulate the heating process of thermal textiles. After understanding how electrical resistance, thermal conductivity and other parameters of thermal textiles change in a certain environment during heating, the thermal behaviour of thermal textiles can be controlled accurately. Therefore, a systematic study on thermal textiles is needed for precise thermal control.

1.2 Aims and objectives

This thesis is concerned with a systematic investigation of the working principal of thermal textiles containing silver-coated yarns and their temperature control during the heating process. The study aims to establish a theoretical model to accord with the performance of thermal textiles in heating process. This model is based on studies of thermal textiles' electrical resistance, thermal conductivity and fabric size and external environmental factors. The specific objectives of the study can be summarized as follows:

1. To investigate the electrical resistance change of a conductive knitted fabric during heating process and how the temperature influences the electrical resistance.

2. To establish a model in which the relationship between temperature and electrical resistance is added to simulate the thermal performance of the conductive knitted fabric during heating.
3. To study the electrical resistance change of conductive knitted fabrics of different sizes and improve the model to simulate the heating process of fabrics of various sizes.
4. To study how the airflow and its flow direction influence the heating process of a thermal fabric.
5. To investigate the heating process of a thermal fabric when covered with external layers.

1.3 Significance and value

The research in this thesis serves as a systematic study of thermal control in thermal textiles. Recently, thermal textiles have become increasingly popular on the market and have been adopted by many people to improve their quality of life. However, the working principles and the properties of thermal textiles have not been fully studied, which has hindered the achievement of precise thermal control. Moreover, current thermal textiles are not designed for a changing environment and the performance of these thermal textiles will deteriorate in a rapidly changing environment. The study presented in this thesis aims to investigate every factor that is related to the thermal behavior of thermal textiles and to develop a systematic model for thermal textiles under different environments.

The results in this thesis not only complement the fundamental study of thermal textiles but also benefit the function and applicability of thermal textiles. The research results can also be used as a reference when selecting materials or constructions for fabricating thermal textiles.

1.4 Organization of thesis

The organization of this thesis is as follows.

Chapter one provides an outline of the thesis including the background information of the study, the previous research in related works, the existing research gap, the research aims and objectives, and the significance and value of the study.

Chapter two presents the reviewed literature that is related to this study. The literature review can be divided into two parts. The first part introduces the conductive polymer-coated textiles, their properties and their applications as sensors. The second part of chapter two is focused on thermal functional textiles, which constitute the main topic of this thesis. Previous research on conductive textiles, its electrical properties and thermal behavior has been reviewed.

Chapter three presents the methodology adopted in this thesis. The research work began with the study of internal factors that can influence the thermal properties of the conductive fabric, followed by the study of external factors that may influence the temperature control.

Chapter four discusses the research results and findings of this study. The research was developed around the temperature control of thermal fabrics. Different factors that can influence the temperature of the fabric are studied and discussed. The factors include the resistance, thermal conductivity, airflow, external cover and so on. A theoretical model that takes all the factors into consideration could be established to simulate how the thermal fabric works and what temperature it can achieve (Figure 1.1). The factors include the electrical resistance, thermal conductivity, and size of the fabric. The relationship between these factors and the achieved temperature was explored and a theoretical model was established.

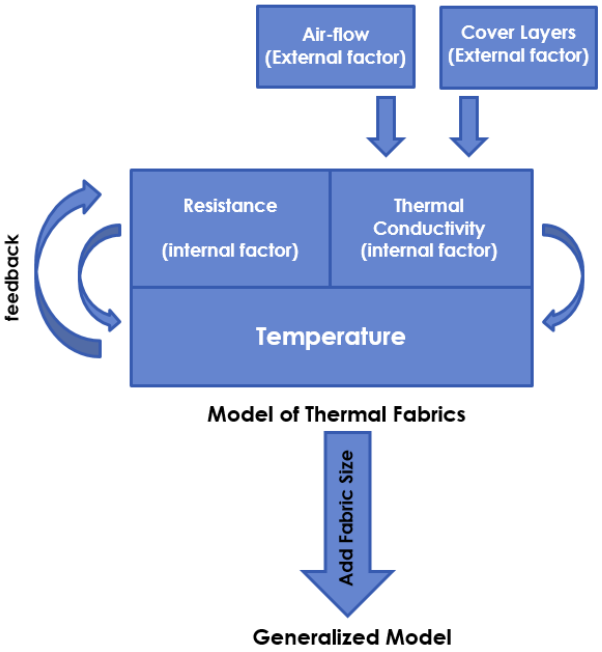

FIGURE 1.1. Diagram of the research topic

Chapter five summarizes the research findings obtained in this study. Some limitations of the research results are also discussed. Finally, future works that would complement the theory presented in this thesis or have promising applications are mentioned.

CHAPTER TWO
LITERATURE REVIEW

2.1 Introduction

First, this chapter will introduce some application of wearable electronics. Fabrics featuring conductive polymers are widely used for sensing functions such as chemical sensing, gas sensing and stretch sensing. Then this chapter will focus on fabrics with thermal functions which is the topic of this thesis. The previous research that has been conducted on thermal textiles will be reviewed. First, this chapter will introduce some popular thermal functional wearable electronics in the current market. Next, the literature review will focus on the properties of thermal textiles and the heating process. Thermal control in thermal textiles means controlling the applied electrical power to achieve the expected temperature. According to Ohm's law, the applied electrical power is related to the applied electrical voltage and the objective's electrical resistance. Thus, this chapter will review previous research on the electrical resistance of conductive textiles. The review of the resistive property of conductive textiles will include the calculation of its resistance under static conditions as well as under strain. Moreover, the heat flux in thermal textiles determines the thermal condition of thermal textiles, which is related to the thermal conductivity of the material (Fourier's law). Thus, in the next section of this chapter, the previous work on the thermal behaviour and thermal conductivity of conductive textiles will be reviewed.

2.2 Application of electrical textiles as sensors

2.2.1 Electromechanical property of PPy-coated fibers

In the last decades, a number of different kinds of sensors have been developed such as electrically conducting sensors, piezoelectric sensors and so on. Of all these sensors, the electrically conducting sensor is the most selected one in the

market because it is simple, cost-efficient and durable. When applying electrically conducting materials into textiles, people have a lot of choice such as carbon fibres, conductive polymers and metal. Polypyrrole (PPy) is one of the most widely used conductive polymers because it owns good electrical conductivity, good stabibility and fewer toxicological problems. However, the brittleness of PPy limits its practical applications. It can be solved either by blending some polymers or by forming copolymers of PPy. Thus PPy coated fibers not only shows excellent physical properties of polymer composites such as strength and flexibility but also owns electrically conducting functions. These advantages of PPy coated fiber makes it an excellent candidate as an electrically conducting sensor. Chemical vapour deposition process is always used to coat PPy on the textile substrate.

The electrically conducting sensing function is mainly based on the electromechanical property of the material. In other words, the sensing function is achieved by the connecting between the resistance and the strain. As a candidate of electrically conducting sensors, the electromechanical property of PPy-coated fibers is the key to its sensing functionality (Xue P, Tao XM, Kwok WY, Leung MY, 2004). When the PPy-coated fiber is in strain, its dimensional change is considered as the main cause of the resistance variation. This behaviour is similar to that of some intrinsically electrically conductive fibers such as copper wire. When the fiber is applied with strain, its length and cross-sectional area will change,

$$L = L_0(1 + \varepsilon)$$
$$A = A_0(1 - v\varepsilon)^2$$

Where ε is the applied strain and v is the Poisson's ration of PPy-coated fibers when elongated along the longitudinal direction. Thus the resistance variation of the PPy-coated fibers in stretch can be obtained,

$$R/R_0 = \frac{(1+\varepsilon)}{(1-v\varepsilon)^2}$$

Where R_0 is the initial resistance and R is the resistance of fiber in stretch. It is found that this model can fit PA6 fibers (multi-filaments of polycaprolactam) coated with PPy very well. The PPy-coated PA6 fibers provide very good linearity which can be observed in Figure 2.1. It is also observed that the PPy-coated PA6 fiber can be stretched to 46% before fracture, which means that The PPy-coated PA6 fibers shows excellent sensing performance up to a strain of 43%, while other conductive fibers such as copper wire can only be stretched below 1.5%. Therefore, PPy-coated PA6 fiber is a better candidate as the electrically conducting sensor.

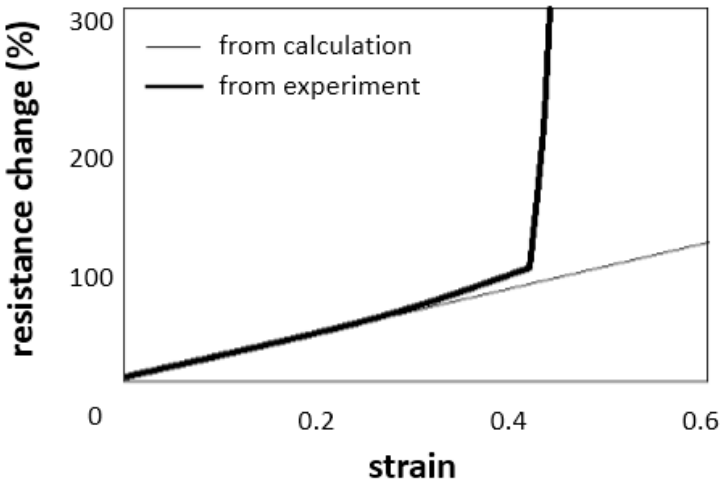

FIGURE 2.1. Comparison of calculated and measured results: R/R_0 versus strain curve of PPy-coated PA6 fibers

The selected fiber substrate can influence the electro-mechanical property greatly. It is reported that the Lycra fibers coated with PPy shows totally different electromechanical property from the PPy-coated PA6 fibers. The resistance variation versus strain curve of PPy-coated Lycra fibers shows non-linearity in big strain (Figure 2.2). Thus selection of the suitable fiber substrate is the very first important process of fabricating polymer-coated fiber sensors.

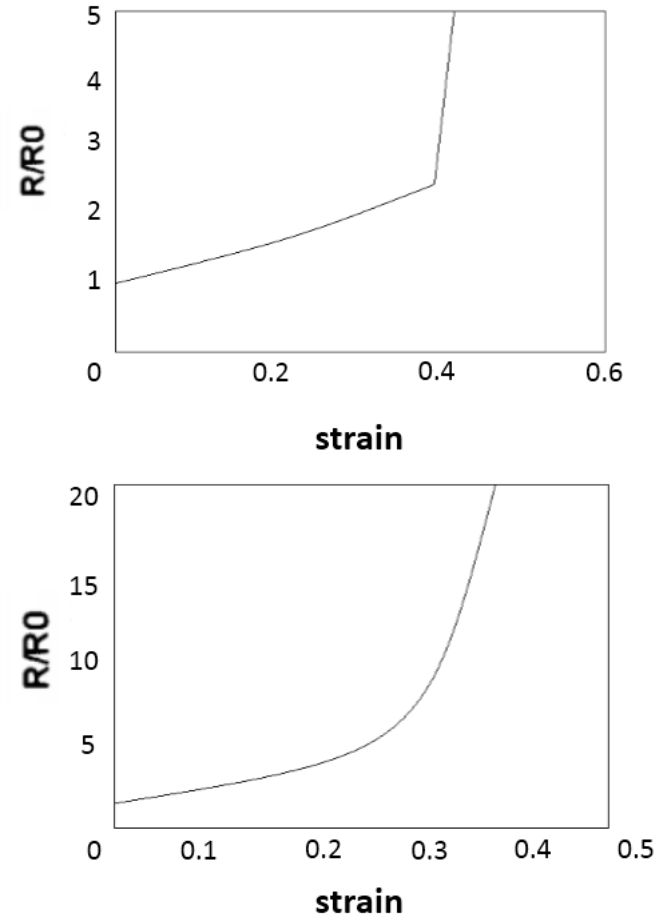

FIGURE 2.2 Resistance variation versus strain curves of PPy-coated PA6 fibers (up) and PPy-coated Lycra fibers (down).

It is also found that the coating of polymer can change the mechanical property of the substrate fiber in different ways. Figure 2.3 presents that the coating of PPy makes the PA6 fiber more stretchable but makes the Lycra fiber less stretchable. It is because the stretchability of the PPy material is above PA6 fibers but below Lycra fibers. When the fibers are coated with PPy material, the stretchability of the coating fibers will be between the coating material and the bare fibers.

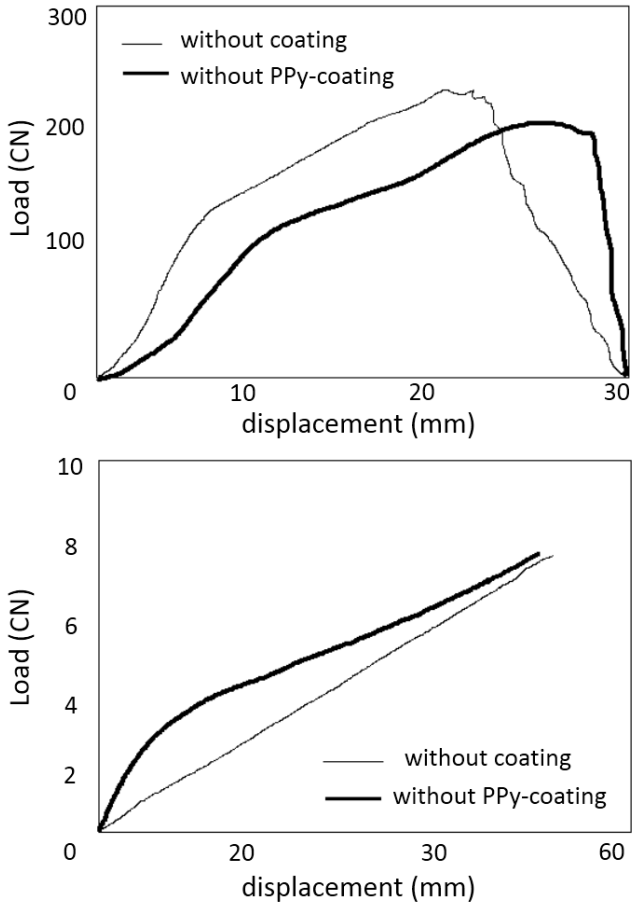

FIGURE 2.3. Load versus displacement curves of PPy-coated PA6 fibers (up) and PPy-coated Lycra fibers (down).

2.2.2 Electromechanical property of PPy-coated fabrics

The property of PPy-coated fabrics also have been studied (Oh KW, Park HJ, Kim SH, 2002). The PPy-coated fabrics can either be accomplished by weaving PPy-coated yarns or coating PPy on fabrics directly. Oh KW, Park HJ and Kim SH used in situ polymerization process to coat PPy on nylon-spandex stretch fabric to achieve PPy-coated fabrics that owns flexibility, elasticity and conductivity. The polymerization on the fabric ensures that each fiber is individually coated with PPy. Different pyrrole concentrations were adopted to process the polymerization of pyrrole and an optimum concentration of 0.5M was achieved (Figure 2.4).

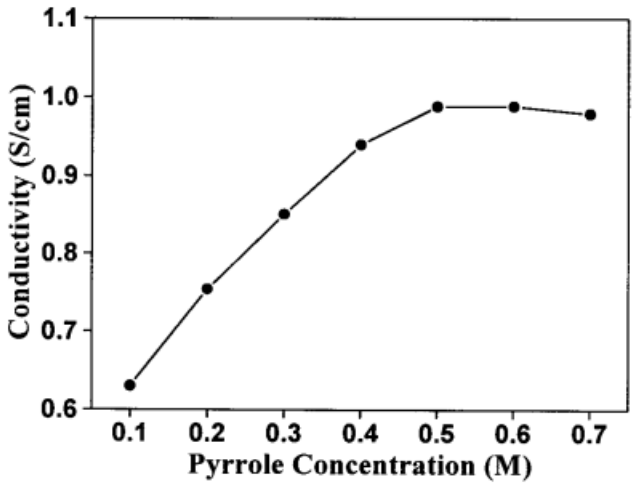

FIGURE 2.4. Conductivity varying with pyrrole concentration.

Figure 2.5 presents the conductivity changes during stretching and relaxing. The conductivity trace of stretching is a little different from the relaxing trace especially when the extension is very big. It is because the fabric is impaired in stretching process. The fabric shows good recovery performance when stretch can be controlled below 40%. Repeated extension test shows that the conductivity of the fabric will decrease to a great degree after repeated 40% stretch, which also supported that the stretch controlled below 40% is important to maintain the fabric conductivity after repeated use. SEM microphotographs (Figure 2.6) shows that damage happened on the surface of fiber after the fabric was under repeated extension over 30 cycles at 60%.

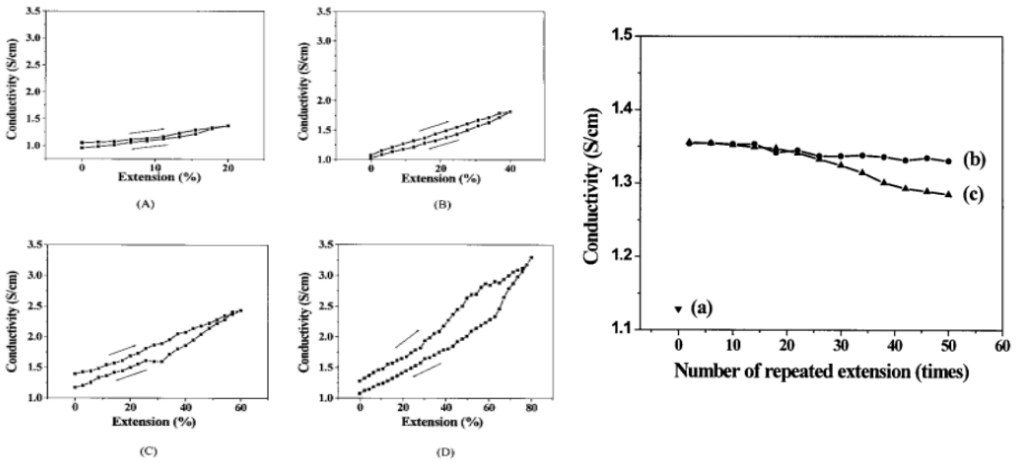

FIGURE 2.5. Conductivity changes during stretching and relaxing: (A) 20%, (B) 40%, (C) 60%, and (D) 80% extension and conductivity changes during repeated extension test: (a) initial conductivity, (b) 40%, and (c) 60%.

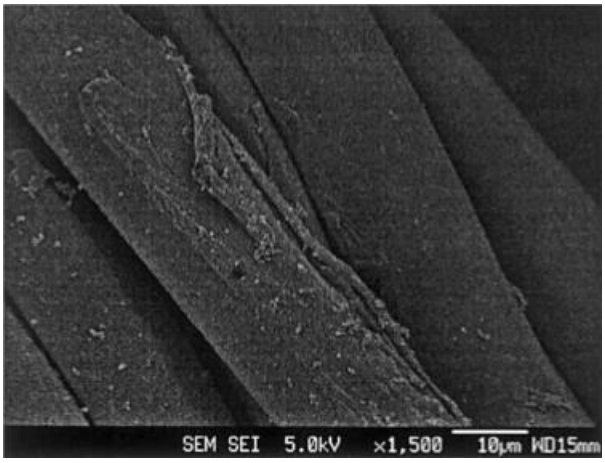

FIGURE2.6. SEM microphotographs of fabric after repeated extension over 30 cycles at 60% strain.

2.2.3 Applications: wearable sensing textiles

The combination of traditional fabrics and smart materials (conducting polymer, piezoelectric material, etc.) provide the fabrics with unique properties that traditional fabrics don't own. The electro-mechanical property of the polymer-coated fabric enable the realization of wearable sensing textiles that are capable of recording posture, sensing movement, detecting chemical gas and so on.

It is proposed that the sensors arrays can be distributed on garment to achieve a sensor network in order to obtain the stretching information of every point on the garment (Rossi DD, Carpi F, et al. 2002). In this way, the posture or movement of the subject can be detected and recorded. A network of sensors were established to read the signals from every point in the network and further to confirm the stretch situation of the entire row and column (Figure 2.7).

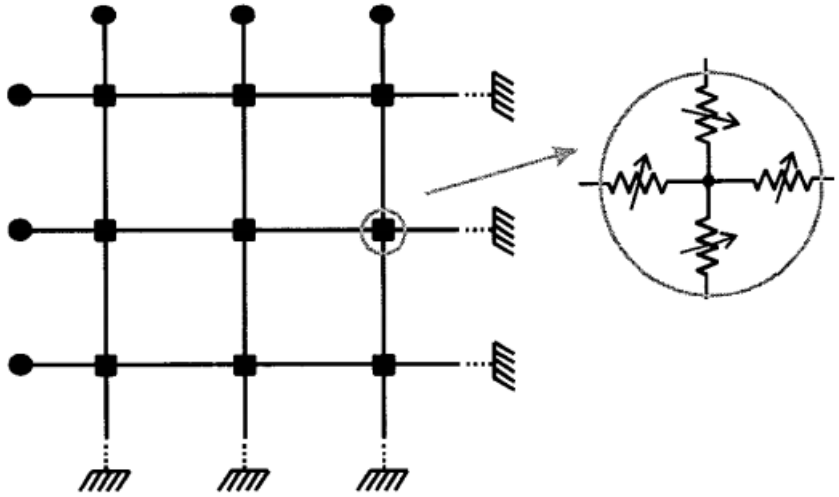

FIGURE 2.7. Network of Sensors Arrays

Piezoelectric materials were also used in wearable sensing textiles. A special glove were developed which utilize piezoelectric material as shape sensors (Edmison J, Jones M, Nakad Z, Martin T, 2002). In this design, the piezoelectric films were placed at the finger joint and fingertips to capture the hand movement during typing (Figure 2.8).The fingertip and mid-finger sensors for each finger were each connected to a single channel on an A/D converter and the collected and packed data were sent to PC for processing. Finally, the movement of the finger was determined. The glove shows promising application of keyboard function.

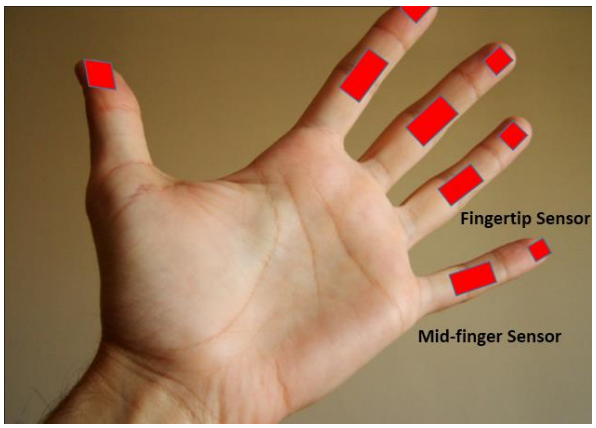

FIGURE 2.8. Sensor arrangement

As mentioned before, the electromechanical property of PPy-coated fabrics makes them good candidates as movement sensors. It is also reported that PPy-coated fabrics showed good potential as candidates of gas sensors (Kincal D, Kumar A, Child AD, Reynolds JR, 1997). It is found that the conductivity of the PPy-coated fabric decreases upon exposure to NH3 and is regained with HCL. The PPy-coated fabric during cycling with HCl/N2/NH3/N2 presented conductivity switching (Figure 2.9). However, there is a slow decay in the overall conductivity with repeated cycles. When the fabric is exposed to the cycling of HCl and NH3 gas, they will combine into NH4Cl salt on the surface of the fabric. Thus this conductivity decay can be attributed to the formation of a layer of salt on the surface of the fabric, which reduces the further interact between the gases and the fabric. This explanation was further confirmed by observing that the conductivity of the fabric was recovered after water washing and dry. In order to solve this problem, formation of salt should be avoided and weak acid gas can be a better choice. When HCl was replaced with CO2, the PPy-coated fabrics under cycling with NH3/CO2 still shows conductivity switching. It can be seen that the switching amplitude was decreased but the switching is more stable and reproducible. Therefore, the PPy-coated fabrics presents their gas sensing capabilities through monitoring their conductivity changes.

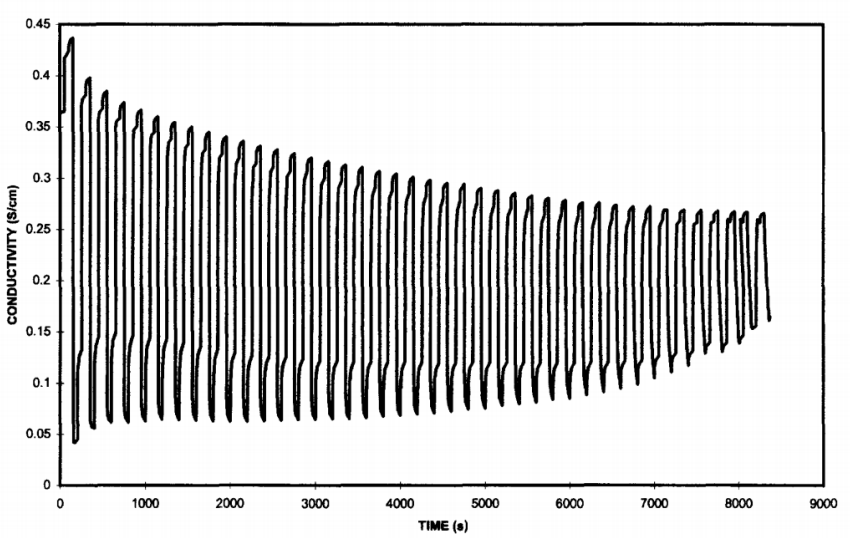

(a)

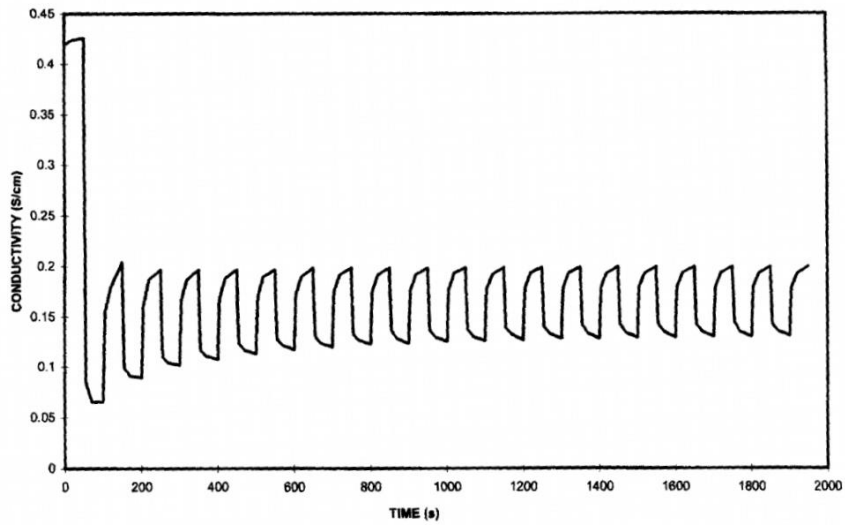

(b)

FIGURE 2.9 Conductivity change for the PPy-coated fabric during cycling with (a) HCl/N2/NH3/N2 and (b) NH3/CO2

2.3 Products of thermal textiles in market

Thermal functionality is one of the critical topics in wearable electronic textiles. Thermal textiles now in markets can provides thermal functionality that is significant to healthcare, safety insurance and resisting extreme environment. These smart textiles with thermal function will be applied in various fields, for instance, medical, sports, healthcare and so on.

Nowadays, a number of thermal functional textile products have emerged in the commercial market (Figure 2.10) and they are mainly divided into four typical types. The first type of product for daily heating is presented by Nuanshou Po. It uses the oxidation of iron to generate heat to achieve thermal function. However, the temperature of this product is hard to control due to the incontrollable chemical process and consequently it may injure users' skin which limits the application of this kind of product. The second type of heating product is the spontaneous thermal protective clothing such as spontaneous thermal kneecap. This kind of heating product generates heat based on special material such as tourmaline, which can release far-infrared rays and negative ions with the help of human temperature environment. The shortcomings of this kind of products is the relative expensive price resulted from complicated manufacture process. The third type of heating products in the current market is the heating home textiles and electric blanket is one of the most popular products of this type. Even though this kind of products are widely accepted in market, they have some shortcomings in common, such as poor flexibility, distributing electromagnetic radiation, low energy efficiency, risk in electric shock and so on. According to the weakness of the products, some industry manufacturers and labs use a temperature controller to insure the safety. However, the most fundamental problem of this kind of products is that the heating material in the products is metal wire. In some products, carbon fibres or carbon coated fibres are used and the products present excellent properties, flexibility, safety, etc.

With the huge potential demand of heating products, the thermal textiles are developing rapidly and research on thermal textiles is becoming a fast growing topic in textiles industry. As mentioned before, as a heating product, temperature control and energy management are the most important topics in thermal textiles. Well developed products now in market, including WarmX, iTermx, MET5 jacket, Gorix diver suit, Brookstone and so on, do a relatively better job on temperature

control and energy management and they are the fourth type of heat products, which use conductive materials. A notable application of thermal function in textile including WarmX, a German company which focuses on thermal knitwear research to retain warmth during outdoor sport activities and work protection which are made of conductive polyamide fiber by weaving technology (knitting technology). In the last decade, much attention has been paid to heated jackets that usually attach a carbon fiber material layer inside the jacket to support heating energy. Another issue is advanced control system; Solaris ski-gloves were produced by Reush with a new microcontroller platform named iTermx. In addition, the heating products presented by Gerbing are constructed with an interior protective moisture barrier and breathable membrane to generate heat. Yet, sew processes and electronic control systems are necessary to realise its thermal function. The thermal garments are also designed for specific situation of sub-aqua heated by piped hot water. Aside from retail clothing and the industrial sector, other research works have also been conducted. However, most thermal garment operate by attaching a heating layer that may be a piece of conductive fiber or metal materials, and some products incorporate conductive heat fabric with normal fabric sewn together by the patchwork method to format a heating area and electronic routing. Few studies can provide a systemic method to develop the thermal function garment incorporating a heating area and resistive network together in one formation.

FIGURE 2.10. Thermal functional products in market

2.4 Resistance calculation for conductive textiles

Thermal textiles are also conductive textiles because they generate heat based on the conductive yarns embedded in them. The conductive yarns in thermal textiles form a network which conducts the electrical current from the power supply. As mentioned above, thermal control is the most significant topic in textiles. And thermal control is controlling the heating temperature by adjusting the applied electrical power accordingly. According to Ohm's law, the electrical power applied to the objective is related to the applied electrical voltage and the resistance of the objective,

$$P = \frac{U^2}{R} \tag{2.1}$$

Thus calculation of the resistance of the network in thermal textile is the very first step in thermal control. In previous research, a resistive network model was proposed to calculate the resistance of conductive knitting stitches (Li Li, Wai Man Au, et al. 2010). Knitting structure is one of the most used structures in textiles and its network can be regarded as the combination of many loops (Figure 2.11). The loop is a basic unit in the knitting structure and they are in a repetitive sequence. In a single loop, there are both length-related resistance and contact resistance. The length-related resistance is positively linear correlated with the length of conductive yarn. The contact resistance is result from contact of conductive yarns and thus vary with the pressure between conductive yarns. Consequently, the conductive knitting stitches for different numbers of courses and wales can be represented as a resistive network that is comprised of a number of length-related resistor and contact resistors. Contact Resistance R_c could be divided into four equal resistances ($0.25\,R_c$) and be absorbed to their four neighbouring length-related resistor without altering the equivalent resistance of the stitch. When the knitting fabric is in a static status, the contract resistance can

be regarded as unchanged. To simplify the resistance in network, the three equivalent resistance is used as follows:

$$R_1 = R_{l3} + 0.5R_c \tag{2.2}$$

$$R_2 = R_{l2} + 0.5R_c = R_{l4} + 0.5R_c \tag{2.3}$$

$$R_3 = R_{l7} + 0.5R_c \tag{2.4}$$

Where R_1, R_2 are used to specified the inner resistance along the course and wale direction, while, R_3 represents the outer resistance, which is located along the boundary between the conductive yarn and the non-conductive yarn.

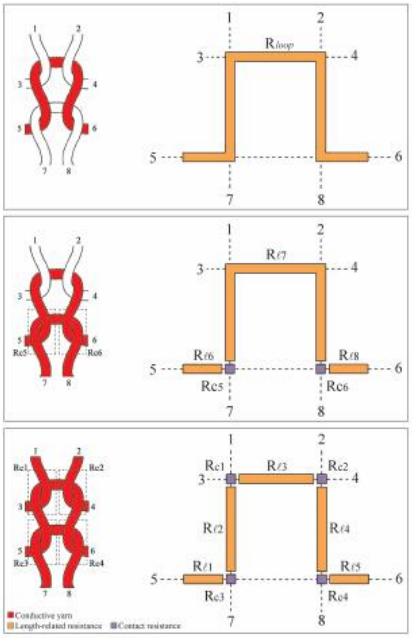

Figure 2.11. A lump resistor model represents the unit loops in the knitting fabric

According to the signal flow theory (Haykin, 1970), the contact resistance could be divided equally into four resistances and then be absorbed to their four neighboring length-related resistors. In this way, the resistance network could be

simplified, as shown in the following figure. Since R_1 is not equal to $R_{1//3}$, According to signal flow graph theory, equal portion of Δ of R_1 could be transferred to both R_2 and $R_{1//3}$ to achieve

$$\frac{R_1-\Delta}{R_{1//3}+\Delta}=\frac{R_{1//3}+\Delta}{R_1-\Delta}=\frac{R_1}{R_1} \tag{2.5}$$

Where,

$$\Delta=\frac{R_1-R_{1//3}}{2} \tag{2.6}$$

Thus the "bridge" resistors R_2 in the resistive network can be neglected due to the equal voltage potential and the resistive network can be furthermore simplified. Finally, the equivalent resistance for a conductive knitting fabric (M courses, N wales) along a course direction can be obtained as follows:

$$R_{equivalent}=\begin{cases} NR_{loop}, & M=1 \\ 2NR_{1//3}, & M=2 \\ \frac{2NR_1(R_1+R_{1//3})}{(M+1)R_1+(M-3)R_{1//3}}, & M\geq 3 \end{cases} \tag{2.7}$$

With this formula, the manufacturer can design the resistance of the conductive textiles to achieve an expected target.

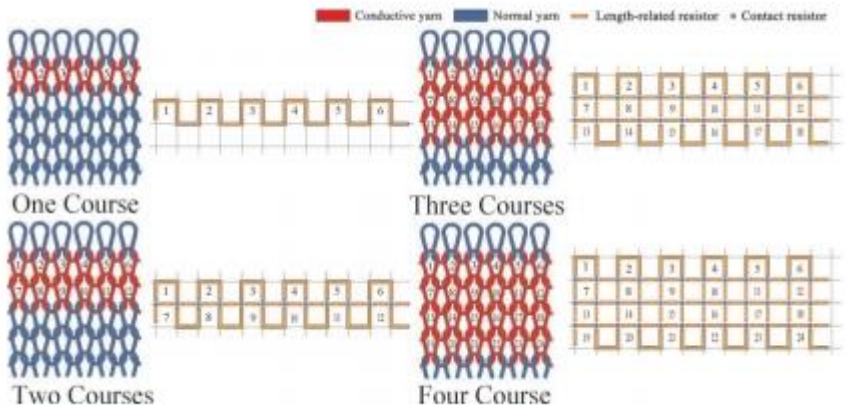
Conductive yarn
Normal yarn
Length-related resistor
Contact resistor
One Course
Three Courses
Two Courses
Four Course

(a)

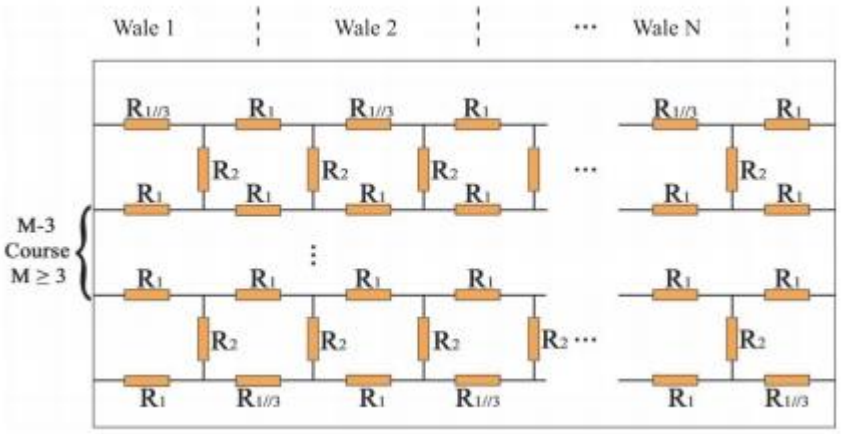
Wale 1
Wale 2
Wale N
M-3
Course
M ≥ 3

(b)

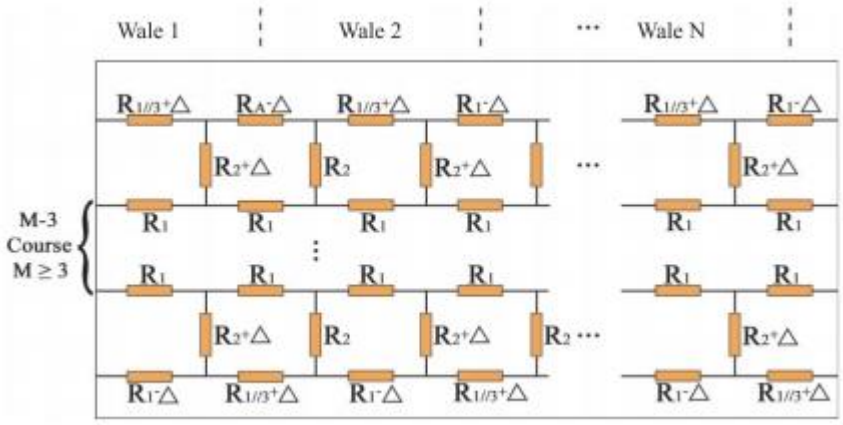
Wale 1
Wale 2
Wale N
M-3
Course
M ≥ 3

(c)

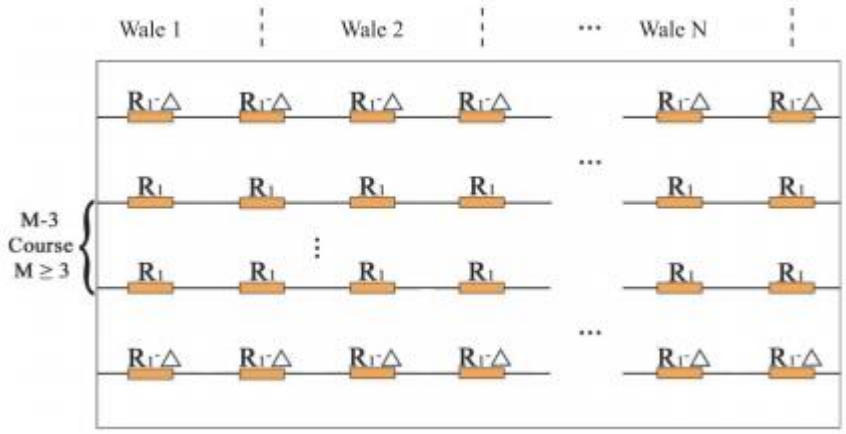

(d)

FIGURE 2.12. The resistive network of a conductive knitted fabric and its simplified procedure

Same calculation method applies to the knitting textiles which have float stitches (Figure 2.13, Liu S, 2014). Resistive network and the simplifying process of it are still an effective way to calculation the resistance of knitting textiles with float stitches.

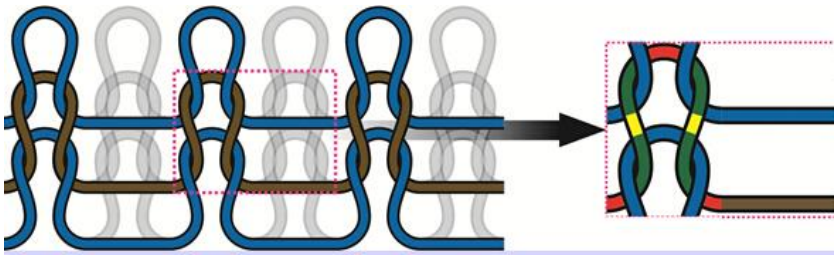

Figure 2.13. Knitting structure with float stitches

Another calculation method is adopted to calculate the resistive network of knitting structure in previous research. Kirchhoff's Law is the core concept in that method

(Zhang Hui, Tao Xiaoming, 2005). The conductive kitting textile is also treated as a pure electrical circuit network. A unit loop, which is a repeatable unit in structure, is also composed of contact resistors and length-related resistors. It is shown in the figure that one unit loop contains two contact resistance R_c and three length-related resistance R_l , related the contacting force of the overlapped yarns and the length of yarns respectively.

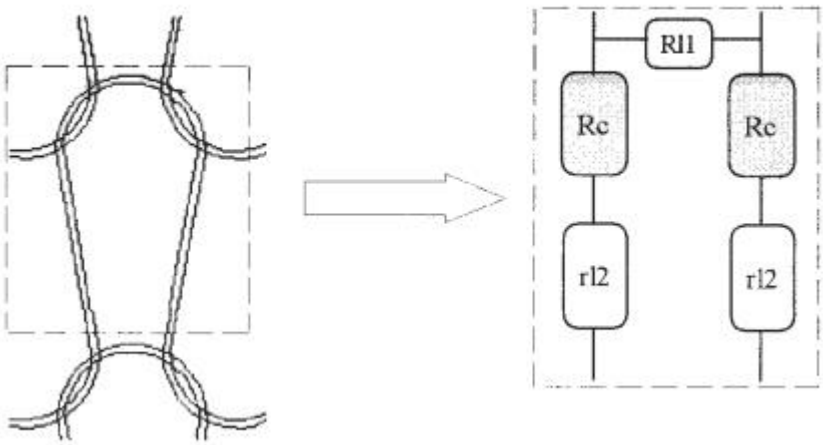

FIGURE 2.14. A unit loop and its resistive network

Thus the circuit diagram for the conductive knitting fabric can be obtained, which is presented in the following figure (Figure 2.15). Because, in general, according to the experimental results, the length resistance is far smaller than the contact resistance in conductive textiles, the circuit diagram can be further simplified. In order to calculate the equivalent resistance of the whole resistive network, Kirchhoff equation is established for every local circuit in the resistive network and the equation set is obtained as follows,

$$\left[R_{i,j}^{*}\right][i_i] = [U_j](i = 1,2,3 \dots j = 1,2,3 \dots) \tag{2.8}$$

By solving this equation set, every local electrical current i_i in the network can

be calculated. Thus the total electrical current of the whole network I_{total} can be obtained. After that, the equivalent resistance of the whole resistive network can be obtained from dividing the applied voltage by the total electrical current,

$$R_{equivalent} = \frac{U}{I_{total}} \tag{2.9}$$

The advantage of this method is that the calculation process is programmable. What's more, it is not limited to some specific structures and is very versatile in applications. But the calculation process is complicated and time-cost, which are the disadvantages of solving Kirchhoff equations.

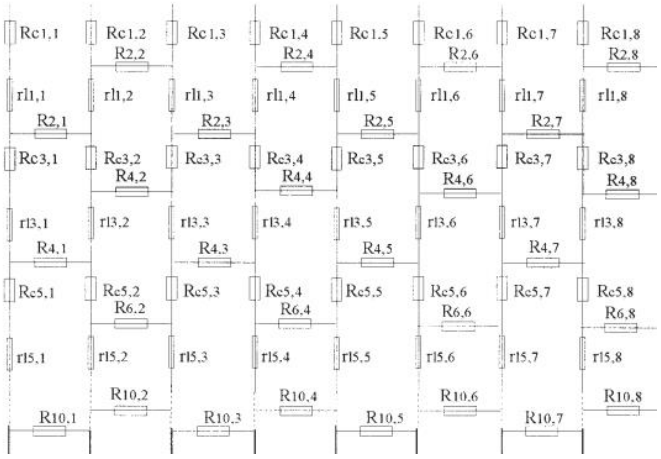

(a)

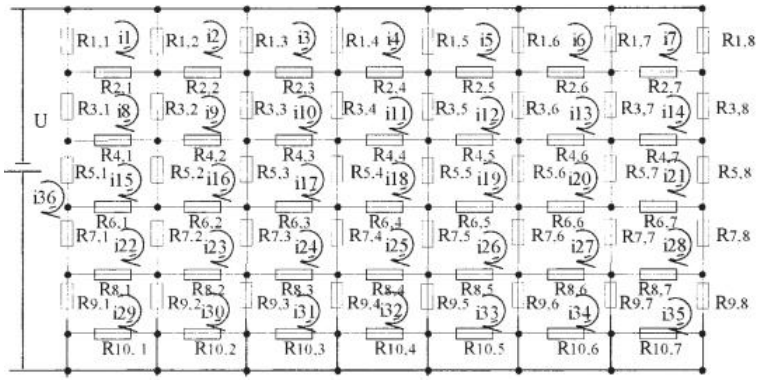

(b)

FIGURE 2.15. (a) Resistive circuit network of a fabric;

(b) the simplified resistive circuit network

Woven structure is also one of the most used structure in textiles. Calculation of the resistance of conductive woven fabrics should also be conducted. Compared with the complicated knitting structure, the structure of woven textiles is straightforward. In a woven structure, the contact resistance does not exit and the length-related resistance is the only type of resistance that should be considered (Figure 2.16, Zhao YF, 2013). It is because, in a woven structure, the conductive yarns do not cross with each other and consequently there's no contact at all. Therefore, the most important thing step of the calculation process is to calculate the length of the conducting yarns along the current flow in woven textiles.

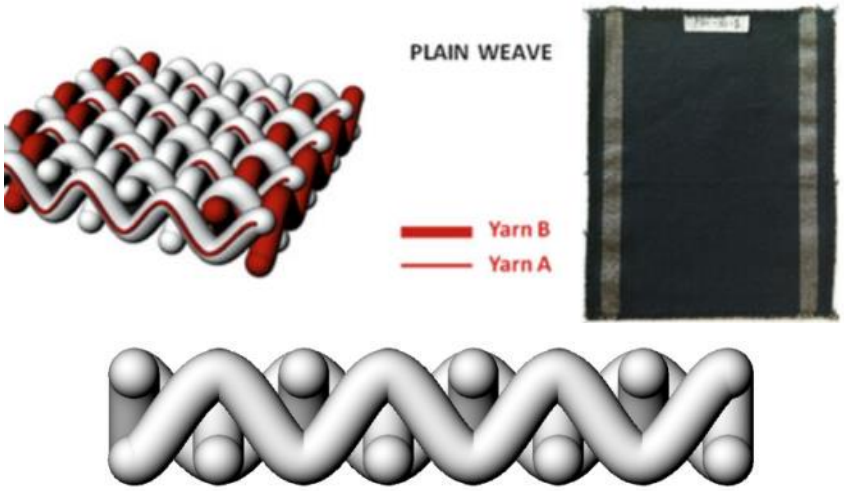

Figure 2.16. 3D Image of Plain Woven Structure

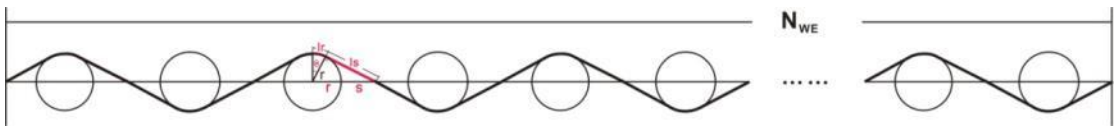

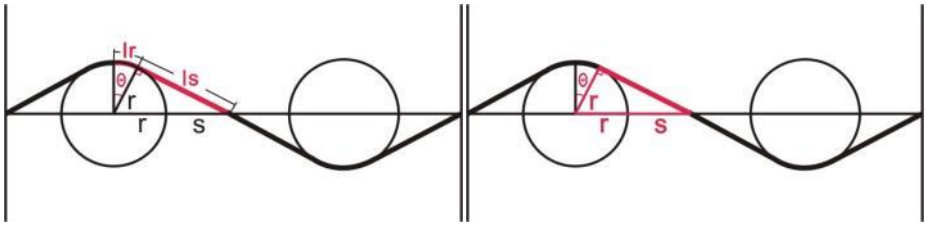

Figure 2.17. Schematic Diagram of Plain Woven Structure

The adjacent two yarns are considered as a unit and the whole length of the weft yarn can be divided into two parts: lr, ls. It is assumed that lr is part of a circle and ls is straight in line (Figure 2.17). Along with the radius of the cross section r and the angle corresponding to length lr, the following relationship can be obtained,

$$\begin{cases} I_r = \theta r \\ I_s = \sqrt{2rs + s^2} \\ sin\,\theta = \frac{r}{r+s} \end{cases} \tag{2.10}$$

Considering the course number and wale number of the plain weave structure M and N, the warp yarn and weft yarn together make a criss-cross pattern, which is firm and resist yarn slippage. Each of the weft yarn goes up and down through the warp yarns, which is shown in figure. The length of one weft conductive yarns can be calculated,

$$L_P = 2N(I_r + I_s) = 2N\left(\theta r + \sqrt{2rs + s^2}\right) \tag{2.11}$$

Therefore, the resistance of the whole plain woven structure can be express as,

$$R_P = \frac{2NR_0\left(\theta r + \sqrt{2rs + s^2}\right)}{M} \tag{2.12}$$

Where the R_0 is the line resistance density of the conductive yarns. With the above formula, the conductive yarns can be arranged based on requirement in the fabrication of woven fabrics and people can make different conductive woven

fabrics with different resistive parameter.

The core principal in the calculation of resistance of conductive textiles is to establish a resistive network and simplify the network in a proper way. With the calculation method, people can design the conductive textiles they want for thermal purpose. Moreover, the resistance of a conductive textiles can be estimated by using the resistive network.

2.5 Conductive textiles in stretch

In daily use, the conductive textile for thermal purpose can be stretched and the condition of the conductive yarns in it may change. Consequently, there may exist shift in the resistance of the conductive textile in stretch. Thus how the resistance of conductive textile will change when external strain is applied is an important topic. Some study has been conducted on this electro-mechanical property of conductive textiles (Li Li, Au WM, et al. 2008). As is known to all, in a conductive knitting structure, there exit length-related resistance and contact resistance. So now the mission can be converted to explore how the external strain will influence the length-related resistance and contact resistance respectively.

The length-related resistance for a given object is inversely proportional to the cross-sectional area and proportional to the length of the object. The resistance of a conductive wire can be computed as,

$$R = \rho \frac{l}{A} \tag{2.13}$$

Where l is the length of the wire, A is the cross-sectional area of the wire, ρ is the electrical resistivity of the material that is used to make the wire. When external strain is applied to the conductive wire and it is in stretch, the length of the wire will increase and the cross-sectional area of the wire will decrease, which makes

the resistance of the wire increase rapidly. The length resistance of the conductive textile in stretch can be expressed as follows,

$$R_l = \frac{1}{W} . \sum_{n=0}^{N} \sum_{m=0}^{N} C_{mn} F^n L^n \tag{2.14}$$

The stretch applied to conductive textiles will not only influence the length-related resistance but also the contact resistance. The contact resistance is generated from the contact between conductive yarns and the contact level will decide the value of contact resistance. Basically, better contact makes bigger contact area, which will reduce the contact resistance. Thus, when the external strain force increases, the conductive yarns in textiles will become tight and the contact between them is enhanced. In other words, the contact resistance part in the total resistance of conductive textile is inversely correlated with the strain, which can be expressed as follows,

$$R_c = \frac{1}{W} . \frac{a_1}{P_0 + a_0 F} \tag{2.15}$$

When the above two formulas are combined, the total resistance of conductive textiles in stretch is obtained and it can be calculated by the following formula,

$$R\ (F, L, W) = \frac{1}{W} \left(\sum_{n=0}^{N} \sum_{m=0}^{N} C_{mn} F^n L^n + \frac{a_1}{P_0 + a_0 F} \right) + W . b_0 \tag{2.16}$$

Where F is the external strain force, L is the length of the fabric, W is the number of wales, b_0 is the terminal resistance between the connector and the fabric. This formula implies that, in the initial stretch when strain force F is small enough, the length related resistance term $\sum_{n=0}^{N} \sum_{m=0}^{N} C_{mn} F^n L^n$ can be neglected compared with the contact resistance term $\frac{a_1}{P_0 + a_0 F}$. Thus, in the initial stretch, the contract resistance change represents the total resistance change, which means the total resistance decreases. However, when the strain force furthermore increases, the length-related resistance will dominates the total resistance for further stretch,

which makes the total resistance increases. This model shows that the length-related resistance and contact resistance altogether form two competing factors that determine the overall resistance and it is consistent with the actual textile behaviors (Figure 2.18). In conclusion, the contact resistance acts as a decreasing factor during the initial stretching process, whereas the length-related resistance dominates the total equivalent resistance for the further increasing of tensile force in the stretching process.

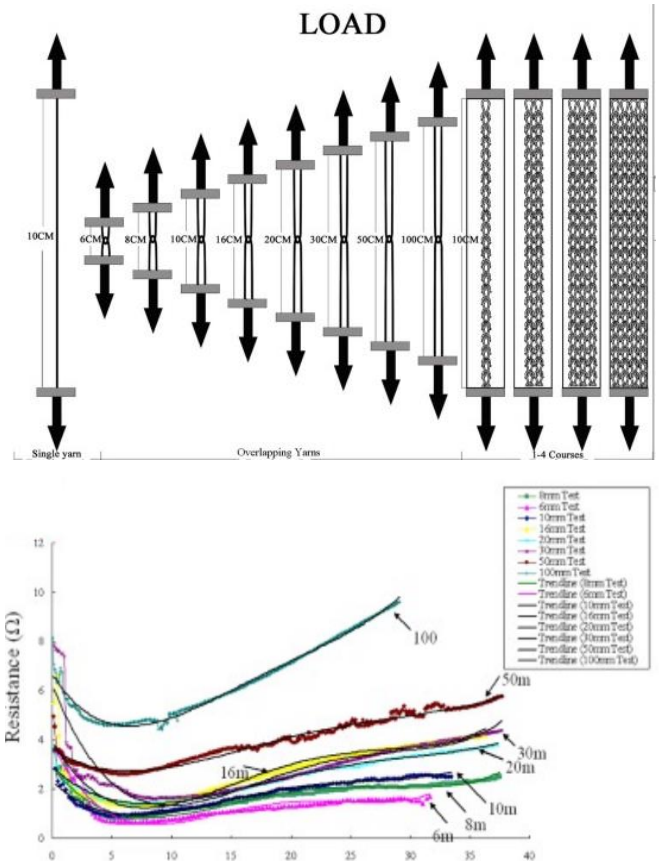

Figure 2.18. The electro-mechanical test for different conductive textiles

People also proposed an empirical model to describe relationship between the contact resistance between contacting yarns and the force between yarns (Zhang Hui, Tao Xiaoming, 2005). An exponential function is established in this theory,

$$R_c = R_0 + (R_1 - R_0) \times e^{-\frac{F}{c}} \tag{2.17}$$

Where R_1 is the contact resistance without the applied force, R_0 is the minimal contact resistance with applied force and c is the coefficient. According to Holm theory (Holm R, 1967), the contact resistance between conductors is inversely proportional to the contact area between them. Thus the resistance will decrease rapidly due to the relatively fast increase of the contact area between contacting yarns when the force increase in the initial stage, which completely accords with the exponential relationship in the above formula. When the force between contacting yarns further increases, the contact area between contacting yarns is already big enough and cannot increase in a big degree, which makes the contact resistance decrease slowly. The experimental results also indicates that the resistance-force curve can be divided into two part: the “sharp stage” with small contacting force and the “stable stage” with the large contacting force (Figure 2.19).

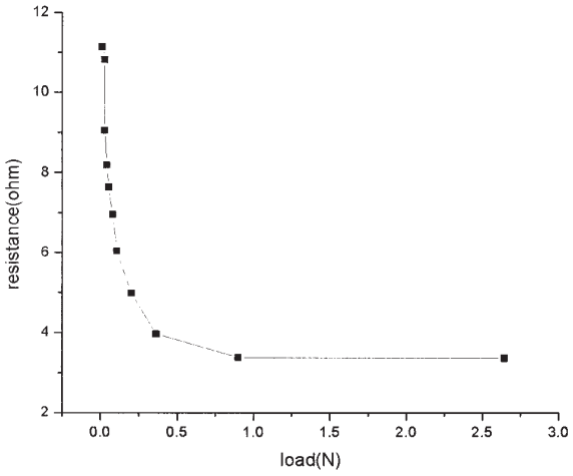

Figure 2.19. Relationship between the contact resistance between contacting yarns and the force between them

2.6 Thermal process of conductive textiles

In order to achieve temperature control of thermal textile, it is necessary to explore the its thermal process. The heat flux condition in thermal textile is the key to the whole thermal process. When the heat flux is fully studied in the whole thermal system, the temperature can be estimated. In previous research,

the thermal property of conductive knitted fabrics has been studied (Li Li, Au Waiman, et al, 2014). When electric power P is applied to a thermal textile at an time interval of dt, the change of the heat energy in fabric dQ is balance of input electric power and the heat loss to the surrounding environment,

$$dQ = Pdt - dS \tag{2.18}$$

Where dS is the heat loss from the fabric to the surrounding environment. According to Fourier's Law, the heat flux is proportional to the temperature gradient. Thus the heat flux from the fabric to the surrounding environment is proportional to the temperature difference between them,

$$dS = \alpha * (T - T_0) * dt \tag{2.19}$$

Where α is the thermal diffusivity of the fabric, T_0 and T are initial temperature and current temperature of the fabric, respectively. Moreover, the change of the heat energy in fabric is proportional to its temperature change,

$$dQ = C * dT \tag{2.20}$$

where C is the thermal capacity of the fabric, which measures the fabric's ability to store heat energy. Thus combine the above two equations and solve the differential equation, the temperature that the thermal fabric can achieve is obtained,

$$T - T_0 = \frac{P}{\alpha}(1 - e^{-\frac{\alpha.t}{C}}) \tag{2.14}$$

This result indicates an exponential relationship between the temperature of the fabric and time. The temperature will increase rapidly at the beginning and then

tend to be stable. When $t \to \infty$, the term $1 - e^{-\frac{\alpha.t}{C}} \to 1$, the thermal fabric system will reach the stable state and the electric power input equals the heat loss rate. Hence, the maximum temperature can be achieved at the stable state,

$$T = T_0 + \frac{P}{\alpha} \tag{2.14}$$

It can be concluded that the stable-state temperature only depends on the electric power input and the thermal diffusivity. The thermal capacity only decides how fast the temperature is raised. In previous research, thermal process of thermal fabrics with different loop densities and different materials were studied and the temperature they can achieve was tested (Figure 2.20). The result shows that the wool is the best of the three materials for heat retention, which accords with the thermal diffusivities of the three materials.

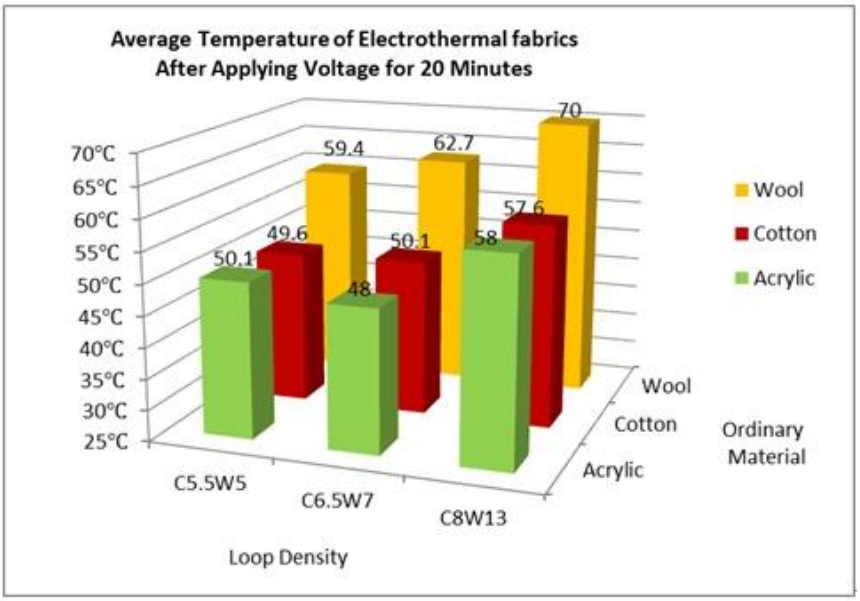

FIGURE 2.20. Average temperatures of nine fabrics after heating for 20 minutes.

2.7 Summary

In previous research, the electromechanical properties of conductive fabrics have been studied and a calculation method for the resistive network has been proposed. Thus, the resistive property of conductive fabric has been fully explored. However,

in previous research, the influence of temperature on resistance has never been considered. The influence of temperature on the resistance is important for temperature control in thermal fabrics and is worth studying. The thermal behavior of the conductive fabrics has been studied. However, additional factors such as environmental factors that may influence the thermal behavior of the conductive fabrics remain to be studied.

CHAPTER THREE

RESEARCH METHODOLOGY

3.1 Introduction

Our research work aims to explore the thermal behavior of a thermal textile and develop a textile with precise temperature control function. It is known that a number of factors can influence the thermal behavior of thermal textiles including internal factors such as resistance changes, the fabric size and the thermal diffusivity and external factors such as the surrounding environmental conditions. Our research methodology will be based on exploring these factors. The research was conducted theoretically and experimentally.

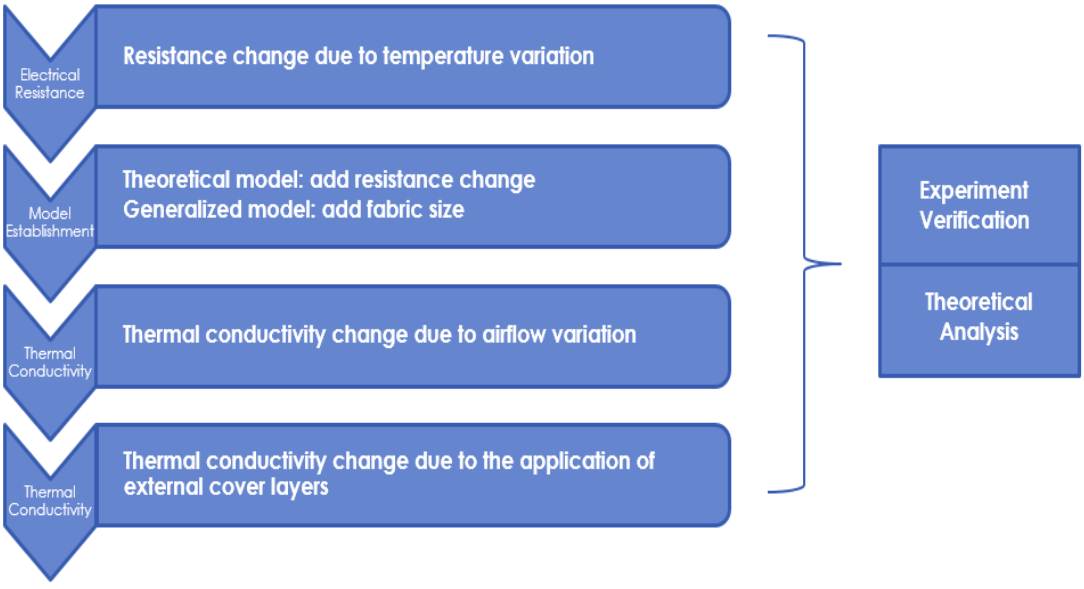

FIGURE 3.1. Procedure used in the research

3.2 Investigation of the resistance change during heating

In previous research, the resistance change of conductive textiles has never been

explored. Because resistance is one of the most important parameters of thermal control, our research is conducted to fill this gap.

The resistance of conductive knitted fabrics may continue changing during the heating process. Thus, primary experimental observation and analysis of the fabric resistance will be adopted in the first stage. Fabrics of different densities with different levels of applied electric power will be studied and compared with one another during heating.

To further identify the essential factors that are responsible for resistance changes or whether heating contributes to resistance change, a control trial will be carried out. The resistance of conductive knitted fabric without external applied electric power will be measured with increasing environmental temperature serving as a control trial.

Previous research concluded that the resistance of a conductive fabric usually includes two types of electrical resistance: length-related conducting resistance and contact resistance. It is also necessary to identify which of these types contributes more to the resistance change during heating. Therefore, a test of the resistance change of a woven fabric in which there exists no contact resistance will be conducted as a control trial.

In the final part of this stage, a theoretical model based on the experimental data and theoretical deduction will be proposed to simulate the thermal behavior of conductive knitted fabrics while taking resistance change into consideration. The model establishes the relationship between the stable-state temperature of a conductive knitted fabric and the external applied electric power to achieve temperature control.

3.3 Establishment of a theoretical model for fabrics of different sizes

Different sizes of thermal fabrics are required for different applications. Thus, there is a demand for a modified model that can simulate the thermal behavior of thermal fabrics of different sizes. When the size of the fabric changes, its electrical resistance also changes accordingly. Consequently, the temperature of the thermal fabric changes which influences its resistance. Thus the theoretical model obtained in 3.2 should be generalized for fabrics of different sizes. The generalized model will be obtained by theoretical deduction and verified by tests of fabrics of different sizes. The theoretical deduction is based on the core idea that the temperature effect on the fabric resistance is independent of the fabric size.

3.4 Influence of external airflow

The surrounding environment can influence the thermal behavior of a heating textile and its temperature control accuracy. One of the most important environmental factors should be wind or airflow. It is obvious that better ventilation or faster airflow is conducive to heat dissipation, which can further result in a lower temperature achieved by the thermal fabric. The precision of the thermal control would decrease if the airflow around the thermal textile is neglected. In this stage of the research, the effect of external wind or airflow on the thermal behavior of a thermal fabric will be investigated. We will investigate both the airflow speed and air flow angle and determine their relationship with the heating process.

3.5 Influence of cover materials

In this stage of the work, the influence of cover materials on thermal textiles will be explored. Sometimes, a thermal functional garment does have a good appearance when worn. Moreover, in certain situations involving extreme environments, additional cover layers are necessary over thermal textiles to strengthen the ability to retain heat. Because of the above issues, adding layers to

cover thermal functional textiles has become common for thermal textiles. It is obvious that the cover layers play an important role in preventing heat loss and improving heat retention. The precision of temperature control would greatly decrease if the effect of an external cover is not taken into consideration. Common sense dictates that external cover layers made of material with lower thermal conductivity are better able to aid the heat retention of thermal fabrics keep warm than cover layers made of material with higher thermal conductivity.

In our research, the effect of cover on thermal textiles will be quantified. First, thermal fabrics will be covered with different numbers of fabric layers. The studies will focus on quantifying the change in the conductivity of the heating system due to cover layers. It is known that the conductivity of a fabric material can be measured directly by a thermal conductivity metre. However, it is speculated that the measured conductivity cannot be applied to the heating process simulation. In other words, when we measure the temperature of a thermal system during heating, the thermal conductivity of the cover can be obtained. It is questionable whether the thermal conductivity of the cover that is obtained from the heating process is the same as that measured directly by the metre. Thus, in the second step of this stage, we will directly measure the conductivity of different types of covering materials using a thermal conductivity metre and then assess whether the measured values are consistent with the values obtained from the actual heating process.

3.6 Summary

The research study in this thesis was conducted based on theoretical calculations and experimental verification. The study is focused on two important parameters of conductive fabrics: electrical resistance and thermal conductivity. The factors that can influence electrical resistance and thermal conductivity were fully considered. Finally, a thermal model was established for conductive fabric, and

experimental tests were performed to ensure the correctness and accuracy of the model.

CHAPTER FOUR

FINDINGS AND DISCUSSION

4.1 Introduction

This chapter presents novel research findings and discussion related to thermal conductive fabrics. This study evaluates the thermal effect on the electrical resistance, the airflow influence on the thermal conductivity, the external cover effect on the thermal behaviour and model establishment. The research findings aim to fill the gaps and complement the previous theory of conductive fabrics.

4.2 Materials and equipment

In our research work, two kinds of silver-coated yarns are selected as the conductive yarns used in thermal textile fabrication. They are both from German company Statex GmbH. Yarn A, a monofilament with resistivity of 68.6 Ω per cm (2.2 tex), was used as the conductive material to form the heating area of thermal textiles. Yarn B, which is a balanced two-plied yarn made from multifilament single yarns, with much smaller resistivity of 1Ω per cm (47 tex), was used to fabricate the electrode of the thermal textiles. Both of them are selected from 9 candidates of silver-coated yarns because they show better performance in stability and durability after a series of testing experiments including SEM detecting, Laundering test, stretching test and corrosion resistance test.

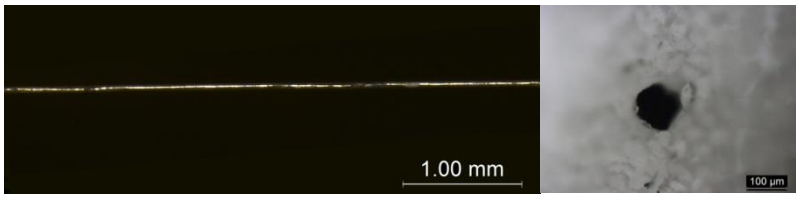

(a)

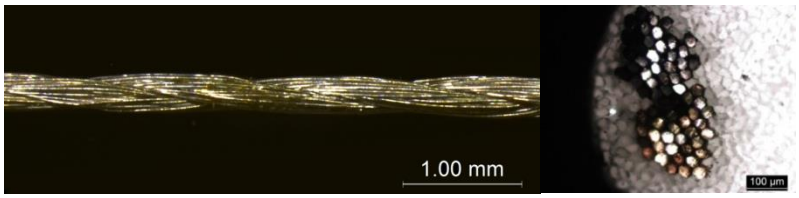

(b)

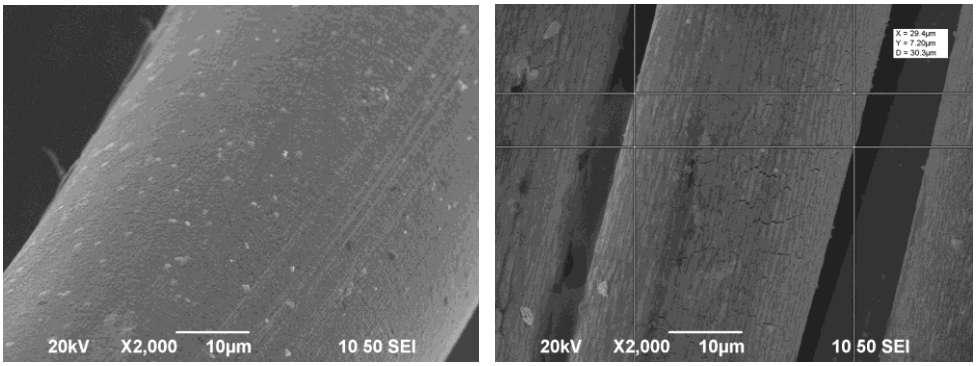

(c)

FIGURE 4.1. (a) Longitudinal view & Cross-sectional view of Yarn A and (b) Yarn B; (c) SEM images of conductive yarns: (left) yarn B and (right) yarn A

Knitted and woven structures were both adopted in this research. For the knitting structure, the silver-coated yarns were embedded into the fabrics together with other non-conductive yarns. STOLL (H. Stoll GmbH & Co. KG) M1 programming flat knitting machine, which can arrange different loop densities, was used to fabricate the thermal fabrics used in our research. And for the weaving structure, the silver-coated yarns were only embedded as the weft yarns to accord with voltage drop direction. A CCI tech automatic dobby sampling loom was used to fabricate the weaving structure fabrics we need in our research.

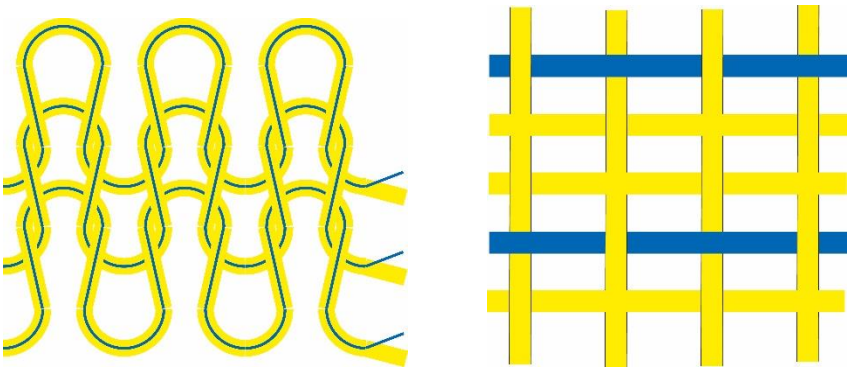

FIGURE 4.2. Silver-coated yarns (blue) in knitting structure and weaving structure and non-conductive yarns (yellow).

The power supply we used to provide electricity in our test is a variable electric DC power supply. The thermal process of thermal fabrics was conducted on a foam board, which is a heat insulator. Thus the heat flux from the fabric to the surrounding environment was ensured to be unidirectional. A number of temperature sensors which were evenly embedded into different positions of the fabric matrix were employed to measure the temperature of the fabrics. The temperatures were obtained by the temperature acquisition system with an error of less than one Celsius degree and then averaged to represent the overall temperature of the thermal system. The measurement error of the temperature can be minimized as multiple temperature samples were collected.

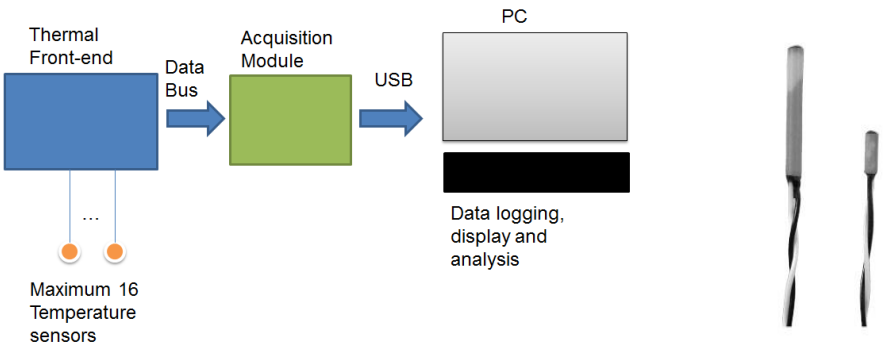

FIGURE 4.3. Temperature acquisition system (left) and Honeywell temperature

sensor HEL-705-T-0-12-00 (-200 to 600 degree Celsius) (right)

When studying the influence of airflow on the thermal process, an electrical fan, which can adjust air flow rate or wind speed, was used to provide good and stable ventilation environment. Model of the electrical fan is Lileng-826 from Lileng company and it offers adjustable free angle function to ensure an accurate air flow direction. An air flow anemometer with an error of $\pm 3\%$ was ready to measure the surrounding air flow rate or wind speed around the thermal fabric.

The thermal conductivity tester used in our research to measure the fabric's thermal conductivity/resistance is THERMOLABO II system. It can measure the thermal conductivity/resistance of a $5 * 5\ cm^2$ fabric.

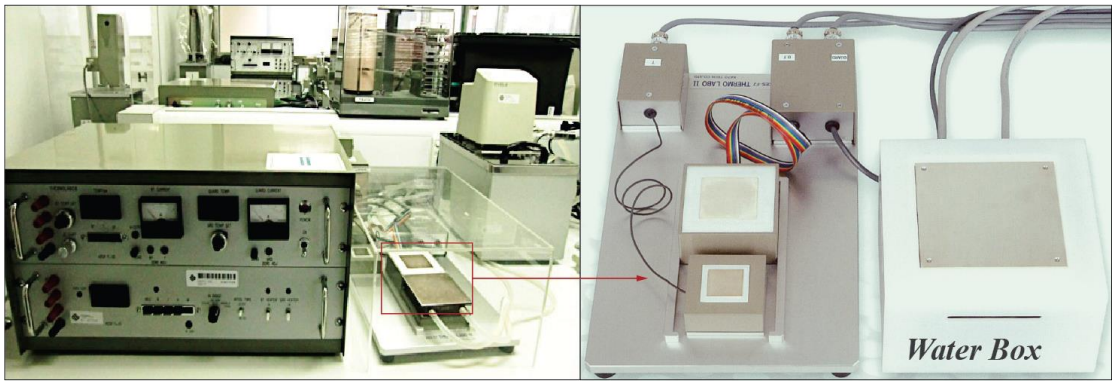

Figure 4.4. Thermal conductivity tester THERMOLABO II

All the research tests were conducted under a standard and stable lab environment with an air pressure of 1 atm, temperature of 21.5±0.5°C, and humidity of 60±2%.

4.3 Temperature effect on conductivity of knitted fabrics

4.3.1 Introduction

In this stage of the research, we will analyse the resistance change of thermal knitted fabrics during heating as well as the related intrinsic factors. Accordingly, a theoretical model that takes the resistance change into consideration will be established to simulate the thermal behaviour of conductive knitted fabrics.

4.3.2 Preliminary investigation of resistance change

In fabrication of conductive knitted fabrics, wool yarns were selected together with the prepared silver-coated yarns, because wool shows outstanding performance in warm-keeping among the common textile materials. Silver-coated yarns A were embedded into the knitted woolen fabrics to make the fabrics conductive (Figure 4.5). Two types of conductive knitted fabric samples with the same knitting structure but different loop densities were prepared by Stoll M1. They are Sample 1 (100 courses, 100 wales, loop density: 9 courses/cm and 12 wales/cm) and Sample 2 (100 courses, 100 wales, loop density: 7 courses/cm and 8 wales/cm).

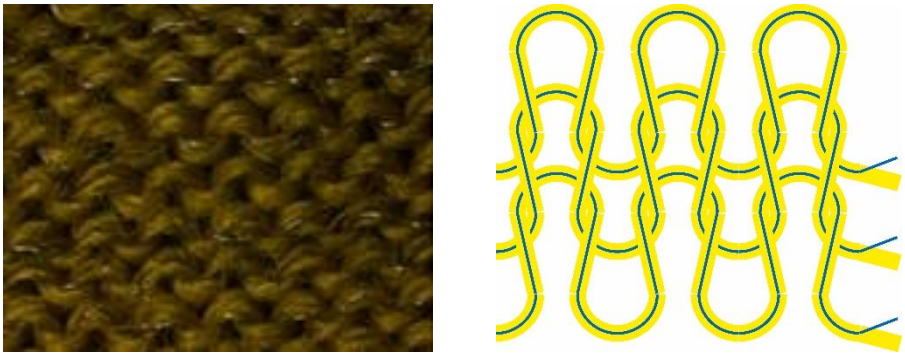

FIGURE 4.5. silver-coated conductive yarns were embedded into the knitted woolen fabrics to make the fabrics conductive.

Sample 1 and Sample 2 are by the power supply heated for 3600 seconds under 5V, 10V and 15V voltage supply respectively. It was observed that the resistance change of the conductive knitted fabric went sharply at the initial time of heating and then slowed down to become stable later. Thus their resistance was recorded every 10 seconds at first and then was recorded every 100 seconds after 600

seconds' heating. After heating, each sample was left for 24 hours to ensure that the fabric could recover to its original state and prepare for the next testing. To compare the resistance before and after heating, the temperature of the fabric should be the same. Thus when the fabric just cooled down after heating but before long time recovering (normally 100 seconds for cooling down after heating), the resistance of each sample was recorded. The temperature of the fabric might still be slightly higher than surrounding environment, but it can be negligible. Finally three resistances of each sample were measured and recorded under three different voltages: the resistance before heating resistance after a long-time heating (3600 seconds) and resistance after cooling down (Figure 4.6).

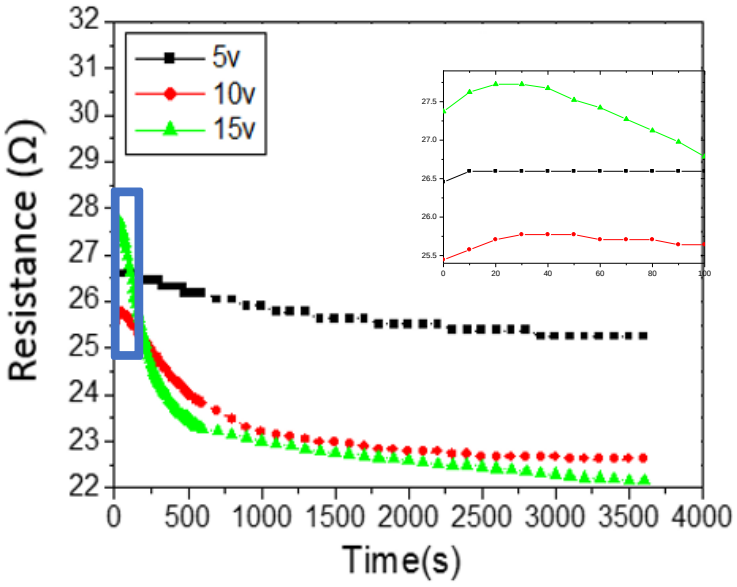

(a)

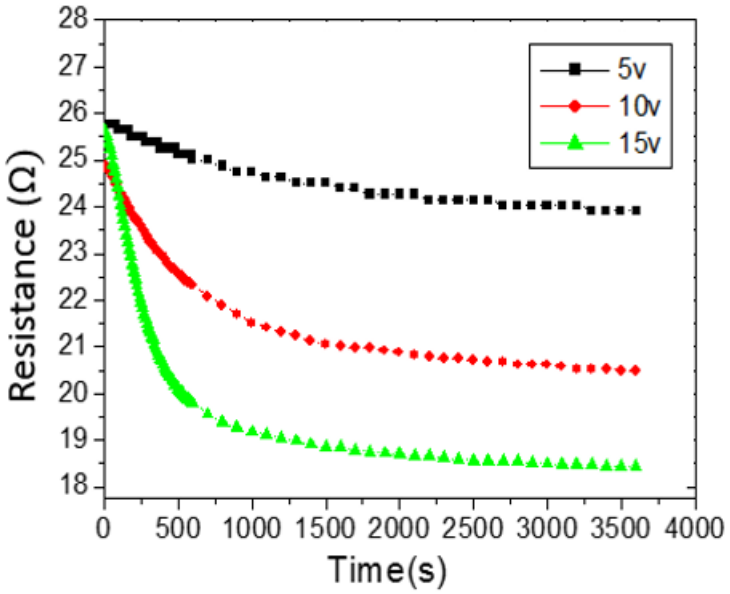

(b)

FIGURE 4.6. The measured resistance of conductive knitted fabric sample 1 (a) and sample 2 (b) varying with time under the applied voltage of 5V, 10V and 15V, respectively

It can be concluded from Figure 4.6 that overall the resistance of the fabrics tended to go down all the way during the heating process. The only exception happened at the very short initial period as presented in the inserted figure in Figure 4.6 (a), where the resistance slightly go rising. The resistance of sample in every test dropped very quickly in the first 500s and then experienced a continuous but slow decrease in the following period of heating. Over the whole heating process, the resistance changed/dropped significantly, which is opposite to the common sense that the resistance of a metal increase with temperature increase. Thus there exists another factor that lead to the resistance decrease. Take the sample 2 as the example, the resistance of Sample 2 decreased greatly at approximately 7%, 18% and 30% respectively under different applied voltages. It is also indicated by the figure that the resistance would go smaller when the applied voltage is higher.

As mentioned before, it is assumed that there're two factors that can influence the resistance of conductive knitted fabrics. One factor is that metal's resistance increases with the temperature increase. Another factor leads to the resistance decrease. These two factors competed with each other in the heating process. And based on the experiment results, the second unknown factor contributed more to the resistance change and even went over the resistance increase. Sample 1 was designed to have higher loop density, which makes its thermal diffusivity lower. When electric power was applied to Sample 1, its temperature rose very quickly. Consequently, the resistance increase effect overcame the resistance decrease and the total resistance increased initially. Because the 5V voltage is not big enough to raise the temperature very quickly, the factor that increased the resistance weighed less than the factor that decreased the resistance and the increase of Sample 1 under 5V at the beginning is not obvious. Similarly, as the loop density of Sample 2 is lower and it has better cooling capacity, the temperature of Sample 2 can't go up very quickly. Thus the resistance increase cannot show up in the initial time. Figure 4.6 shows that the total resistance of Sample 2 goes down all the way under different voltages. However, the total resistance of both samples fell down later after the initial heating period, which means that the decrease factor in resistance became predominating. After long time heating, the total resistance of thermal fabrics tended to be stable and finally reached a steady state. In addition, it is found in Figure 4.6 that there's a little difference between the initial resistances (t=0) under different voltages. The reason is that the resistance of the whole fabric is related to the physical morphology of the fabric and/or the coated yarns in it. And the physical deformation of the fabric and/or yarns is not reversible perfectly and the total resistance cannot go back exactly to the same point.

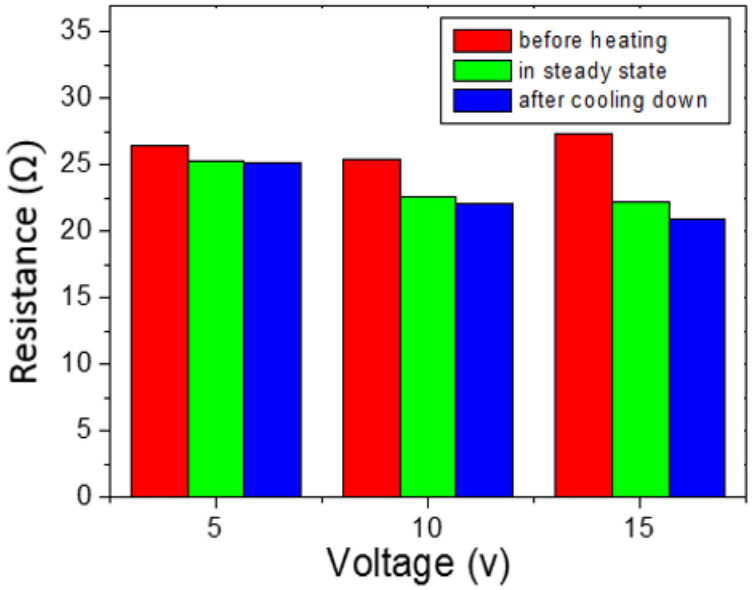

(a)

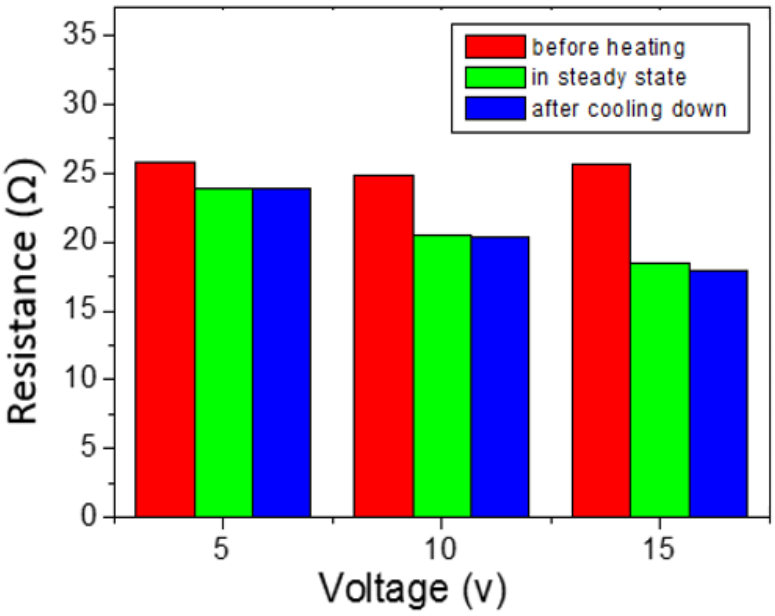

(b)

FIGURE 4.7. (a) The comparison between Sample 1's three resistances (resistance before heating, resistance of steady state and resistance after cooling down) under 5V, 10V and 15V voltage. (b) The comparison between Sample 1's three resistances under 5V, 10V and 15V voltage.

In order to explore the variety range of the resistance, three resistances: the resistances in normal condition (before heating), the resistance in steady state and resistance after cooling down (about 100 seconds after the power is discontinued) under different voltages are compared as presented in Figure 4.7. The resistance of the fabric after cooling down (blue in Figure 4.7) was measured because we need to remove the resistance increase factor by temperature. And the resistance after cooling down is indeed smaller than the resistance during heating as shown in Figure 4.7, which can be explained by the theory that the resistance of a metal increase with temperature increase. The resistance drop between the red and blue indicates that the thermal fabric did change after heating. It can be explained that when applied power was removed from the thermal fabric, the physical deformation of the fabric and/or the conductive yarns will continue for a while and cannot recover from the steady state to the initial state immediately. And it will take very long time for the conductive knitted fabric get out of "working state". That's why the time interval between two tests was set 24 hours. It is observed from Figure 4.7 that higher voltage resulted in bigger drop from the three resistances (from red to green and from green to blue). It is because higher temperature heating contributes to both bigger physical deformation of fabric (bigger drop from red to green) and larger resistivity of silver (drop from green to blue).

It is also shown in Figure 4.7 that the drop in resistance is sharper for Sample 1 compared with Sample 2 even they were applied with the same voltage. It is because Sample 1 has higher loop density and warm-keeping ability. With better warm-keeping ability, Sample 1 provided higher temperature, which contributes to both bigger physical deformation of fabric and larger resistivity of silver-coated yarns. Consequently, sharper resistance drop happened in Sample 1.

4.3.3 Identifying temperature be the resistance decrease factor

From the previous work, it was observed that the resistance of conductive knitted fabric will decrease during the heating process. It is already known that

there exist a resistance increase factor which lead to the peak of resistance curve in the initial time of heating. But the other factor that lead to resistance decrease is still unknown. We assume that temperature is the factor that lead to resistance decrease at the same time. Thus a control trial is necessary to prove this assumption. The resistance of the conductive knitted fabric will be measured when the surrounding environmental temperature increases (No power supply was added to the fabric). The conductive knitted fabrics are placed in a temperature adjustable box for 10 minutes, where the temperature was set at 30°C, 40°C and 50°C respectively. After 10 minutes' heating, the conductive knitted fabrics were left for cooling down for 100 seconds and the resistances for each temperature were measured and recorded (Figure 4.8).

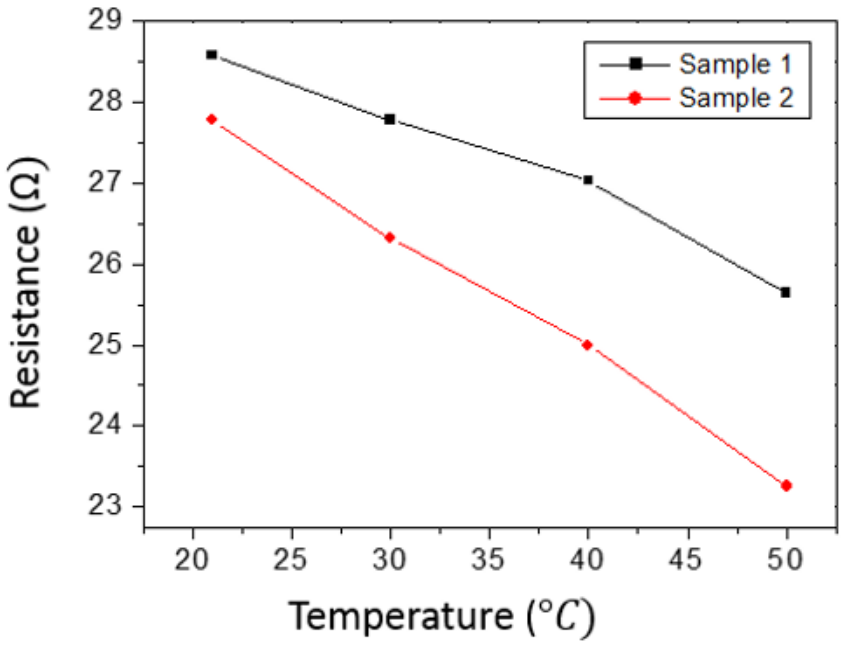

FIGURE 4.8. The resistance of sample 1 and 2 after being heating to 30°C, 40°C and 50°C and cooling down is compared with resistance in standard condition (21°C).

The above figure clearly indicates that the resistances of conductive knitted fabrics will decrease when the temperature increases. This test removed the influence of other variation such as the voltage, electrical current. This result strongly supports the assumption that temperature is also the factor that is responsible for the resistance decrease when the conductive fabrics are under working. In conclusion, the temperature can not only increase the resistance of conductive knitted fabrics but also decrease it. This two effects compete with each other during heating and finally resistance decrease contributes more in this process.

4.3.4 Analysis of the resistance change

Because there exist a lot of contact between silver-coated yarns in the conductive knitted fabrics, the total resistance of the conductive knitted fabric can be divided into the length-related conducting resistance of the conductive yarns and the contact resistance between conductive yarns,

$$R_{total} = R_{yarns} + R_{contact}$$

When take the derivative on both sides of the above equation, the resistance change of the conductive knitted fabric can be obtained,

$$\Delta R_{total} = \Delta R_{yarns} + \Delta R_{contact}$$

It is known that R_{yarns} depends not only on the temperature and but also the

physical condition of silver-coated yarns (e.g., strain, bend). The temperature can influence R_{yarns} through increasing the resistivity of the silver coated on the yarns. And the physical deformation of the yarn can affect R_{yarns} through changing the structure of the silver coating layer on the surface of the yarn, such as increasing the cracks and flaws on the silver coating layer. When the electric power was applied to the conductive knitted fabric, the generated heat from the conducting yarns raised the temperature of the whole fabric. As mentioned before, there must exist a factor that lead to the resistance decrease, which is also resulted from the temperature increase. Thus it can be concluded that the temperature increase in the heating process must improve the structure of the silver coated yarn (ΔR_{yarns} decrease) and/or improve the contact between the silver coated yarns ($\Delta R_{contact}$ decrease).

In order to find out if or how much ΔR_{yarns} contributed to the total resistance change of conductive knitted fabric, a control trial, which removes the $\Delta R_{contact}$, is necessary. As shown in Figure 4.2, in a weaving structure, there's no contact between the silver coated yarns and $R_{contact}$ doesn't exist. Thus the conductive woven fabric Sample 3, which also used Yarn A as the conductive yarns, was prepared. The weaving structure and the inserted silver-coated yarns are presented in Figure 4.2.

In the control trial, Sample 3 was heated under 15V voltage for 1200 seconds and its resistance was recorded every 5 seconds in the first 100 seconds and every 10 seconds in the rest 1100 seconds. Similarly, three resistances of Sample 3: the resistances in normal condition (before heating), the resistance in steady state and resistance after cooling down (about 100 seconds after the power is discontinued) were measured. The resistance curve of Sample 3 under 15V power is shown in Figure 4.9. In order to study how the resistance of a single silver-coated yarn changes during heating process, the resistance change of a single yarn A and B were measured and recorded when they are heated by 60°C

temperature. Three samples of each yarn are measured in each test. Resistances of yarn A and B before and after heating are shown in Table 4.1.

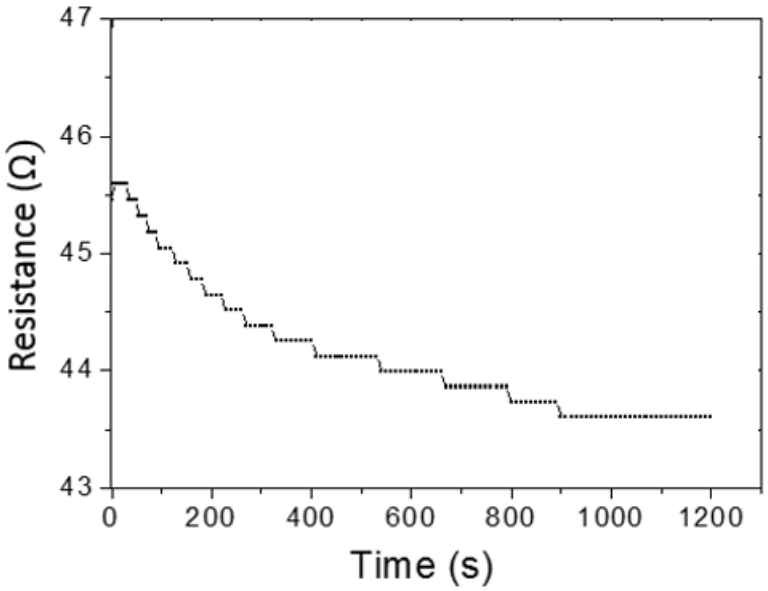

FIGURE 4.9. The resistance of Sample 3 vs. time under 15V voltage

TABLE 4.1. Resistances of yarn A and B before heating and after heating with 60°C

	Resistance after heating and cooling down	Resistance before heating	Rate of change
Yarn A (1)	822.2 Ω	878.0 Ω	6.36%
Yarn A (2)	528.2 Ω	582.6 Ω	9.34%

Yarn A (3)	514.0 Ω	569.4 Ω	9.73%
Yarn B (1)	15.1 Ω	15.2 Ω	0.66%
Yarn B (2)	35.6 Ω	36.8 Ω	3.26%
Yarn B (3)	36.1 Ω	36.8 Ω	1.90%

It is guaranteed that there's no contact between silver-coated yarns in Sample 3 because, in a weaving structure in Figure 4.2, the silver-coated yarns are perfectly parallel with each other. However, Figure 4.9 shows that the total resistance of Sample 3 still all the way went down during heating in the same way as Sample 1 and Sample 2. It is also presented in Table 4.1 that the resistance of a single silver coated yarn decreases after heating. These two results together prove that R_{yarns} decreases with temperature increase and R_{yarns} should be a significant factor that is responsible for the total resistance decrease during heating. It is against our common sense because the resistivity of the silver increase with temperature increase. This result can be explained that there exist local crimps along the conductive yarns during heating and higher temperature generates more crimples. Consequently, crimps along the yarns lead to short circuits and makes R_{yarns} decrease. Table 4.1 also indicates that the resistance of Yarn A is more sensitive to temperature change than the resistance of Yarn B. It is reasonable because Yarn A is a monofilament and is much easier to be crimped when temperature changes.

So far, if how the contact resistance $R_{contact}$ of the conductive knitted fabric will change during heating is still unknown. We combine the previous data together into one table for further analyzing the contact resistance. Resistances of Sample 1, 2, 3 and yarn A, B before heating and after heating are listed in

Table 4.2.

TABLE 4.2. Resistances of Sample1, 2, 3 and yarn A, B before and after heating

		Resistance after heating and cooling down	Resistance before heating	Rate of change
Sample (10v)	1	22.056 Ω	25.445 Ω	13.32%
Sample (15v)	1	20.983 Ω	27.372 Ω	23.34%
Sample (10v)	2	20.345 Ω	24.876 Ω	18.21%
Sample (15v)	2	17.969 Ω	25.641 Ω	29.92%
Sample (15v)	3	42.737 Ω	45.455 Ω	5.98%
Yarn (60°C)	A	514.0 Ω~822.2 Ω	569.4 Ω~878.0 Ω	6.36%~9.73%

Yarn (60°C)	B	15.1 Ω~36.1 Ω	15.2 Ω~36.8 Ω	0.66%~3.26%

Because the resistivity of Yarn A is much larger than the resistivity of Yarn B, the contribution of total resistance of conductive knitted fabric from Yarn B is subtle and can be neglected. Table 4.2 presents that the range of resistance change of Yarn A is close to the range of Sample 3. But the range of resistance change of Yarn A and Sample A is much smaller than the range of Sample 1, 2. Thus It can be deducted that the change of contract resistance did contribute to the total resistance decrease during heating. It can be explained that, when temperature increases, the thermal expansion from the wool fibers lead to tight contact between conductive yarns. In conclusion, the length-related resistance of silver-coated yarns R_{yarns} and the contact resistance $R_{contact}$ between silver-coated yarns are both sensitive to the temperature and they together makes the whole resistance of conductive knitted fabric decrease during heating.

4.3.5 Establishment of model to predict the stable-state temperature

When a voltage is applied to a conductive knitted fabric, electrical current flows along the conductive yarns and the heat is generated. The electric power is transferred to heat energy. The electric power input can be expressed as,

$$\frac{dQ_{in}}{dt} = \frac{U^2}{R(t)} \tag{4.1}$$

Where U is the applied voltage, R is the electrical resistance of the conductive

knitted fabric at time t, and dQ_{in} is the amount of heat generated from the fabric at the time interval of dt. Heat is also dissipated from the fabric to the surrounding environment. The heat dissipation rate from the fabric to environment is proportional to the temperature gradient $T(t) - T_0$,

$$\frac{dQ_{dis}}{dt} = \alpha * (\ T(t) - T_0) \tag{4.2}$$

Where α is the thermal diffusivity, $T(t)$ is the temperature of the fabric at time t and T_0 is the temperature of the surrounding environment. Equation (4.2) indicates that, at the initial time of heating, the heat dissipation level is low because the temperature of the fabric is not high enough. Consequently, the electric power input $\frac{dQ_{in}}{dt}$ is bigger than the heat loss $\frac{dQ_{dis}}{dt}$ and the net energy remaining in the fabric makes its temperature increase. The temperature of the fabric will not stop increasing until the power input $\frac{dQ_{in}}{dt}$ equals to the heat loss $\frac{dQ_{dis}}{dt}$, where the fabric reaches a steady state and its resistance is stable,

$$\mathrm{T(t)} \rightarrow \mathrm{T_s} \tag{4.3}$$

$$R(t) \rightarrow R_s \tag{4.4}$$

$$\frac{dQ_{in}}{dt} = \frac{dQ_{dis}}{dt} \tag{4.5}$$

By combining the above equations, we can obtain

$$\alpha * (\ T_s - T_0) = \frac{U^2}{R_s} \tag{4.6}$$

After rearranging this equation, the steady-state temperature T_s as a function of voltage U can be obtained,

$$T_s = T_0 + \frac{U^2}{\alpha * R_s} \tag{4.7}$$

If the resistance of the conductive knitted fabric is unchanged during the whole heating process, R_s will be a constant and the steady-state temperature can be obtained by Equation (4.7). And by using the Equation (4.7), the temperature of the thermal fabric can be predicted under a given voltage. However, according to the previous research, the resistance of the conductive knitted fabric will change with temperature change and it is related to temperature. Thus R_s is a function of T_s,

$$R_s = R_s(T_s)$$

Rearrange the Eq. (4.7) and move R_s to the left side of the equation, we obtain:

$$R_s(T_s) * (\ T_s - T_0) = \frac{U^2}{\alpha} \tag{4.8}$$

A solution $T_s = T_s(U)$ can be found to solve the Equation (4.8). Thus, when the resistance change is taken into consideration, the steady-state temperature of the conductive knitted fabric can also be calculated and predicted under a given voltage U, though the calculation process is more complicated. Because there is only one independent variable among *T, U* and *R*, The steady-state temperature of the knitted fabric R_s can also be regarded as a function of the applied voltage *U* instead of a function of T_s.

$$R_s = R_s(U)$$

In this way, the steady-state temperature under a voltage U can be easily obtained,

$$T_s(U) = T_0 + \frac{U^2}{\alpha * R_s(U)} \tag{4.9}$$

This solution is completely equivalent to the solution from Equation (4.8) but much easier to achieve. Hereafter, Equation (4.9) will be used to simulate the steady-state temperature instead because the calculation process is more straightforward and less complicated. Equation (4.9) indicates that the deviation of the predicted temperature T_s can be very large if the resistance of the fabric R_s sensitivity to the applied voltage is ignored. Thus the sensitivity of the conductive knitted fabric to the temperature or applied voltage determines the level of accuracy when predicting the achieved steady-state temperature.

According to Equation (4.9), the very first step to obtain the steady-state temperature of a conductive knitted fabric is to measure the resistance varying with applied voltage $R_S(U)$. In our calculation, we will take Sample 2 as a study case as the loop density of Sample 2 is closer to a regular knitted fabric in applications. Sample 2 was heated for 3600 seconds in each test under the applied voltage ranging from 5V to 15V (2V step between two tests). The fabric sample was heated for 3600 seconds so that the fabric can reach its steady-state and its temperature will be stable. The resistance of Sample 2 was measured and recorded when the temperature was stable. Thus the corresponding *R-U* curve and was presented in Figure 4.10. Similarly, the *T-U* curve (Figure 4.11) was obtained through a similar process, where Sample 2 were heated for 3600 seconds in each test under the applied voltage ranging from 5V to 18V (1V step between two tests). As mentioned before, morphologic change happens to conductive knitted fabric when it experiences heating. Thus before Sample 2 took the next test, it was left for 24 hours so that it can recover to its initial condition.

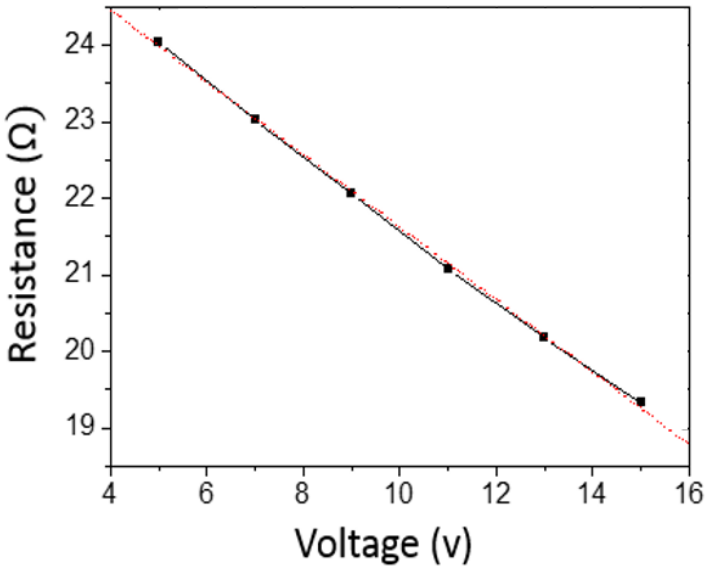

FIGURE 4.10. R vs. U curve of Sample 2 and the linear fitting of the data (dot line).

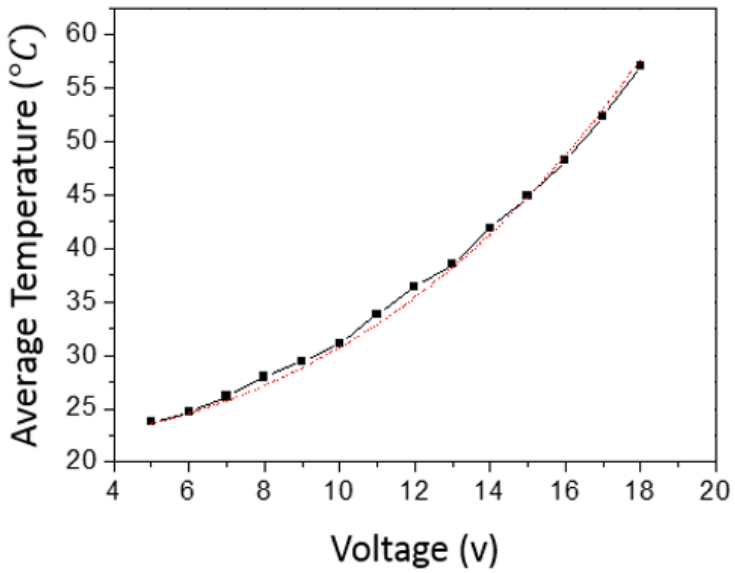

FIGURE 4.11. The measured (solid line) and fitted (dot line) temperature of Sample 2 as a function of voltage.

It can be observed in Figure 4.10 that there's a good linear relationship between the resistance and the applied voltage. Thus linear fitting is used to fit the relationship. The fitted curve y=26.35-0.47x was shown in Figure 4.10 (red line). The coefficient of determination- R^2 of 0.9995 indicates that there does exist a linear relationship between the steady-state resistance of the conductive knitted fabric and the applied voltage. Now the steady-state resistance $R_s(U)$ can be written as,

$$R = 26.35 - 0.47U \ \ (\Omega) \qquad (4.10)$$

Add it into Equation (4.9), we can obtain,

$$T_s = 21.5 + \frac{U^2}{\alpha*(26.35-0.47U)} \ (°C) \tag{4.11}$$

Equation (4.11) is used to fit the relationship between the steady-state temperature and the applied voltage. The fitting curve together with *T-U* curve were presented in Figure 4.11. The fitted thermal diffusivity α = 0.5176 (w/$°C$) is obtained and the fitting correlation coefficient is 0.9976. The correlation coefficient is very close to 1, which indicates that Equation (4.11) is a very suitable function to fit the *T-U* curve. Add $\alpha = 0.5176(\mathrm{w}/°C)$ into the equation, we obtain the final result,

$$T_s = 21.5 + \frac{U^2}{13.6-0.24U} \ (°C) \tag{4.12}$$

In Figure 4.11, the error of the fitting curve is within 1$°C$. Thus, this formula can perfectly fit the *T-U* curve and can be applied to predict the temperature of conductive knitted fabric. Furthermore, it proves a relationship like Equation (4.9) exist between the temperature and the applied voltage. Resistance change should not be ignored during heating or large error may happen. In Figure 4.12, it is shown that the error of the predicted temperature can be more than 10 $°C$

under an 18 V applied voltage if the resistance change is ignored. The actual temperature that the thermal textile can reach will be underestimated, which can lead to severe problems.

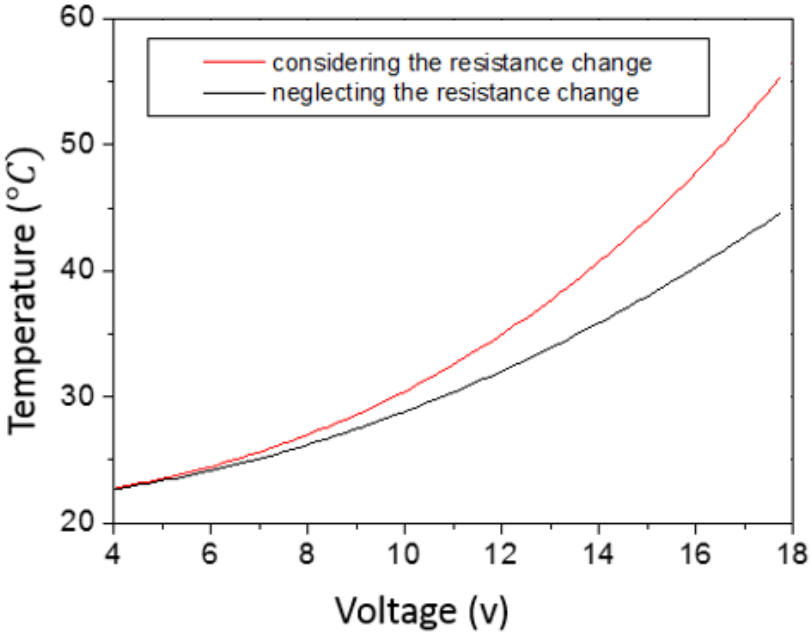

Figure 4.12. The temperatures of Sample 2 vs. applied voltage for two cases: (i) the resistance change is considered and (ii) ignored.

4.3.6 Summary

In conclusion, in this stage of research, not only the length-related conducting resistance of the conducting yarns but also the contact resistance between conducting yarns will play an essential role in the total electrical resistance of the conductive knitted fabric. Both types of resistance will decrease with increasing temperature. In conclusion, the total resistance of a conductive knitted fabric will decrease dramatically when the fabric is heated, and we must pay more attention to this characteristic of conductive knitted fabrics in future

applications. A linear relationship is achieved between the stable-state resistance of the fabric and the voltage applied, and a theoretical model is established to precisely predict the stable-state temperature of a conductive knitted fabric.

4.4 Conductive knitted fabrics of different sizes

4.4.1 Introduction

On the market, different sizes of conductive knitted fabrics are required to meet the needs of different applications. Temperature control of a conductive knitted fabric is related to a number of parameters, such as electrical resistance and thermal diffusivity. However, these parameters of conductive knitted fabrics are closely related to the size of the fabric. Therefore, the theoretical model proposed in 4.1 should be modified and generalized to take into consideration the size of the fabric.

4.4.2 Theoretical

The research work in 4.1 tells that the resistance of a conductive knitted fabric in heating will decrease and then tend to be stable after long-time heating. And the steady-state resistance of the fabric can be regarded as a function of temperature. In order to find out this function, relationship between the steady-state resistance and the applied voltage should be obtained, as we did in 4.1. In our previous research work, a linear relationship between the steady-state resistance and the applied voltage is found for the conductive knitted fabric in heating and thus the steady-state resistance of the conductive knitted fabric can be regarded as a linear function of applied voltage. The linear relationship between stable-state resistance of fabric and the voltage applied is a representation relationship. The relationship in the whole temperature range

would not be linear. But the temperature range of thermal fabrics in application is narrow (below 60 ° and the silver-coated yarns are not resistant to high temperature). A good fitting of relationship in that range is enough for research.

$$R_s(U) = R_0 - kU \tag{4.13}$$

Or

$$U = \frac{R_0 - R_s(U)}{k} \tag{4.13}$$

Where $R_s(U)$ is the resistance of the conductive knitted fabric in steady-state, R_0 is the initial resistance of the fabric and k is the slop, which measures the resistance decrease speed during heating. When Equation (4.13) is added into Equation (4.9), the variable U is removed,

$$R_s = R_0 + \frac{1}{2}\ \alpha k^2(T_s - T_0) - \frac{1}{2}\sqrt{4R_0\alpha k^2(T_s - T_0) + \alpha^2 k^4 (T_s - T_0)^2} \ldots (4.14)$$

Formula (4.14) presents how the steady-state temperature T_s can change the steady-state resistance for a conductive knitted fabric. Now $\frac{R_s}{R_0}$ will be adopted to represent the percentage change of the resistance when temperature changes,

$$\frac{R_s}{R_0} = 1 + \frac{1}{2}\frac{\alpha k^2}{R_0}(T_s - T_0) - \frac{1}{2}\sqrt{4\frac{\alpha k^2}{R_0}(T_s - T_0) + \frac{\alpha^2 k^4}{{R_0}^2}(T_s - T_0)^2} \quad \text{.....(4.15)}$$

Because $\frac{R_s}{R_0}$ is the percentage change of the resistance based on the initial resistance for the conductive knitted fabric whose temperature is T_s, $\frac{R_s}{R_0}$ should be irrelevant to the initial resistance R_0. Thus the term at the right side of Formula (4.15) should be irrelevant to R_0, which means that $\frac{\alpha k^2}{R_0}$ should be irrelevant to R_0. Therefore, we can conclude that,

$$\frac{\alpha k^2}{R_0} = \beta^2 \qquad (4.16)$$

Where β is a constant, which is irrelevant to either the initial resistance of the fabric or the size of the fabric. β is a parameter that is only related to the property of the knitted conductive fabric. Only fabrics with different structures or different conductive materials have different values of β. When the loop density of the conductive knitted fabric is unchanged, the value of β should be unchanged. Thus Equation (4.16) becomes,

$$\frac{R_s}{R_0} = 1 + \frac{1}{2}\beta^2(T_s - T_0) - \frac{1}{2}\sqrt{4\beta^2(T_s - T_0) + \beta^4(T_s - T_0)^2} \quad \text{.....(4.17)}$$

From Equation (4.17), we can find out the meaning of the parameter β. The value of β measures how much percentage change happens to conductive knitted fabric when temperature changes. Equation (4.17) can be simplified by

approximate treatment,

$$\frac{R_s}{R_0} = 1 - \beta * \sqrt{(T_s - T_0)} \text{.....(4.18)}$$

Equation (4.18) can also be used in addition to Equation (4.17) when the temperature change is not that large. According to Equation (4.16), the resistance decrease speed k can be obtained,

$$k = \beta \sqrt{\frac{R_0}{\alpha}} \quad (4.19)$$

Now we can combine Equation (4.9), (4.13), (4.19) together and solve the steady-state temperature. The steady-state temperature of the conductive knitted fabric varying with the applied voltage can be obtained,

$$T_s(U) = T_0 + \frac{U^2}{\alpha * R_0 - U * \beta * \sqrt{\alpha * R_0}} \text{.....(4.20)}$$

This formula removes the temperature decrease speed k and adopt a more intrinsic parameter β. With the help of this formula, we can easily predict what temperature a conductive knitted fabric can achieve, when the applied voltage U, the initial resistance R_0, the thermal diffusivity α and the β value of this kind of fabrics are obtained. β value of the fabric can be summarized and obtained by testing a series of this kind of fabrics (same knitting structure and

loop density but different sizes). In the above theoretical calculation process, Equation (4.19) is the key formula and it illustrates that the resistance decrease speed of a conductive knitted fabric during heating is not only determined by the initial resistance but also by its thermal diffusivity.

4.4.3 Methodology and experimental design

In section 4.3, Sample 2 is used as the case study because its loop density is close to a regular knitting textile in applications. Thus in this stage of study, the same loop density will be applied to the fabric samples. Stoll M1 programming system can set knitting parameters and offer various knitting fabrics for testing. We selected five different sizes ($100\ \text{courses} \times 100\ \text{wales}$, $100\ \text{courses} \times 110\ \text{wales}$, $100\ \text{courses} \times 120\ \text{wales}$, $110\ \text{courses} \times 100\ \text{wales}$, $120\ \text{courses} \times 100\ \text{wales}$) for the conductive knitted fabric and three samples per each size were prepared. The loop density of these fabric samples were unified (7 courses/cm and 8 wales/cm) to make sure that they have the same β value.

The fabric samples were heated by the DC power supply under the voltage from 5V to 17V (2V step between two testing). The fabric sample were heated for 3600 seconds in each test to make sure that the temperature of the fabric was stable enough. And at the same time, both the resistance and temperature of the knitted fabric in steady-state were measure and recorded. The *R-U* curve and *T-U* curve for each sample can be drawn base on the obtained data. Each of the fifteen samples were treated under the same testing procedure and the *R-U* curve and *T-U* curve were well obtained.

4.4.4 Discussion of β value

In this section, we will measure the β value of the fabric samples and discuss the correctness of Equation (4.16). According to Equation (4.16), values of k, R_0, and α should be obtained first before calculating the value of β. Thus we

should obtain the *R-U* curve and *T-U* curve for each sample and then use fitting method to obtain the values of k, R_0, and α. We will take the fabric sample with size of 100 courses $\times 100$ wales as the study case in the following process. The *R-U* curve and *T-U* curve for this fabric sample are presented in Figure 4.13, 4.114.

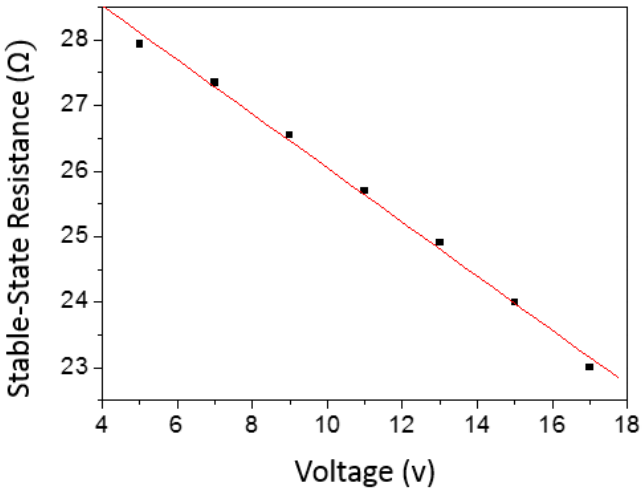

FIGURE 4.13. Stable-state resistance R_s vs. U curve of the sample(100 courses $\times 100$ wales) and the linear fitting of the data (red line).

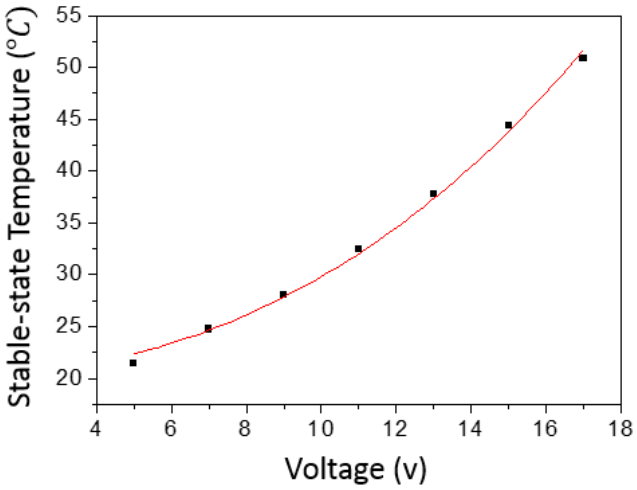

FIGURE 4.14. The measured and fitted (red line) temperature of the sample (100 courses $\times 100$ wales) as a function of voltage.

The fitting method is the same as used in Section 4.1. The linear fitting is adopted to fit the relationship between the resistance and the applied voltage and the fitting curve is y=32.06-0.38x. The fitting correlation coefficient of 0.998 is achieved, which indicates a good fitting result. There's a good linear relationship between the steady-state resistance and the applied voltage for the fabric sample and the resistance varying with applied voltage is,

$$R_s = 32.06 - 0.38U \ \ (\Omega) \tag{4.21}$$

In the same way, add Equation (4.21) into Equation (4.9) and we obtain,

$$T_s = 21.5 + \frac{U^2}{\alpha*(32.06-0.38U)} \ \ (°C) \tag{4.22}$$

Equation (4.22) is used to fit the relationship between the steady-state temperature and the applied voltage, which is also known as *T-U* curve. The fitting curve together with *T-U* curve were presented in Figure 4.14. The fitted thermal diffusivity α = 0.3891 (w/$°C$) is obtained and the fitting correlation coefficient is 0.997. The achieve correlation coefficient is very close to 1, which indicates a very good fitting result. Thus Equation (4.22) can be used to simulate the temperature of this fabric sample perfectly. With the obtained $R_0 = 32.06 \ (\Omega)$, $k = 0.380 \ (\Omega/V)$ and $\alpha = 0.389$(w/$°C$) , $\beta = 4.186 \times 10^{-2}(°C^{-0.5})$ for the fabric sample can be achieved by Equation (4.16). Other 14 fabric samples were also processed in the sample procedure as shown above and their data were recorded in Table 4.3 and their β values were calculated

and presented in Figure 4.15.

TABLE 4.3. Four parameters of all the samples

Size(cm)		$R_0(\Omega)$	$k(\Omega/V)$	α(w/°C)	$\beta(°C^{-0.5})$
100 × 100	s1	32.05812	0.37999	0.38906	4.186×10^{-2}
	s2	35.23581	0.37330	0.42720	4.110×10^{-2}
	s3	30.17468	0.41283	0.38337	4.653×10^{-2}
100 × 110	s1	33.49344	0.42242	0.43360	4.806×10^{-2}
	s2	31.44610	0.42737	0.42049	4.942×10^{-2}
	s3	34.89066	0.36146	0.39156	3.829×10^{-2}
100 × 120	s1	33.94293	0.41162	0.43804	4.676×10^{-2}
	s2	38.38969	0.31752	0.41870	3.316×10^{-2}
	s3	40.62800	0.31892	0.39665	3.151×10^{-2}
	s1	26.32729	0.36118	0.39622	4.431×10^{-2}

110	× 100 s2	28.18211	0.45510	0.40951	5.486×10^{-2}
	s3	28.01121	0.37367	0.41285	4.536×10^{-2}
	s1	25.75316	0.35083	0.42844	4.525×10^{-2}
120	× 100 s2	24.77041	0.37443	0.42873	4.926×10^{-2}
	s3	24.00011	0.37187	0.46732	5.189×10^{-2}

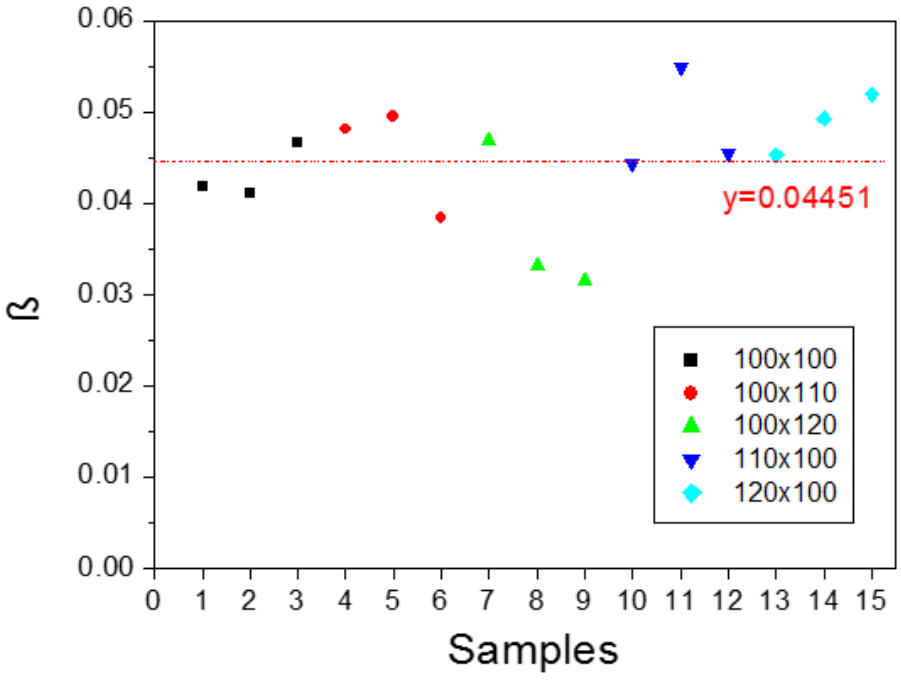

FIGURE 4.15. Distribution of the β values of these fifteen fabric samples and their mean (red dot).

It can be observed from Figure 4.15 that the β values of the fifteen samples are distributed around their mean value $\beta = 4.451 \times 10^{-2}$ ($°C^{-0.5}$). However, the points in Figure 4.15 fluctuate greatly to some degree. It is mentioned before in the theoretical section that β value is irrelevant to the size of the fabric but determined by the loop density. As the loop densities of the fifteen samples were unified, they should have the same β value and the distribution of the β points in Figure 4.15 should be a horizontal line. The actual situation can be different from the theory, because the variation in samples is not considered in theory. Especially, in the situation of textile industry, it is more common. As presented in Figure 4.15, it seems that the points go without any pattern. But when the attention is paid to the overall trend of the points, it can be found that the points are all the way around a certain value (mean value), even though the variation of the distribution if a little large. Therefore, we can conclude that the data obtained from the testing did accord with what the theory predicted. The point distribution is not that convergent for the following reasons. First and foremost, the physical morphology of the fabric sample cannot fully recover to the same initial point, which was already discussed in Section 4.3. It means that, even for one sample, the β value obtained from today's testing cannot be the same as that obtained from tomorrow's testing. Because, when the today's initial resistance is different with tomorrow's initial resistance, their calculated β values must be different. In other words, the β value is determined by the initial condition of the fabric sample and can vary in different testing. The second reason is that the structures and parameters of these fifteen samples cannot be totally the same and may vary to some degree. Though they were fabricated by the same machine and same process, it is impossible to make totally identical fabrics. Especially in textile industry, the variation between samples is considerable large. In addition to the above two reasons, error in every measuring step cannot be avoided. In conclusion, the big fluctuation of the data in Figure 4.15 is reasonable and can be explained from two aspects: limitation of quality control and morphologic change of textile materials. According to this situation, measurement of β value can be conducted by the statistical method. Enough samples should be prepared and tested to obtain a mean value to

estimate the β value.

4.4.5 Estimation of initial resistance

According to Equation (4.20), study of the initial resistance is necessary to calculate the steady-state temperature of conductive knitted fabrics. Fortunately, the calculation of the resistance of the conductive knitted fabric has already been studied before, which has been discussed in Chapter Two. The initial resistance that we are discussing in this section is the static resistance in Chapter Two. Equation (2.7) in Chapter Two illustrates that the resistance of a conductive knitted fabric is positively correlated with the wale number N and negatively correlated with the course number M. In general, the course number M and wale number N of a knitted fabric can be big enough (M,N ~100 in our experiment),

$$\mathrm{M}, \mathrm{N} \gg 1 \tag{4.23}$$

In this situation, Equation (2.7) can be simplified through removing the edge effect. Thus we can obtain the static resistance formula in a compact form,

$$R_0 = \rho \frac{N}{M} \tag{4.24}$$

Where ρ is the resistivity of the fabric, which measures the resistance per unit area of the fabric. Formula (4.24) can be regarded as the initial resistance R_0 in Equation (4.20). We used the Formula (4.24) to fit the initial resistance of the fifteen sample and the fitting result is shown in Figure 4.16.The fitted resistivity of the samples is $\rho = 30.94\Omega$ and correlation coefficient 0.8306 is achieved.

The correlation coefficient of 0.8306 and the data distribution in Figure 4.16 together indicate that the variation of the initial resistance is not small to some degree. As mentioned before in discussion of β value, two reasons lead to big variation. The first reason is that the measure initial resistance can be different in two tests for the same fabric due to the morphologic change after heating. The second reason is that inconsistency always happens to two textile products made by the same machine and same fabrication procedure, which is inevitable. Fortunately, the overall trend of the data in Figure 4.16 is consistent with Formula (4.24). Thus Formula (4.24) can be successfully applied to represent the initial resistance of the samples in our testing, where the resistivity is $\rho = 30.94\Omega$.

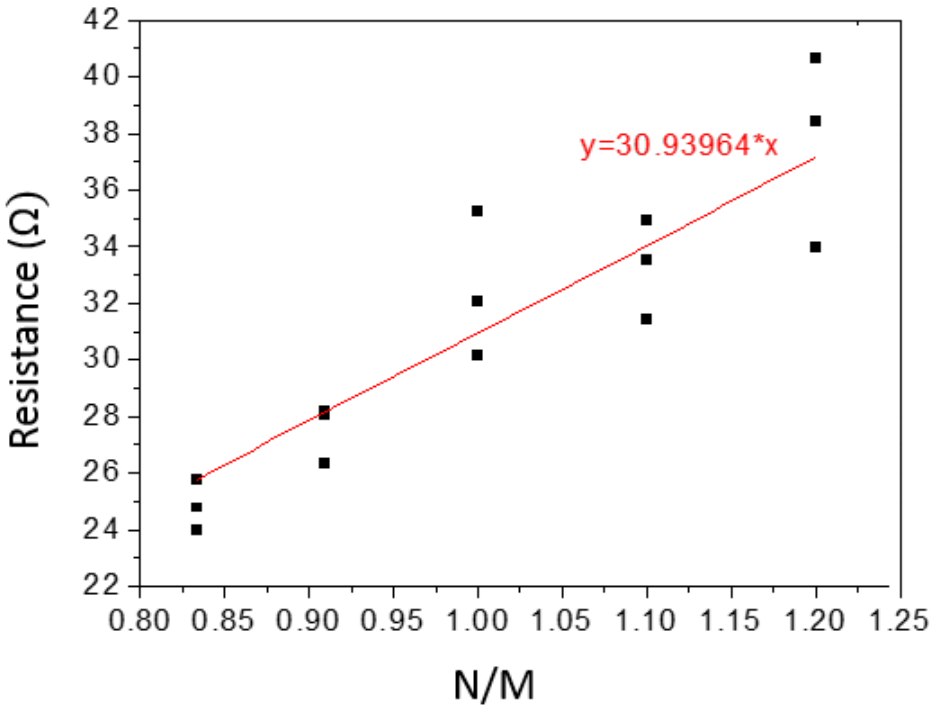

FIGURE 4.16. Initial resistance of these fifteen samples and the fitting of the data (red line).

4.4.6 Study of thermal diffusivity

In Section 4.4.4 and 4.4.5, the β value and the initial resistance R_0 were already discussed. According to Equation (4.20), the remaining parameter that should be studied is the thermal diffusivity of the fabric. The thermal diffusivity of a material measures its ability to conduct heat and in our test it measures how fast the heat can dissipated from the hot side (thermal fabric) to the cold side (surrounding environment). Generally speaking, the thermal diffusivity is proportional to the cross-sectional area of the heat flux. In our test, the cross-sectional area if the area of conductive knitted fabric. Because the only difference between the fabric samples are the course number M and wale number N, these fifteen fabrics can be regarded as the same material and have the same diffusivity density. We use the value $\mathrm{M} * \mathrm{N}$ as the area of the fabric,

$$\mathrm{S} = \mathrm{M} * \mathrm{N} \tag{4.25}$$

Thus the thermal diffusivity density or thermal diffusivity per unit area a can be obtained,

$$\mathrm{a} = \frac{\alpha}{S} = \frac{\alpha}{M*N} \tag{4.26}$$

Theoretically, the thermal diffusivity density of the fifteen samples should be unified as they have the same knitting structure and same loop density. The thermal diffusivity density or thermal diffusivity per unit area is presented in Figure 4.17,

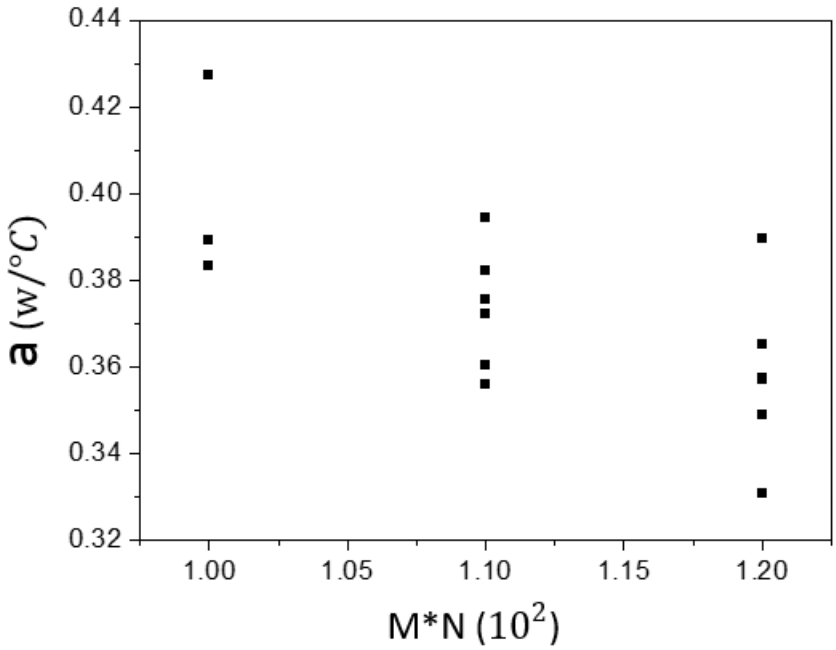

FIGURE 4.17. Thermal diffusivity per unit area of the fifteen samples

Figure 4.17 gives a totally different result. The thermal diffusivity per unit area in Figure 4.17 has a decrease trend when the area of the fabric increases, which is a big departure from the prediction that diffusivity densities of samples are the same. The reason behind this result is that the heat flux model is simplified (Figure 4.18). Theoretically, we assume that the heat flux is totally perpendicular to the thermal fabric and ignored the edge effect, which leads to limitation in applications. In actual situation of heating process, there must exist other heat flux model other than the one presented in Figure 4.18 (a). For example, there exist horizontal mode of heat flux at the edge of fabric as shown in Figure 4.18 (b). When the edge effect is taken into consideration, the calculation of the thermal diffusivity becomes complicated. We assume that the thermal diffusivity contributed by the edge effect is related to the perimeter of the fabric. In Figure 4.19, there are two thermal fabric with the same heating area. However, the shape of the heating area in the fabric on the right side gives it longer

perimeter and thus gives it more contact with the surrounding environment and thus the fabric on the right side has a higher thermal diffusivity. Therefore, the conclusion that the thermal diffusivity from edge effect is related to the perimeter is reasonable. Therefore, the total thermal diffusivity of a conductive knitted fabric in actual situation can be divided into two parts. One is proportional to the area of the fabric and the other one contributed by the edge effect is proportional to the perimeter of the heating area,

$$\alpha = \theta_1 * S + \theta_2 * P \tag{4.27}$$

Where S is the heating area of the fabric, P is the perimeter of the heating area, θ_1, θ_2 are the coefficients of S and P. Equation (4.27) may be not accurate enough but can already explain what happened in Figure 4.13. When the area of the fabric increases, the edge effect distributed on the unit area becomes smaller and consequently the thermal diffusivity per unit area decreases as shown in Figure 4.17. It is known that the area is square-related to the size of the fabric and the perimeter is linear-related to the size of the fabric. Thus when the size of the fabric is large enough, the second term in Equation (4.27) or the edge effect can be ignored compared with the first term. However, in our test, the fabric samples used is not that large enough. Now the calculation of the thermal conductivity of a fabric becomes rather complicated in an actual situation and judgment based on experience becomes important. Fortunately, it is found that the thermal diffusivities of these fifteen fabric samples are very close, even though their thermal diffusivity densities differ. The thermal diffusivities of fifteen thermal fabrics are presented in Table (4.3) in Section 4.4.4 and the mean value of $\alpha = 0.416\ (\mathrm{w}/^{\circ}C)$ was adopted in the following study and modelling.

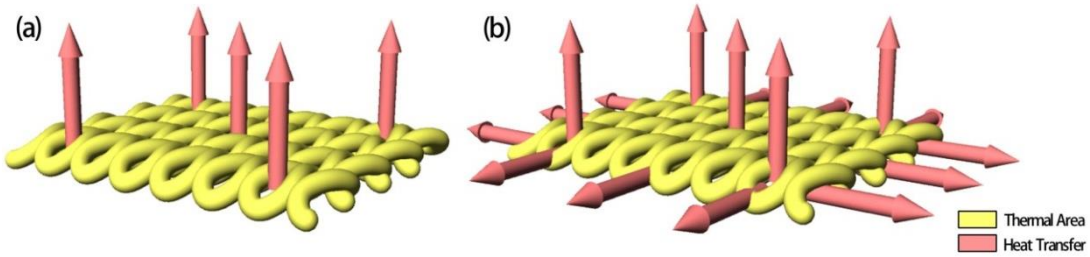

FIGURE 4.18 (a) Simplified thermal diffusion model which neglects the edge effect; (b) There exist other heat transfer mode at the edge of the fabric

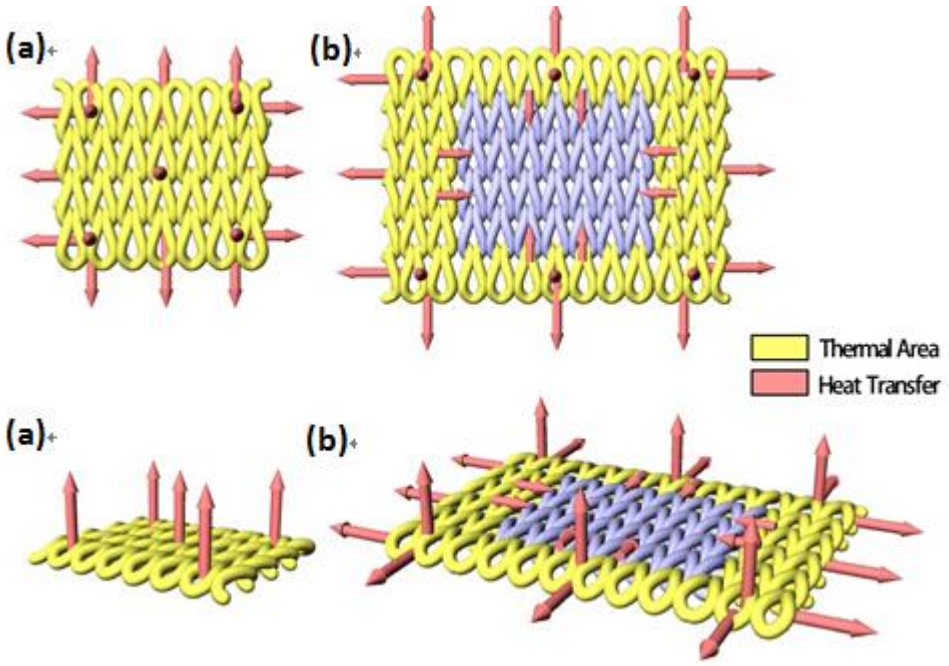

FIGURE 4.19. Two fabrics have the same area. The fabric in “ring” shape (b) on the right has much more contact with the surrounding environment

4.4.7 Temperature simulation for fabrics of different sizes

In Section 4.4.4, 4.4.5 and 4.4.6, the β value, initial resistance R_0 and thermal diffusivity α, which are the three important parameters in Equation (4.20), were already discussed and the calculation formula were also obtained. Thus in this section, we can simulate the steady-state temperature of the conductive knitted fabric samples based on the results obtained from Section 4.4.4, 4.4.5 and 4.4.6. The error between the simulation and experimental data will be evaluated. A good simulation of the theoretical model will indicate the correctness of Formula (4.20) and applicability of the heating process theory. Formula is our key point to predict what temperature a conductive knitted fabric can achieve. Thus Formula (4.20) will be used to simulate the steady-state of fifteen samples. As the β value, initial resistance R_0 and thermal diffusivity α were already studied, we can combine them together with formula (4.20) and finally obtain,

$$T_s(U) = T_0 + \frac{U^2}{\alpha*\rho*\frac{N}{M} - U*\beta*\sqrt{\alpha*\rho*\frac{N}{M}}} \quad \text{.....(4.28)}$$

Where $\alpha = 0.416$ $(\mathrm{w}/^{\circ}C)$ and $\rho = 30.94\Omega$. Formula (4.28) is the ultimate result for the conductive knitted fabric, which gives the relationship between the temperature of the fabric T_s, applied voltage U, course number M, wale number N. With the help of this formula, the course number and wale number can be adjusted to obtain the requested fabric. With the thermal diffusivity α and initial resistivity ρ known, Formula (4.28) becomes,

$$T_s(U) = T_0 + \frac{U^2}{12.87*\frac{N}{M} - 0.16*U*\sqrt{\frac{N}{M}}} \quad \text{..... .....(4.29)}$$

Now Formula (4.29) is used to fit the steady-state temperature of the fifteen fabric samples. The *T-U* curve together with the fitting curve are presented in Figure 4.20. Figure 4.20 shows a satisfactory fitting result, which indicates the applicability of Formula (4.20) and (4.28) and proves the correctness of the generalized model for fabric in different sizes. However, we can still find some deviation in the fitting results, especially the one in Figure 4.20 (d). A significant deviation of the actual result from the theoretical modeling sometimes can happen just like Figure 4.20(d) for two reasons, which were already mentioned before. Firstly, due to the irreversible morphologic change, the parameters of the same sample such as the initial resistance can be different in two tests to some degree. Secondly, it is impossible to obtain two exactly consistent fabric samples made by the same machine and made from the same fabrication process.

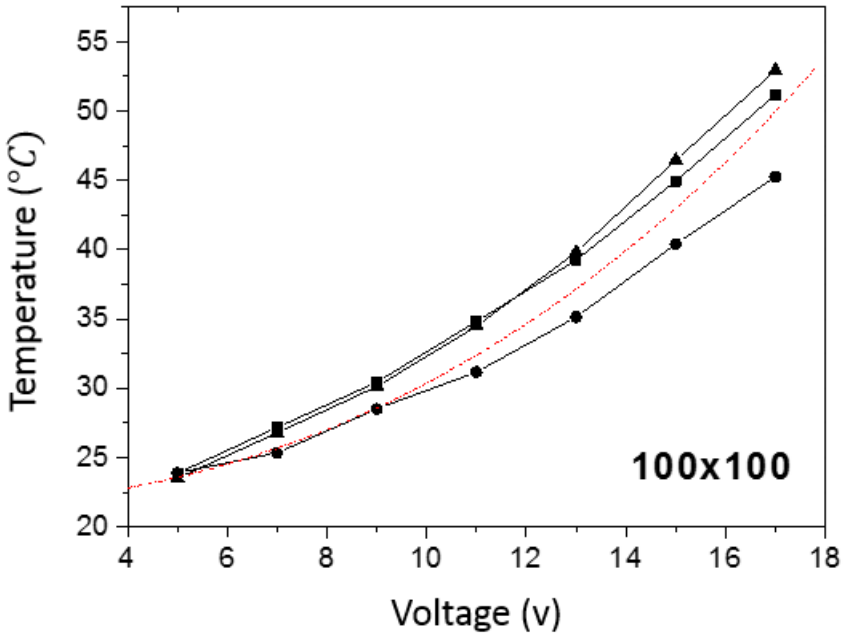

(a)

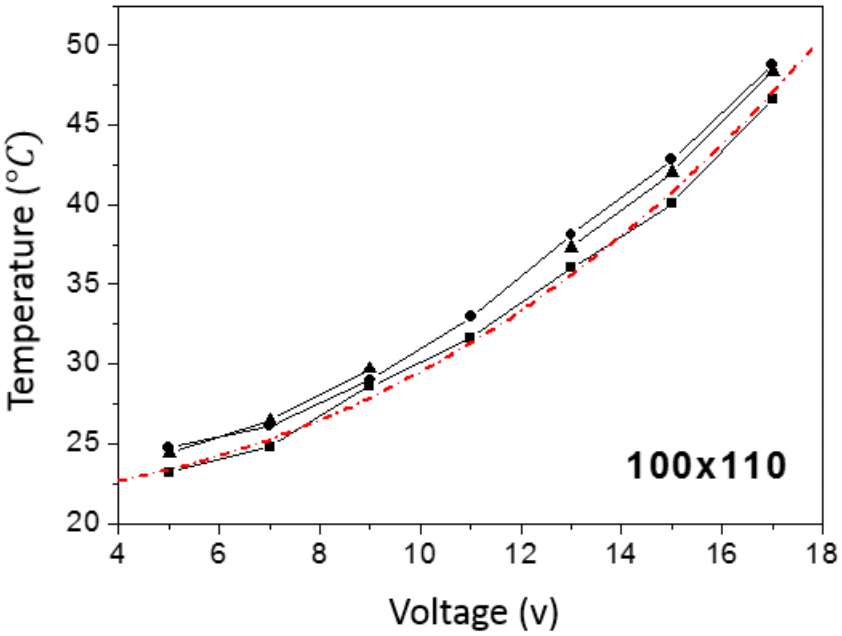
Temperature (°C)
Voltage (v)
100x110
50
45
40
35
30
25
20
4
6
8
10
12
14
16
18

(b)

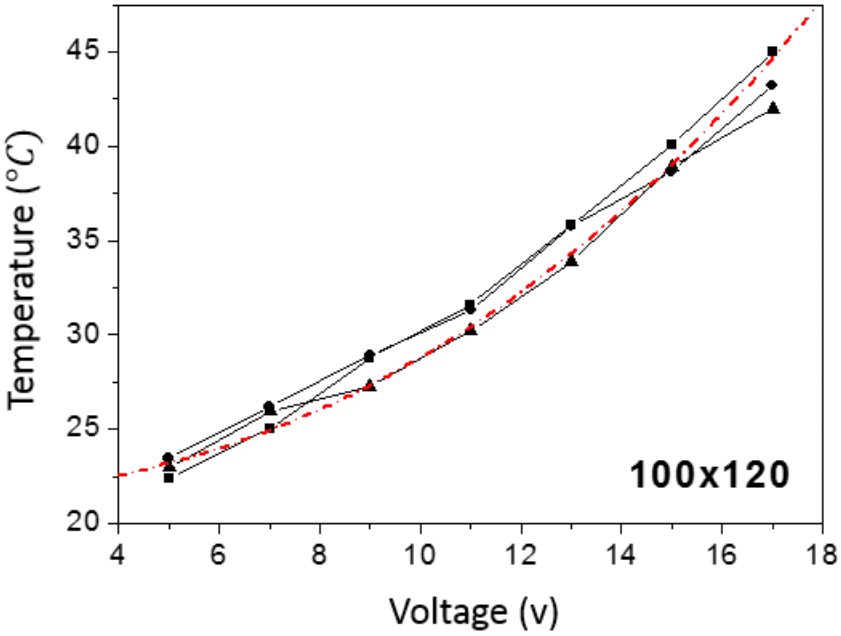
Temperature (°C)
Voltage (v)
100x120
45
40
35
30
25
20
4
6
8
10
12
14
16
18

(c)

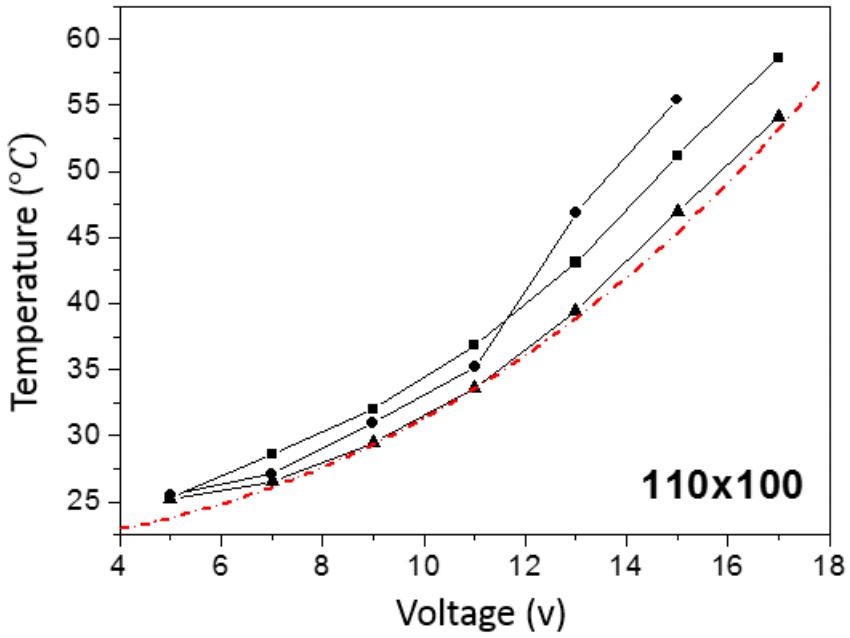

(d)

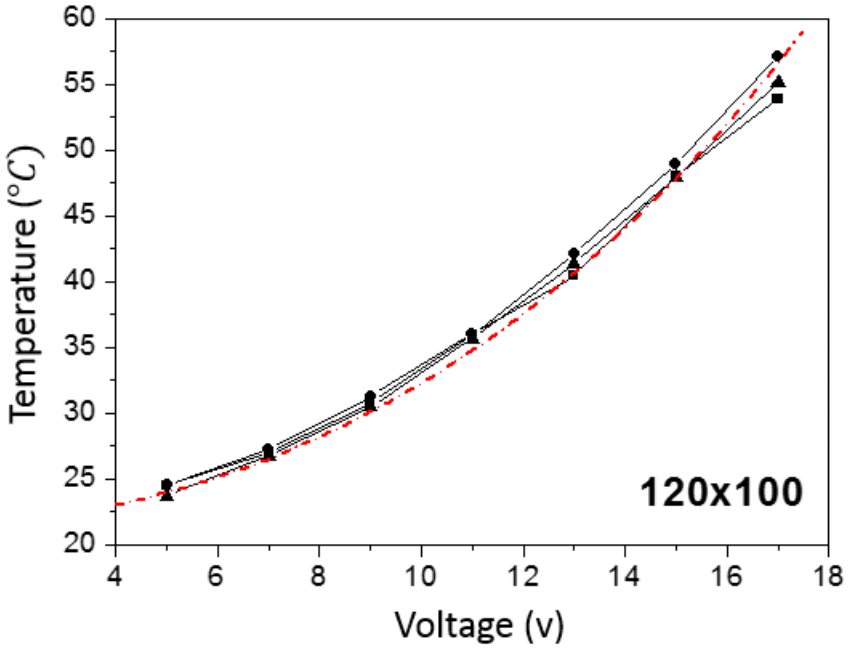

(e)

FIGURE 4.20. The comparison between the experimental $T_s(U)$ curves and simulated ones of the fifteen samples knitted in five different sizes.

4.4.8 Summary

In conclusion, verification of a generalized theoretical model for conductive knitted fabrics of different sizes and identification of the parameters of the fabrics was conducted in Section 4.4. The satisfactory simulation result indicates that the theoretical model can be used for temperature prediction or temperature control of conductive knitted fabrics in future applications. In addition, great deviation may occur mainly due to two unavoidable reason: limitation of quality control in textile industry and morphologic change of textile materials. We should pay attention to such deviations.

4.5 Influence of airflow on thermal fabrics

4.5.1 Introduction

In Sections 4.3 and 4.4, the thermal behaviour of thermal functional fabric was studied, and the parameters that are related to the thermal behaviour were also explored. However, some external factors or environmental factors have never been taken into consideration. When a thermal functional fabric is in use, the surrounding environmental conditions will certainly influence its functions. The surrounding environment also plays an important role when the thermal fabric is attempting to achieve a certain temperature. Undoubtedly, the airflow or wind around a thermal fabric should be one of the most important environmental factors. The airflow can greatly influence the heating process of thermal fabrics. It is obvious that stronger airflow (better ventilation) leads to faster heat loss from a fabric and results in a lower achieved temperature. When a thermal fabric is in a ventilated environment, the influence of the airflow should be taken into consideration, or the accuracy of the temperature control will be decreased. Because precise temperature control is the key to thermal fabrics, there is a demand for exploring the influence of airflow or wind on thermal fabrics during

heating. The research carried out is meaningful for the use of thermal fabrics when a ventilated environment cannot be avoided.

4.5.2 Theoretical

The heat transfer theory of heat conduction and heat convention has been explored in Physics. However, there's still a demand to investigate the heat transfer process on a textile base for two reasons. Firstly, there exist heat conduction and heat convention in the textile base and the theoretical calculation behind is very complicated. It is not feasible to apply the over-complicated theory into an actual situation of a thermal fabric in heating and it is impossible to process the simulation. Thus a more compact model is needed to analyze the heat transfer process in thermal textiles which is in a ventilated environment. Secondly, the actual situation may be different for a textile based material because of the unique properties of textiles. The structure of textiles can have unexpected influence on the surrounding airflow such as air transmission and air reflection, which will complicate the heat transmission and heat reflection. Thus the previous theory may not be applicable in the thermal textiles. In our study, theoretical analysis combined with experimental verification will be carried out to investigate the influence of the surrounding airflow on the thermal textiles.

In addition to the strength of the airflow, its flow direction is also required to be taken into consideration. It is highly possible that the flow direction of the airflow plays an important role and different flow directions can lead to different achieved temperatures.

Heat transfer is a process of heat energy transfer between physical systems (generally from hot system to cold system). The heat transfer process is always driven by temperature difference, which is also known as temperature gradient. Thus the heat transfer process will continue until all the involved systems reach

the same temperature and the thermal equilibrium is achieved. There're three modes of heat transfer: heat conduction, convective heat transfer and radiation. In thermal fabrics, radiation is subtle and can be ignored. Thus we only consider the heat conduction process and convective heat transfer process in thermal fabrics. Especially, the convective heat transfer plays a more important role in heat transfer in thermal fabrics because fabric and air are both weak heat conductors and heat conduction in thermal fabrics can be neglected to some degree.

Heat conduction theory tells that the heat transfer rate in a material is proportional to the temperature gradient in the material. The temperature gradient refers to the temperature difference between the thermal fabric and its surrounding environment. Thus the heat flux from the fabric to the surrounding environment $\frac{dQ_{out}}{dt}$ is proportional to the difference between the temperature of the fabric T and the temperature of its surroundings environment T_0,

$$\frac{dQ_{out}}{dt} = \lambda * (T - T_0) \tag{4.30}$$

where λ is the thermal conductivity contributed by heat conduction and λ is related to the thermal conductivity of thermal fabric and the air in it. It is known that both the textile and air are bad heat conductors and thus the thermal conductivity contributed by heat conduction is low. In this situation, the heat conduction process can be ignored and the convective heat transfer dominates the whole heat transfer process. The mechanism of convective heat transfer is totally different from the heat conduction. The heat flux of convective heat transfer is driven by air flux, which is much more complicated. Theoretically, the process of convective heat transfer is achieved when the hot object is moved to a cold system. Thus the convective heat transfer in thermal fabric is achieved by transferring the air from the fabric to the surrounding environment.

Consequently, the heat flux $\frac{dQ_{out}}{dt}$ is proportional to the air flow rate and the heat capacity of air,

$$\frac{dQ_{out}}{dt} = A * v * \rho * c * (T - T_0) \tag{4.31}$$

where $\frac{dQ}{dt}$ is the heat flux rate, A is the cross-sectional area of the flow, v is the air flow rate or wind speed, ρ is the density of air, and c is the heat capacity of air. As mentioned before, the direction of airflow can also influence the heat transfer process in thermal fabric. We assume that the air above the fabric flows away from the fabric at a rate v regardless of whatever direction the air flows across the fabric. The the thermal conductivity contributed by the convective heat transfer process is also irrelevant to the airflow direction,

$$\lambda' = A * v * \rho * c \tag{4.32}$$

Thus the total thermal conductivity of the thermal fabric can be obtained,

$$\lambda_{total} = \lambda + A * v * \rho * c \tag{4.33}$$

Where the first term is from the heat conduction process and the second term is from the convective heat transfer process. In general, the first term is much smaller than the second term and thus can be ignored. Formula (4.33) is just a result of the assumption and it remains to be verified. According to (4.33), the total thermal conductivity of a thermal fabric in ventilated environment is proportional to the airflow rate v regardless of its flow direction,

$$\lambda_{total} \sim v \tag{4.34}$$

In the following study, the influence of the airflow rate and airflow direction on the thermal conductivity of thermal fabrics will be investigated and the correctness of Equation (4.34) will be explored.

It should be mentioned that the thermal conductivity or thermal resistance of the fabric in this thesis may be a little different from the regular "thermal conductivity" of a material. The thermal conductivity/resistance here is the total thermal conductivity/resistance of the fabric regardless of its area or thickness. It only scale the fabric's ability to conduct heat and thus its unit is w/$°C$ instead of w/$(\mathrm{m} * °C)$.

4.5.3 Methodology and experimental design

Conductive fabric with weaving structure was selected as the thermal fabric in the following tests because the woven fabric is more stable and uniform in resistance distribution. The finished conductive woven fabric was 4.8 inches x 5.9 inches in size while its weft and warp densities were 30 picks/inch and 40 ends/inch respectively as shown in Figure 4.21.

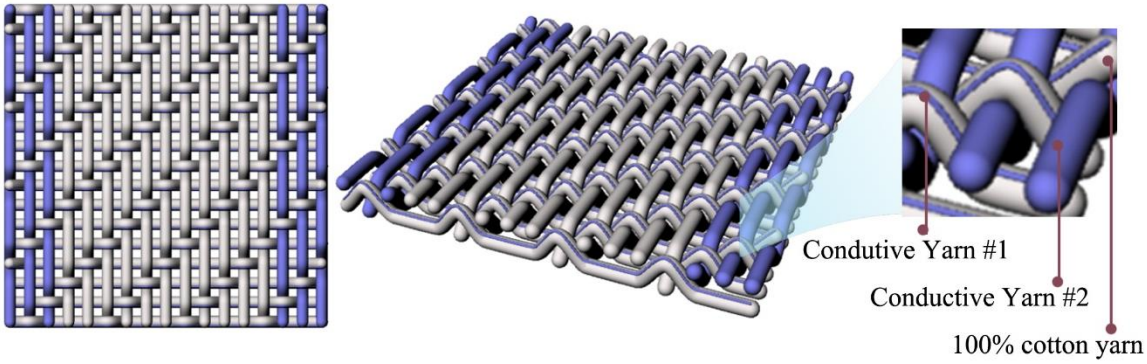

Figure 4.21. 3D model of fabricated structure of conductive woven fabric and arrangement of conductive yarns

The thermal fabric was heated by the DC power supply and the thermometer sensors were prepared to collect the temperature data of the fabric, which is just the same process as in Section 4.3 and 4.4. An electrical fan, which can adjust

its working wind speed, was used to provide stable airflow around the thermal fabric. And at the same time, a wind anemometer was ready to record the wind speed around the fabric. The wind speed was measured for five times in one test and averaged to reduce the error. The whole testing systems is shown in Figure 4.22.

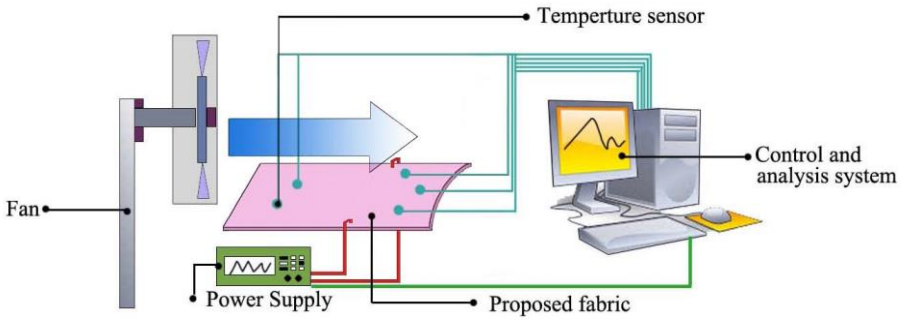

Figure 4.22. Testing equipment and control and analysis system

In this section, we aim to find out the relationship between the thermal conductivity of the thermal fabric and the surround airflow. Influence of both the airflow rate and the flow direction will be taken into consideration. Thus the thermal conductivity of the thermal fabric should be obtained when airflows of different wind speed and different direction are applied. We aim to find out how the airflow rate/wind speed and flow direction can influence the thermal conductivity of the fabric. In order to obtain the thermal conductivity of the thermal fabric, according to Equation (4.30), $\frac{dQ_{out}}{dt}$ and $T - T_0$ should be measured. When the thermal fabric achieve an equilibrium state, $\frac{dQ_{out}}{dt}$ equals to the input electric power,

$$\frac{dQ_{out}}{dt} = P_{in} \tag{4.35}$$

Thus with Euqation (4.30), we have the following relationship,

$$P_{in} = \lambda * (T - T_0) \tag{4.36}$$

Therefore, the thermal conductivity of the fabric can achieved by fitting the relationship between the input power electricity and the temperature difference $T - T_0$. Thus the temperature difference $T - T_0$ under different input power should be measured for the further fitting process.

4.5.4 Influence of airflow on thermal conductivity

According Equation (4.36), the temperature difference $T - T_0$ will be measured under different input electric power. The DC power supply was used to provide different power to heat the thermal fabric and the thermal fabric was heated for 1800 seconds to achieve thermal equilibrium in each test. The conductive knitted fabric in previous research was heated for 3600 seconds because it was found that it takes longer for conductive knitted fabric to reach equilibrium state. The equilibrium temperatures under different power were recorded for further fitting. In addition, the airflow rate around the thermal fabric was also measured and recorded.

In the first step of this section of research, we will test the thermal fabric without airflow and thus the fan was turned off. Our lab environment is poor-ventilated to ensure the airflow around the fabric can be neglected. Furthermore, the wind anemometer showing 0 (m/s) of the airflow rate again guaranteed the poor-ventilated environment. Three appropriate output powers of the DC power supply were set to heat the thermal fabric and the corresponding obtained temperature was recorded. The temperature difference between the fabric and environment $T - T_0$ was obtained by subtracting the room temperature from the temperature of fabric. Thus the relationship between the input electric power P_{in} and the temperature difference $T - T_0$ was obtained (Figure 4.23). Equation (4.36) indicates a linear relationship between the input electric power

P_{in} and the temperature difference $T - T_0$. Thus Equation (4.36) was used to fit the data and the fitted curve $y = 0.30x$ was obtained. Thus the fitted thermal conductivity λ is 0.30 (w/$°C$) when airflow rate $v = 0\ m/s$. The fitting correlation coefficient of 0.992 indicates that the proportional relationship between the input power and temperature difference was proved.

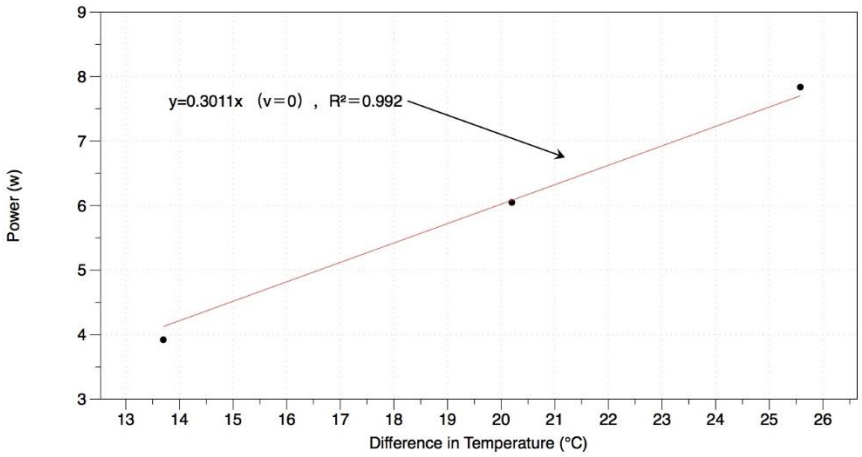

Figure 4.23. Temperature difference under different power and its fitting curve (red line) when airflow rate $v = 0\ m/s$.

The following tests were conducted when airflow rate $v \neq 0$. Thus the fan was turned on to provide different airflow around the thermal fabric and the board under the fabric can be adjusted to change the air inflow angle (airflow direction). The fan was set to provide small airflow at first and the air inflow angle was set $\theta = 0°, 45°, 90°$ in each test. In each test, the inflow angle was set and the temperature of the fabric was measured under four different input electric power. Then the fan was set to increase the airflow rate and the above process was conducted repeatedly. Finally, the relationship between input electric power and temperature difference under different airflow rate and different air inflow angles (airflow direction) was obtained. Figure 4.24 presents the relationship between the input electric power and the temperature difference under different air flow rates when the applied air inflow direction is parallel to the fabric ($\theta = 0°$) and the achieved good fitting results illustrate that a

proportional relationship between electrical power input and the temperature difference under different air flow rates (Equation 4.36) is verified. This result indicates that thermal conductivity contributed either by heat conduction or by convective heat transfer can be obtained either from dividing the heat flux by the temperature gradient (temperature difference), as shown in Equation (4.37) or from the fitting slop between the input electric power and the temperature difference. The fitting results are presented in Figure 4.24 and the fitting slop in Figure 4.24(a)~(d) is the thermal conductivity of the fabric under a specific airflow rate.

$$\lambda = \frac{P_{diss}}{T - T_0} \tag{4.37}$$

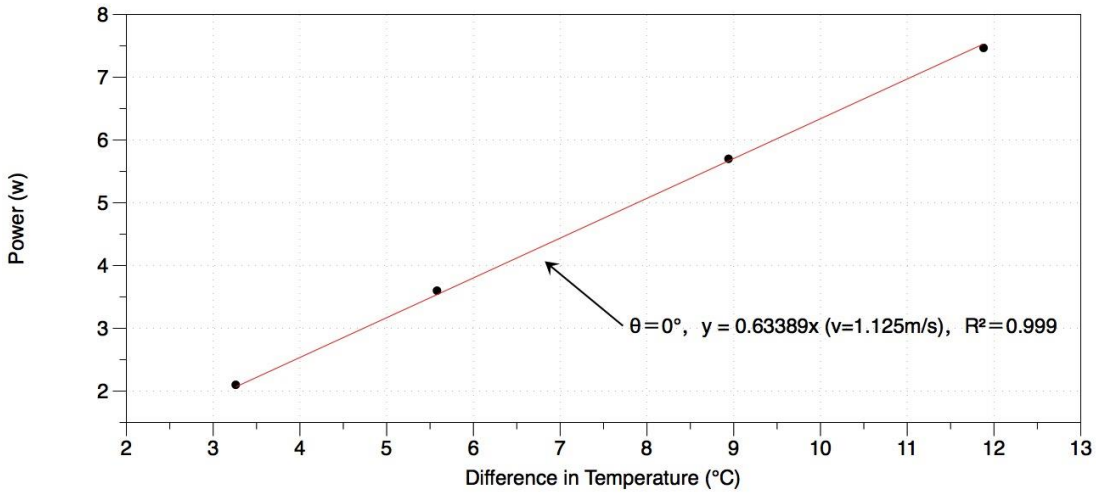

(a)

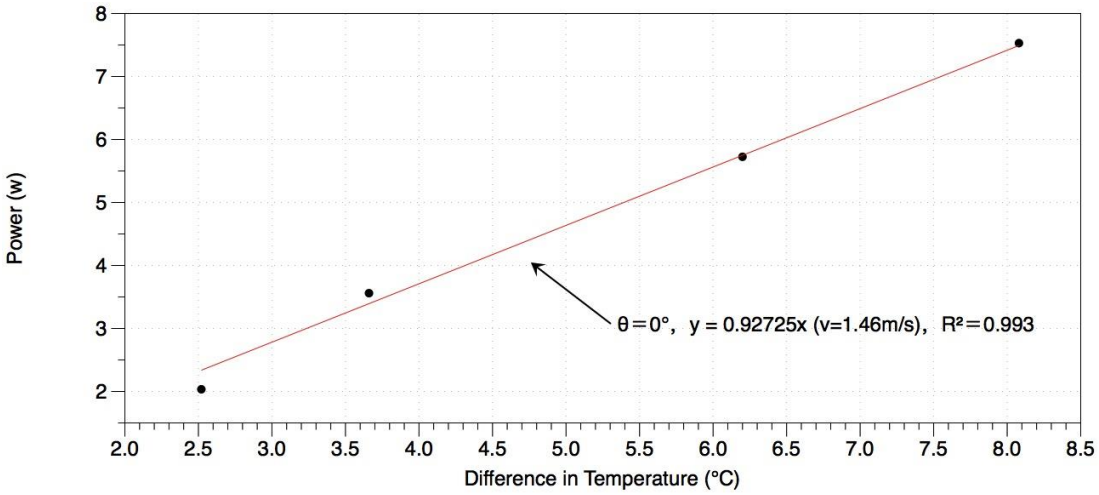
Power (w)
Difference in Temperature (°C)
θ = 0°, y = 0.92725x (v=1.46m/s), R² = 0.993

(b)

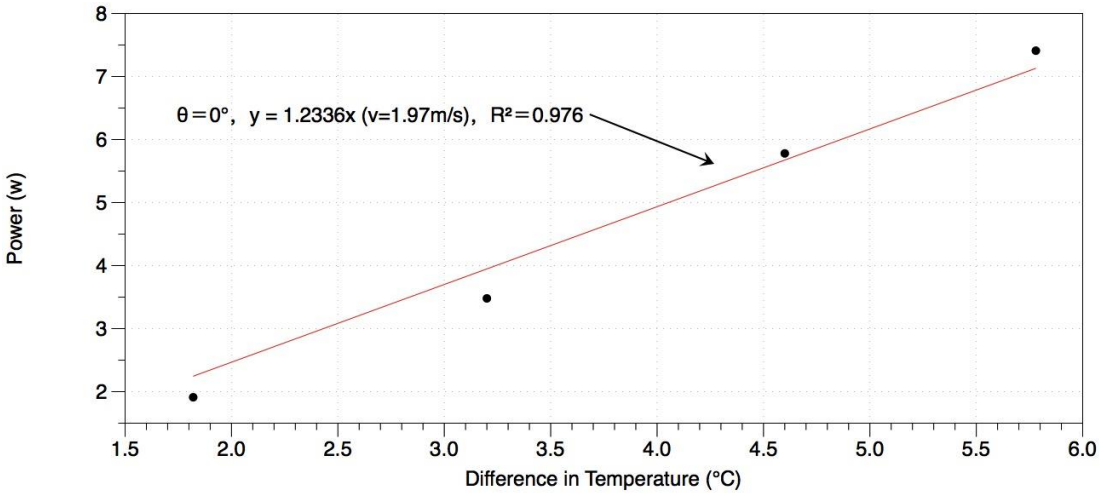
Power (w)
Difference in Temperature (°C)
θ = 0°, y = 1.2336x (v=1.97m/s), R² = 0.976

(c)

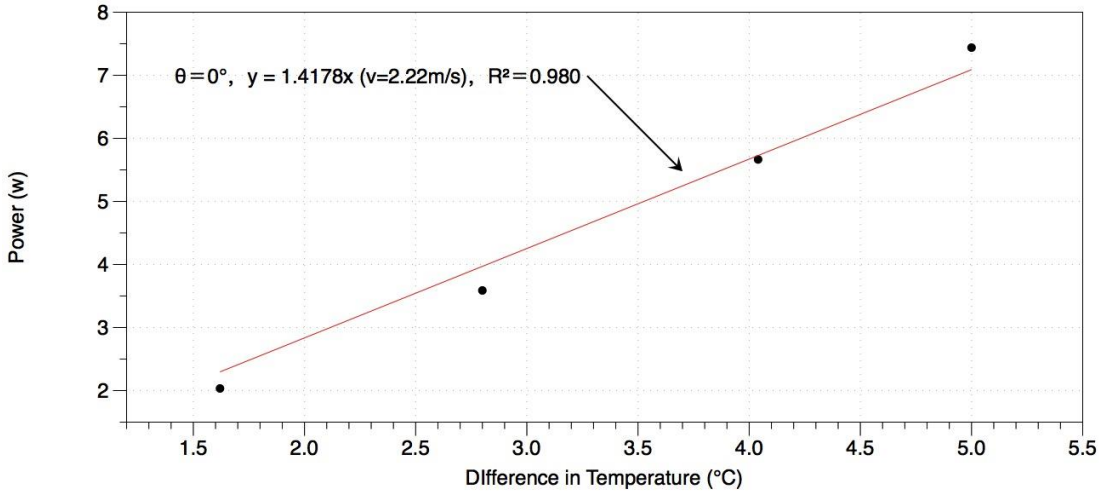
Power (w)
DIfference in Temperature (°C)
θ = 0°, y = 1.4178x (v=2.22m/s), R² = 0.980

(d)

Figure 4.24. Relationship between the electrical power input and temperature difference of thermal fabric under different airflow rates (1.25 m/s , 1.46 m/s , 1.97 m/s and 2.22 m/s) when air inflow angle $\theta = 0°$ and the fitting results (red line). It is clearly shown from a to d that with increasing airflow rate the thermal conductivity increases continuously.

As the thermal conductivities of the thermal fabric under different airflow rates were obtained in Figure 4.24, $\lambda - v$ curve ($\theta = 0°$) can be drawn (Figure 4.25) by integrating the fitting results from Figure (4.24 a~d). As Equation (4.34) in the theoretical section that the thermal conductivity λ is proportional to the airflow rate v, a proportional functional was used to fit the relationship. The fitting result "$\theta = 0°, y = 0.62627x$" was obtained to simulate how the thermal conductivity of the fabric changes with the changing airflow rate when the airflow direction is parallel to the fabric surface. Now the $\lambda - v$ curve under other air inflow angles remains to be explored. The same testing and fitting procedure was applied when the air inflow angle $\theta = 45°, 90°$. The obtained $\lambda - v$ curve ($\theta = 45°, 90°$) is presented in Figure 4.25. Figure 4.25 shows how thermal conductivity changes with air inflow rate or air inflow angle changes. Good fitting result shown in Figure 4.25 proves both the correctness of the heat transfer theory of fabric and the Equation (4.34). It is confirmed that the thermal conductivity of a thermal fabric in ventilated environment is proportional to the airflow rate. It is reasonable because the faster airflow can carry thermal energy from the thermal fabric to the environment more quickly. However, this is an exception in Figure 4.25 when the airflow $v = 0$. The point ($v = 0$) is inconsistent with the pattern of other points in Figure 4.25. According to Equation (4.34), the thermal conductivity of fabric equals to zero when the airflow $v = 0$. The reason is that the airflow still exist on the fabric when the fan stops providing airflow. When the fabric is heated, there must exist local temperature drop on the fabric and the airflow is generated locally. Consequently, a weak and self-generated convective heat transfer appears, even though external airflow was not provided. Although the self-generated convective heat transfer is weak, it cannot be neglected when there's no external

airflow applied. What's more, heat conduction still exist, even air and fabric are poor heat conductors. Thus when airflow $v = 0$, the self-generated convective heat transfer and heat conduction both makes the thermal conductivity non-zero at the point $v = 0$. When the airflow rate increases (above around 1.0 m/s in Figure 4.25), the convective heat transfer by external airflow dominates the whole heat transfer process and thus cover the self-generated heat transfer process.

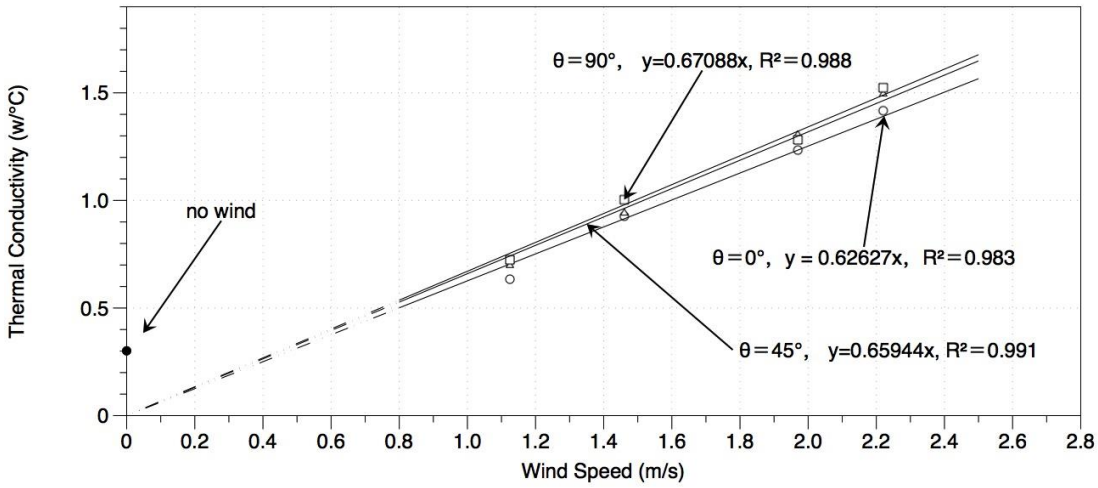

Figure 4.25. Thermal conductivity of thermal fabric vs. wind speed with different inflow angles $\theta = 0°, 45°, 90°$

In Figure 4.25, it can be concluded that the thermal conductivity of the fabric is proportional to the airflow rate ,

$$\lambda = k * v \quad (\ v\ is\ high\ enough) \tag{4.38}$$

where k is the coefficient. It is found that the airflow direction has very little influence on the k value. In other words, it is the airflow rate rather than the airflow direction that influences the thermal process of the thermal fabric, which accords with the assumption in theoretical section. In order to further verify it,

another two fabric samples were prepared and same testing procedure was applied. The k value under airflow angle $\theta = 0°, 45°, 90°$ were obtained. k value with different airflow angles for the three fabric samples are concluded in Table (4.4). Table 4.4 again verify that the airflow direction doesn't affect the thermal conductivity of the fabric. The air above the fabric is blew away at the rate of airflow speed regardless of whatever angle the air flows in.

Table 4.4. k value of fabric samples with air inflow angle $\theta = 0°, 45°, 90°$

Sample/ θ	k($\theta = 0°$)	k($\theta = 45°$)	k($\theta = 90°$)
1	0.6263	0.6594	0.6709
2	0.5845	0.6108	0.6156
3	0.6455	0.6790	0.6931

Finally, the thermal conductivity of the thermal fabric can be obtained by the following formula,

$$\lambda = \begin{cases} \lambda_0 & v \sim 0 \ (m/s) \\ k * v & airflow \ strong \ enough \end{cases} \tag{4.39}$$

This formula fully concludes the study result of the airflow influence on thermal fabric. With the help of Equation (4.39), even though there exist airflow around the thermal fabric, its thermal conductivity can be obtained. And the achieved temperature of the fabric can be further calculated and estimated. Thus precise thermal control can be achieved for the thermal fabric in airflow.

In conclusion, there are mainly two modes of heat transfer in the thermal fabric,

which has airflow around. They are both convective heat transfer modes. One is self-generated convective heat transfer and the other one is convective heat transfer by external airflow. These two modes compete with each other when the airflow rate increases. When airflow is low enough, the self-generated heat transfer plays an important role. With further stronger airflow, the convective heat transfer by external airflow dominates the total heat transfer process and covers the self-generated one. When the airflow is strong enough, the thermal conductivity of the fabric is proportional to the airflow rate. According to the previous research, the achieved temperature of the fabric can be obtained,

$$T_s(U) = T_0 + \frac{U^2}{\lambda * R_s} \tag{4.40}$$

The influence of airflow is never taken into consideration in previous research. Equation (4.40) is not applicable to thermal fabric in ventilated environment because the λ in Equation (4.40) strongly depends on the airflow. Fortunately, $\lambda - v$ is obtained in Equation (4.39). The research result in this section complements the previous theory and applies the formula to the heating process in a ventilated environment. For example, Equation (4.40) can be transformed into the following form when the airflow is strong enough,

$$T_s(U) = T_0 + \frac{U^2}{k * v * R_s} \tag{4.41}$$

Thus the thermal fabric can be designed accordingly to deal with the windy situation. A thermal garment with a heating area on the waist is designed to deal with the windy situation. The fabric structure and the arrangement of the silver-coated yarns were designed based on the heating theory proposed in Formula (4.41). The temperature control system can make adjustment according to the airflow rate and provide required voltage. This garment can achieve more accurate temperature control through providing more power to offset the heat

loss by airflow, which is shown in Figure (4.26). Thus in this section, precise temperature control for the thermal fabric in windy environment is finally achieved successfully.

Figure 4.26. (a) Thermal garment with heating area near the waist area; (b) Infrared image of thermal garment when heated; The left thermal garment taking into consideration air flow (left) vs. garment without taking into consideration air flow; (c) it is shown that the garment considering the air flow (up) achieves more precise temperature than the garment without considering that (down) because it provides more power to offset the heat loss;

4.5.5 Summary

In conclusion, in this section, the influence of airflow on the heating process of thermal fabrics was explored, and the relationship between the heat dissipation capacity (thermal conductivity) and the airflow was determined. A proportional relationship between the thermal conductivity and the airflow rate was found when the airflow was sufficiently strong. The direction of the airflow has a very limited influence on the heat dissipation by the thermal fabric during heating. Moreover, when the airflow rate is zero, the thermal conductivity of the fabric will not be zero due to self-generated convective heat transfer. Based on the above research results, we can adjust the parameters of a thermal fabric to make the thermal fabric applicable in a windy environment. Furthermore, the $\lambda - v$ curve of a thermal fabric makes conductive textiles promising candidates as

wind anemometers.

4.6 Thermal Fabrics under Heat-retaining Cover Layers

4.6.1 Introduction

The effect of a covering material on the thermal fabric, which is also regarded as a type of environmental factor, has never been studied in previous research. Obviously, external cover layers play an important role in preventing heat transfer and improving heat retention. Not taking into consideration the effect of external coverage would seriously affect the precision of thermal control. It is speculated that external cover layers with lower thermal conductivity are better able to help thermal fabrics retain heat, and cover layers with better thermal conductivity have a weaker ability to enhance warmth retention. However, the extent to which an external cover can influence the temperature control of thermal fabrics is still unclear. It is known that a thermal conductivity metre can measure the conductivity of a fabric. Thus, another question is whether the measured thermal conductivity of a fabric cover can be applied to the heating process directly. Precise thermal control is very important in some applications. Taking thermal treatment as an example, some drugs require an optimal working point to function. Thus, there is a demand to investigate the quantitative effect of cover layers on thermal control. In our study, we will focus on the two questions mentioned above. In our first step, a number of fabric cover layers will be applied over thermal fabrics. Studies will focus on what type of change the covers cause in the conductivity of the heating system. In our second step, we will measure the conductivity of the cover layers by a thermal conductivity metre directly and then assess whether the measure values are consistent with the heating process in step 1.

4.6.2 Theoretical

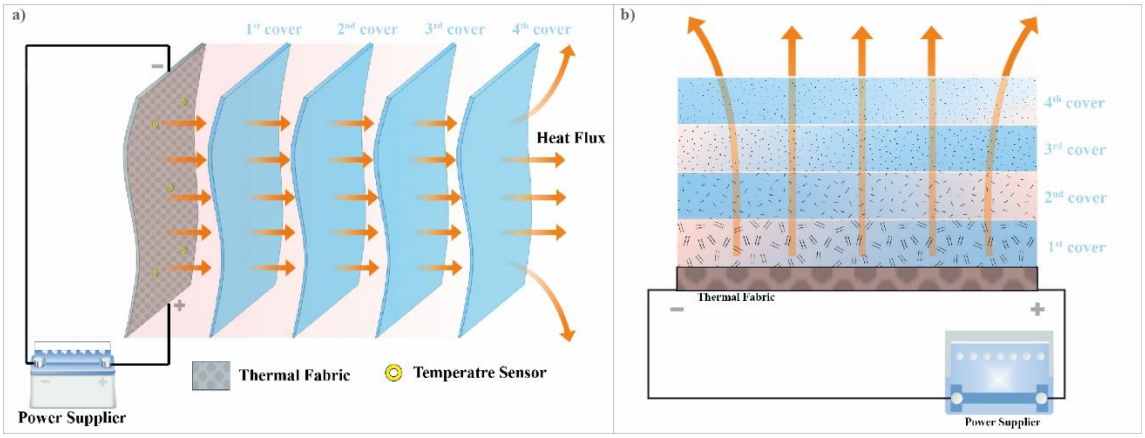

Figure 4.27. Heat flux goes through covers on thermal fabric

Heat transfer is a physical process of thermal energy exchange between systems. It is driven by temperature differences between systems until all involved bodies and surroundings reach the same temperature when the situation is called thermal equilibrium. The law of heat transfer states that the time rate of heat transfer through a material is proportional to the gradient in temperature. That is, for thermal fabrics, the heat flux from the fabric to the surrounding environment $\frac{dQ_{out}}{dt}$ is proportional to the temperature difference between the fabric and its surroundings.

$$\frac{dQ_{out}}{dt} = \lambda * (T - T_0) \tag{4.42}$$

λ is the thermal conductivity under heat transfer, which measures the ability of a material to conduct heat. But in our study, λ refers to the ability of the thermal fabric to conduct heat to its surrounding environment. The amount of heat dissipation from the thermal fabric to the surrounding environment also equals to the electrical power input when thermal equilibrium is achieved.

$$\frac{dQ_{out}}{dt} = P_{in} \tag{4.43}$$

By combining Equation (4.42) and (4.43), we can obtain:

$$P_{in} = \lambda * (T - T_0) \tag{4.44}$$

Equation (4.44) indicates that the temperature increase of the thermal fabric is proportional to the electricity input and the scale factor λ measures the heat dissipation rate from the thermal fabric to the surrounding environment. However, this λ in our study does not only represent the conductivity of one material but also reflect the combination of conductivities of both the thermal fabric and the surrounding air. Actually the whole thermal transfer process in the thermal fabric includes two parts: heat is transferred from the thermal fabric to the surrounding air and then dissipates in the air (into the distance). It is assumed that the temperature of the fabric and the surrounding air is T_f and T_a. So we can obtain:

$$q_{f \to a} = \lambda_f * (T_f - T_a) \tag{4.45}$$

$$q_{a \to infinity} = \lambda_a * (T_a - T_0) \tag{4.46}$$

Where $q_{f \to a}$ is the heat flux from fabric to the surrounding air, λ_f is the thermal conductivity of the fabric part in the whole system, $q_{a \to infinity}$ is the heat dissipation rate in the air (we assume the heat dissipated to infinity), λ_a is the conductivity of the air part in the whole system, and T_0 is the environmental temperature. Because the system is in thermal equilibrium, from the law of conservation of energy, we can infer that the heat flux should be stable all the way. Or there will exist some places, where heat accumulates or dissipates. Consequently, it would lead temperature to increase or decrease infinitely and the thermal equilibrium would be destroyed. In other words, the heat flux from thermal fabric to the surrounding air $q_{f \to a}$ and the heat dissipated from the surrounding air to the environment $q_{a \to infinity}$ should both equal to the input electricity P_{in}:

$$q_{f \to a} = q_{f \to a} = P_{in} \tag{4.47}$$

By transforming Equation (4.45) and (4.46) with combining Equation (4.47), we can obtain:

$$\frac{P_{in}}{\lambda_f} = T_f - T_a \tag{4.48}$$

$$\frac{P_{in}}{\lambda_a} = T_a - T_0 \tag{4.49}$$

Then add up Equation (4.48) and (4.49), we can obtain:

$$P_{in} * \left(\frac{1}{\lambda_f} + \frac{1}{\lambda_a}\right) = T_f - T_0 \tag{4.50}$$

or

$$P_{in} = \frac{1}{\frac{1}{\lambda_f}+\frac{1}{\lambda_a}} * (T_f - T_0) \tag{4.51}$$

Finally, the conductivity of the whole system is obtained as $\frac{1}{\frac{1}{\lambda_f}+\frac{1}{\lambda_a}}$, which takes the thermal property of both the fabric and air into consideration. Now let N fabrics whose thermal conductivities are λ_1, λ_2 … λ_n cover the heating fabric, heat will flow cross these layers of fabrics and then dissipates in the air. The whole process is similar to the previous one and we can obtain a series of equations:

$$\begin{cases} \frac{P_{in}}{\lambda_f} = T_f - T_1 \\ \frac{P_{in}}{\lambda_1} = T_1 - T_2 \\ \frac{P_{in}}{\lambda_2} = T_2 - T_3 \\ \cdots \\ \frac{P_{in}}{\lambda_n} = T_n - T_a \\ \frac{P_{in}}{\lambda_a} = T_a - T_0 \end{cases} \tag{4.52}$$

Sum up these equations, we can obtain:

$$P_{in} * \left(\frac{1}{\lambda_f} + \frac{1}{\lambda_1} + \frac{1}{\lambda_2} + \cdots + \frac{1}{\lambda_n} + \frac{1}{\lambda_a}\right) = T_f - T_0 \tag{4.53}$$

or

$$P_{in} = \frac{1}{\frac{1}{\lambda_f} + \frac{1}{\lambda_1} + \frac{1}{\lambda_2} + \cdots + \frac{1}{\lambda_n} + \frac{1}{\lambda_a}} * (T_f - T_0) \tag{4.54}$$

Thus the conductivity of the thermal fabrics covered with a number of fabrics is obtained as:

$$\lambda = \frac{1}{\frac{1}{\lambda_f} + \frac{1}{\lambda_1} + \frac{1}{\lambda_2} + \cdots + \frac{1}{\lambda_n} + \frac{1}{\lambda_a}} \tag{4.55}$$

This result indicates that more layers of covers lead to worse conductivity, which is consistent with our common sense that more covers help hold warm. If we use thermal resistance R_i to replace $\frac{1}{\lambda_i}$ in the above equations,

$$R_i = \frac{1}{\lambda_i} \tag{4.56}$$

Equation (4.53) becomes:

$$P_{in} * R = T_f - T_0 \tag{4.57}$$

where

$$R = R_f + R_1 + R_2 + \cdots + R_n + R_a \tag{4.58}$$

Equation (4.57) and (4.58) indicate that the temperature increase of thermal fabric $T_f - T_0$ can be easily obtained by multiplying the heat flux (or input electricity) by the total thermal resistance. And the total thermal resistance of the thermal fabric covered with different layers can be achieved by simply adding up the thermal resistance of each layer. In other words, thermal resistance is linear in a layer or sandwich structure where thermal flux is vertical to the plane of each layer. It is a convenient conclusion that we can apply to thermal calculation with multi-cover problems. N layers of same fabrics are applied to cover the thermal fabrics

in our testing. Equation (4.58) can be simplified as:

$$R = R_f \ + R_a + n * R_1 \tag{4.59}$$

where R_1 is the thermal resistance of single layer of the applied cover on the thermal fabric. $n * R_1$ in the above formula indicates the change that the multi-cover effect bring to the system. Moreover, equation (4.59) can also be expressed as:

$$R = R_f \ + R_a + n * R_1 + m * R_2 \tag{4.60}$$

Where $R_1,\ R_2$ are the thermal resistances of two different kinds of covers and $n,\ m$ are the numbers of them. Therefore, in the system, where thermal fabric are covered with layers of same fabrics, it is highly possible that there is a linear relationship between the total thermal resistance and the number of covers. The effect of covers on the thermal fabric remains to be explored and determined by the experimental test.

4.6.3 Methodology and experimental design

Methodology

Part I

The aim of the study in Part I is to explore how the covers on the thermal fabric can have an effect on the thermal process of the whole system. Specifically, this study will focus on the relationship between the thermal conductivity (or thermal resistance) of the system and the cover added. As we mentioned, there may exist a linear relationship between the total thermal resistance and the number of covers. Thus, the thermal resistance of the system will be measured each time a cover is added on. According to Equation (4.57), the thermal resistance of the system can

be obtained:

$$R = \frac{T_f - T_0}{P_{in}} \tag{4.61}$$

It indicates that the thermal resistance can be obtained by measuring the electrical power input and the temperature difference between thermal fabric and the surrounding environment. The linear fitting method is used to assess the thermal resistance with different number of covers applied on the thermal fabric and further to verify the accuracy of the hypothesis in Equation (4.59)~(4.60)

Part II

The aim of the study in Part I is to explore if the thermal resistance of a fabric measured by thermal conductivity tester machine can be used to predict the covering effect in application. In other words, if the thermal resistance of a fabric measured by machine is consistent with the thermal resistance simulated from the heating experiment, the thermal resistance by machine can be a direct and successful parameter in application. In order to explore the relationship, the thermal resistance of different fabric covers will be measured by thermal conductivity tester machine and the simulated resistance of the cover in heating process will be obtained with the help of following formula, which is derived from Equation (4.58),

$$R_1 = R_{total} - R_f \tag{4.62}$$

Where R_1 , R_f , R_{total} are the thermal resistance of cover, heating fabric and their combination and all of them can be measured and calculated by Equation (4.61).

Materials and Setup

Woven structure was selected in fabricating the thermal fabric, as woven fabric is more stable and uniform in resistance distribution, which is conducive to the uniformity of the temperature distribution on the fabric in the heating process. In fabrication, yarn A were embedded into the woven fabric to provide the fabric with conductive properties.

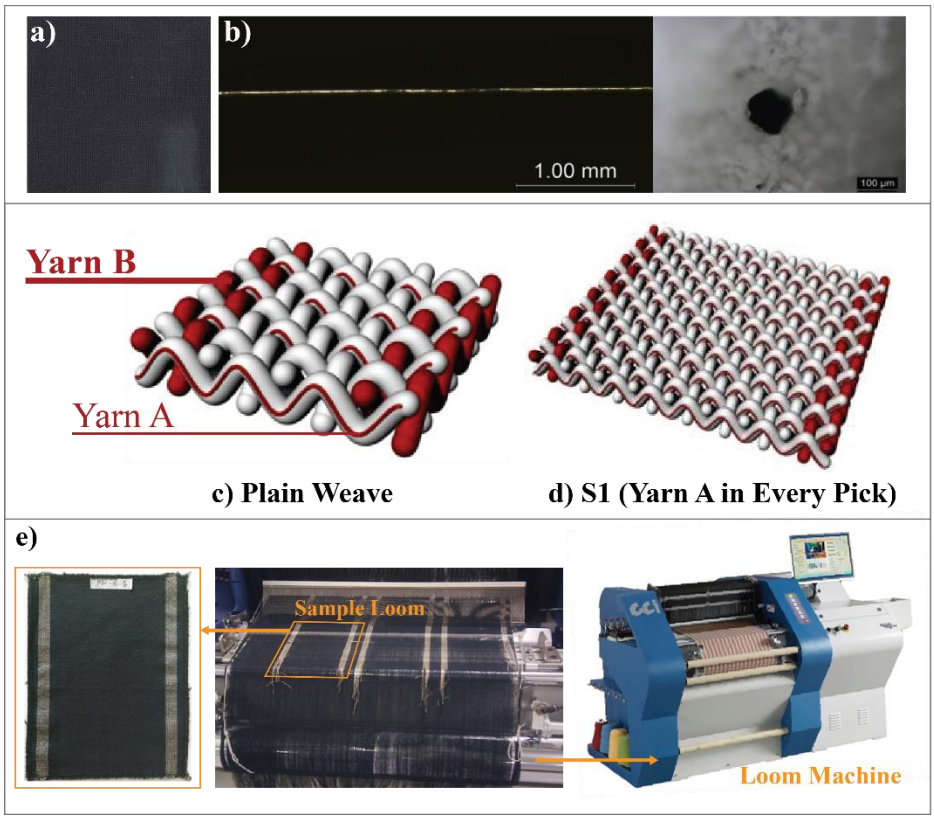

Figure 4.28 (a) The thermal fabric woven with conductive silver yarns; (b) Longitudinal view & Cross-sectional view of the conductive yarn; (c)~(d) structure of woven thermal fabric embedded with conducting silver yarns; (e) the thermal fabric and fabricating process

Ten different kinds of fabrics are selected as the covering materials, whose thermal resistances range from low to high (Figure 4.29). The components and fabricating structures of these ten fabrics also differ and Table 4.5 shows the weight density

of each fabric material.

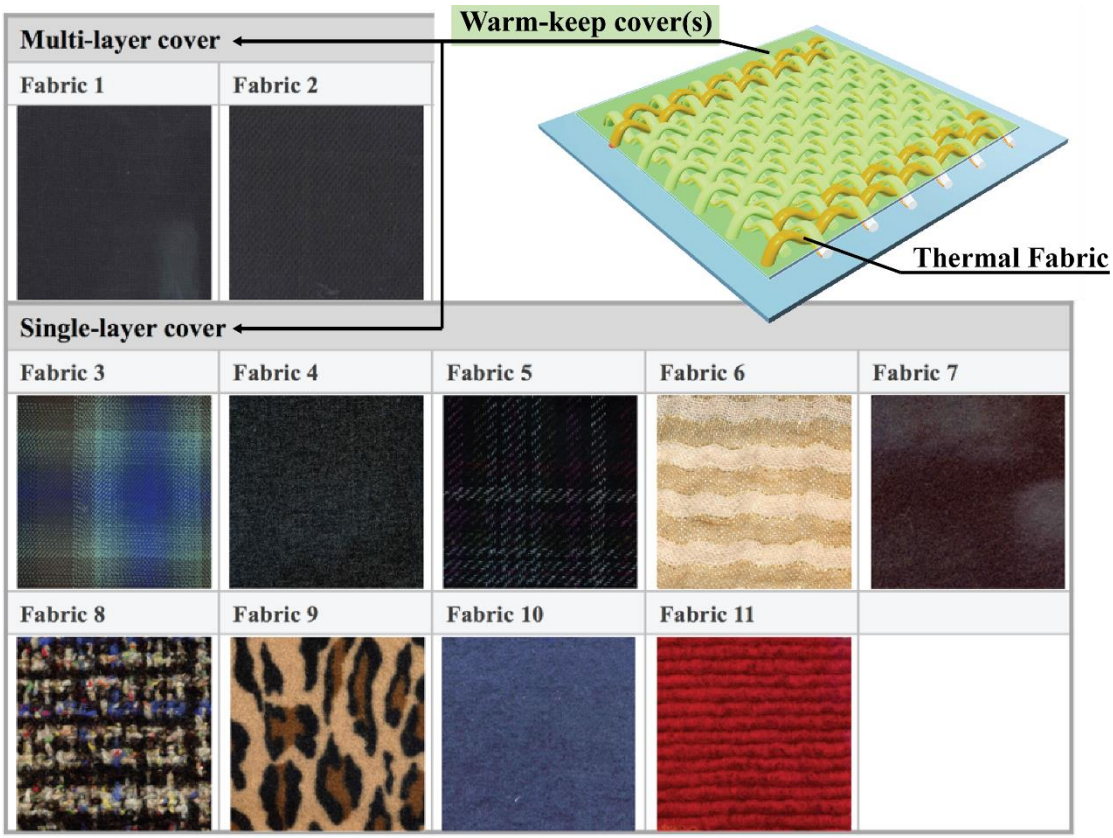

Figure 4.29. eleven different kinds of fabric materials

Table 4.5. Weight density of eleven fabric materials

G/M^2	Fabric 1	Fabric 2	Fabric 3	Fabric 4	Fabric 5	Fabric 6	Fabric 7	Fabric 8	Fabric 9	Fabric 10	Fabric 11
	2637.5	2681.3	167.06	224.81	232.31	165.06	249.38	360.19	347.31	186.38	224.69

The woven fabric was not washed or ironed prior to the testing. Instead, the thermal fabric was dry relaxed and aligned on a rigid, non-conductive foam board for measurement purposes. The power supply was used to heat the fabric in the following test. An electronic thermometer was used to measure and record the temperature of the thermal fabric. The thermometer sensor was evenly placed at five locations on the thermal fabric to measure the temperature, and the average of the five temperatures was taken to represent the apparent temperature of the heated fabric. The thermal conductivity tester

THERMOLABO II system (Figure 4.4) was used to measure the thermal conductivity/resistance directly. But it can measure the thermal conductivity/resistance of a $5 * 5\ cm^2$ fabric. Some adjustment will be made to obtain thermal conductivity/resistance of the covering fabrics.

4.6.4 Part I: multiple-cover effect

The DC power supply was used to heat the fabric with increasing electrical power and the thermal fabric was heated for 1800 seconds to achieve thermal equilibrium. It was guaranteed that thermal equilibrium was achieved in all the testing because the temperature was stable after 1800 seconds' heating. The achieved temperature of the thermal fabric and the applied power were both recorded. Three applied voltages of the DC power supply were set to provide three different powers to heat the thermal fabric respectively and the corresponding obtained equilibrium temperatures were recorded. The temperature difference between the thermal fabric and the surrounding environment was obtained by subtracting the initial temperature. Then the temperature difference varying with power input was obtained in Figure 4.30. Equation (4.57) indicates that the temperature difference is proportional to the power input. Thus Equation (4.57) was used to fit the relationship between temperature difference and the power input. The fitting result is presented in Figure 4.30 that:

$$T_f - T_0 = 4.963 * P \ \ (°C) \tag{4.63}$$

Thus the fitting thermal resistance of the fabric R was 4.963 $(°C/W)$. The regression coefficient was achieved as 0.9933, which indicates that the proportional relationship between the temperature difference and the power input is confirmed and the fitting method is an effective way to measure the thermal resistance of the system.

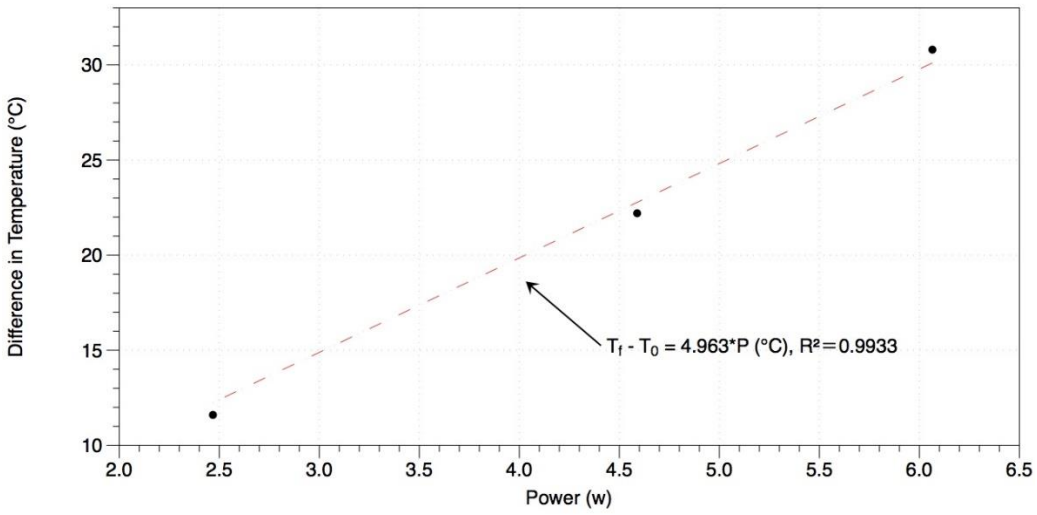

Figure 4.30. Temperature difference between the thermal fabric and surrounding environment varying with the electrical power input.

Then a layer of fabric A was placed on the thermal fabric to cover its surface. Now the system was composed of the thermal fabric and a layer of fabric cover A. The same method would be applied to obtain the thermal resistance of the system. The thermal fabric was again heated for 1800 seconds with three different supplied powers as before to achieve thermal equilibrium of the whole system. The achieved temperature of the thermal fabric and the supplied electrical power were both recorded under thermal equilibrium in each test. With the data of temperature difference and power input, fitting method was used to obtain the thermal resistance of the system as we did before. Then another layer of fabric A was placed on the thermal fabric. As a result, two layers of fabric A were covered on the thermal fabric. The same process was repeated as before to obtain the thermal resistance of the system. The thermal resistance of system was measured each time one layer of fabric cover was added to the system. Finally, the relationship between the thermal resistance of the system and the number of cover A were obtained, which is presented in Figure 4.31. Equation (4.59) presents that there is a linear relationship between the thermal resistance of the system and the number of covers.

Thus the linear fitting method was used to fit the relationship between the thermal resistance and the number of covers. The fitting thermal resistance of the system is obtained:

$$R = 5.0325 + 1.033 * n \ \ (°C/W) \tag{4.64}$$

where the fitting thermal resistance of single layer of the applied cover A on the thermal fabric is 1.033 $(°C/W)$. The regression coefficient of 0.9977 was achieved which indicates that there is a very good linear relationship between the thermal resistance of the system and the number of fabric cover A, which indicates that the experimental result is consistent with Equation (4.59). Then we replaced fabric cover A with fabric cover B and measured the thermal resistance of the system. The relationship between the thermal resistance of the system and the number of cover B were obtained, which is presented in Figure 4.32. The fitted thermal resistance of the system is obtained as:

$$R = 5.0325 + 1.1984 * n \ \ (°C/W) \tag{4.65}$$

where the fitting thermal resistance of single layer of the applied cover B on the thermal fabric is 1.1984 $(°C/W)$. The regression coefficient of 0.9993 was achieved which indicates that there is a very good linear relationship between the thermal resistance of the system and the number of fabric cover B.

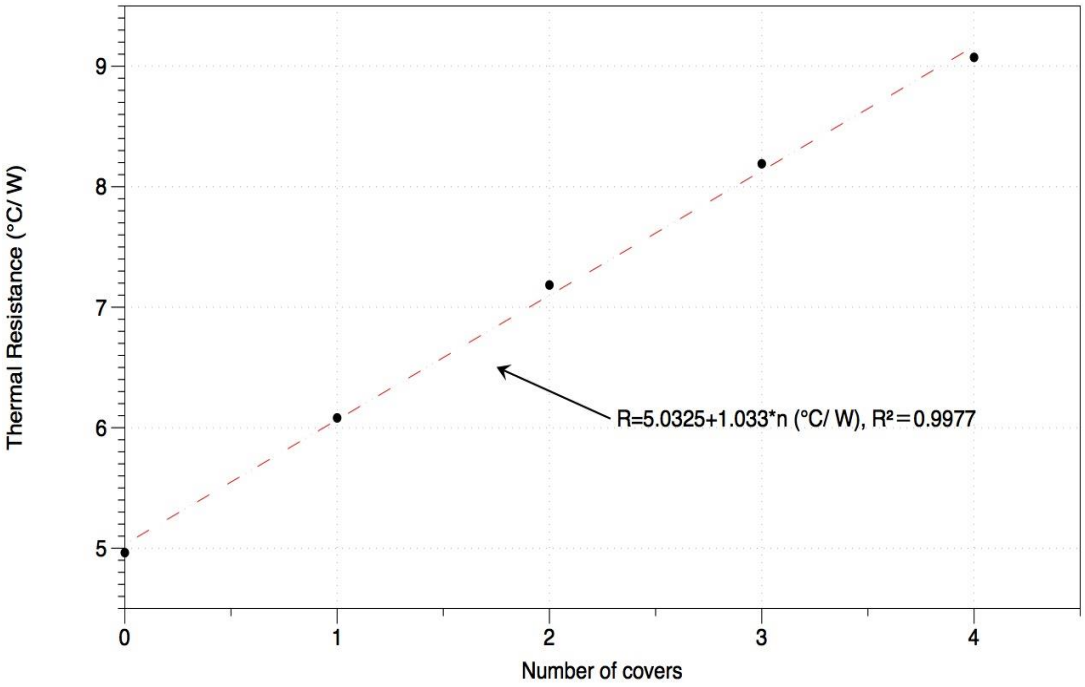

Figure 4.31. Relationship between the thermal resistance of the system and the number of fabric cover A

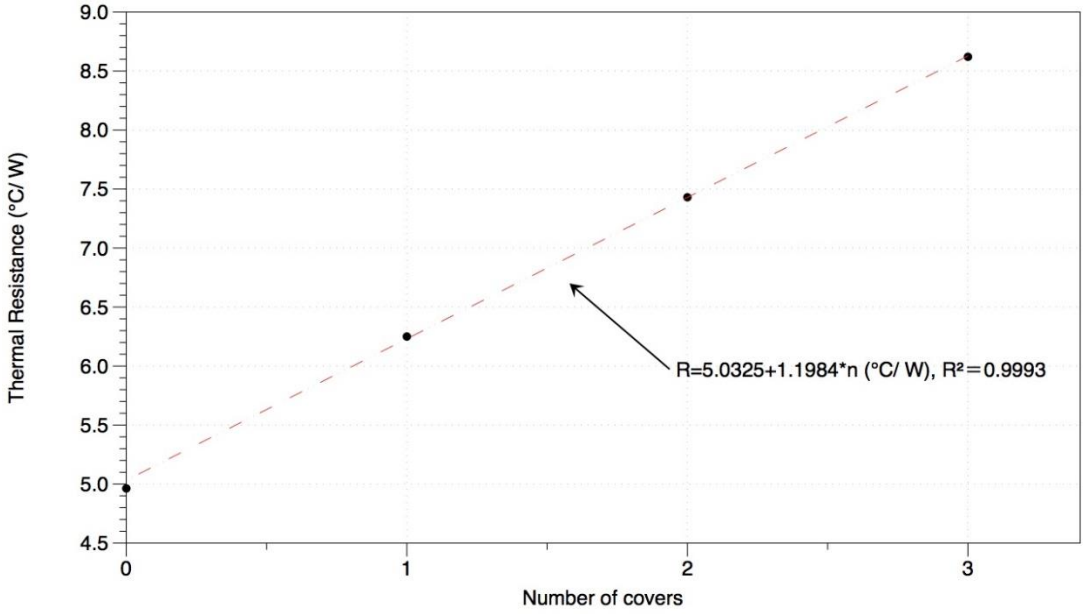

Figure 4.32. Relationship between the thermal resistance of the system and the number of fabric cover B

Then we covered the thermal fabric by mixing fabric cover A with fabric cover B. We aimed to seek how the thermal resistance changes when we applied two

different kinds of covers on the thermal fabric. In this step, we put several pieces of fabric cover A and several pieces of fabric cover B on the thermal fabric and measured the thermal resistance of the system. Finally, we obtain how thermal resistance of system varies with n, m (number of fabric cover A and B). Their relationship is shown in Figure 4.33. Equation (4.60) presents that there is a linear relationship between the thermal resistance of the system and the numbers of fabric cover A, B. Thus the linear fitting method was used to fit the relationship between the thermal resistance and the number of covers. The fitting thermal resistance of the system is obtained:

$$R = 5.0325 + 1.143 * n + 1.429 * m \ \ (°C/W) \tag{4.66}$$

where the fitting thermal resistance of single layer of the applied cover A and B are 1.143 and 1.429 $(°C/W)$ respectively. The SSE of 0.00065 was achieved, which indicates a very good linear relationship between the thermal resistance and numbers of fabric cover A, B.

There's a problem in our fitting results that the fitted thermal resistance in Eq. (4.66) is slightly different with the fitted thermal resistance in Eq. (4.64)~(4.65). Actually it is very common in linear regression method that the fitted coefficients will change when different numbers of variables are applied. What's more, when different fabrics are mixed together, the thermal resistance can be increased. Luckily, the fitted thermal resistance didn't change greatly.

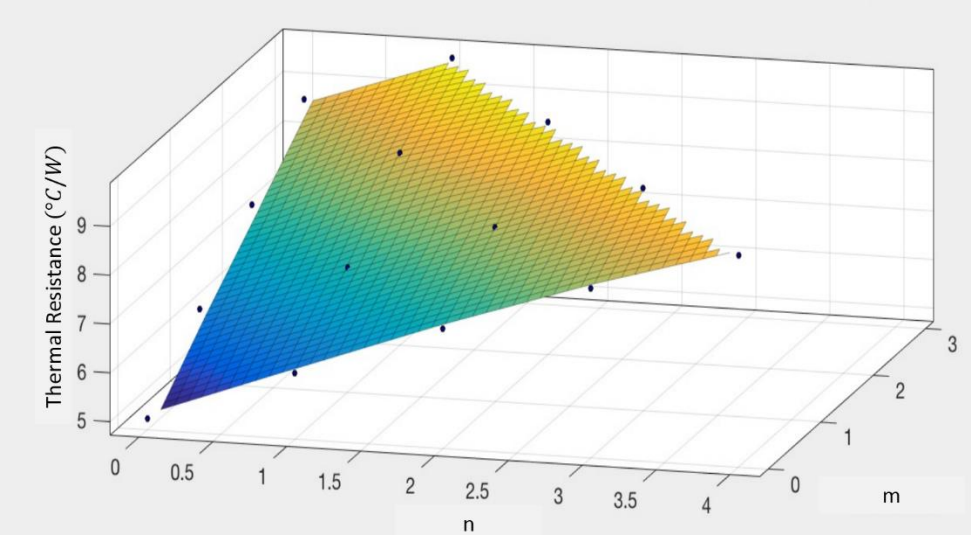

Figure 4.33. Thermal resistance of the whole system when applying different number of fabric covers

The experimental and analytical results are consistent with the heat transfer theory discussed in "II Theoretical" and proved the feasibility of Equation (4.58), (4.59) and (4.60). With proved theory: the thermal resistance of the system could be obtained by simply adding up the thermal resistance of every single part, we can easily obtain the thermal resistance of the thermal fabric covered with external fabrics. With obtained thermal resistance of the system R, according to Equation (4.57), the temperature of the thermal fabric can be obtained by:

$$T_f = P_{in} * R + T_0 \tag{4.67}$$

where

$$R = R_f \ + R_1 \ + R_2 \ + \cdots + R_n \ + R_a$$

Therefore, the problem of thermal fabric with covers on it is solved and the feasibility of the theory is verified. The temperature control of thermal fabric with muti-cover can be achieved by applying Equation (4.67). It is also possible that temperature adjustment of the thermal fabric can be achieved by adding or

reducing the covers on the thermal fabric. Different from the applied electrical voltage and resistance of the thermal fabric, covers become an external factor that can affect the temperature control of thermal fabric. The study results can be very applicable in preparing thermal garments with cold resistance in some extreme environment. With the obtained study results, people can choose the material of the cover and the number of cover to achieve the enough temperature they want. What's more, the method of adding covers to obtain higher temperature saves electrical energy, which is conducive to long-time use of thermal garments.

4.6.5 Part II: Test the Applicability of Measured Thermal Resistance

Firstly, the thermal resistances of these selected fabric covers are measured directly by THERMOLABO II. For each kind of fabric, five samples are prepared to be measured and averaged. THERMOLABO II measures the thermal conductivity/resistance of a $5 * 5\ cm^2$ area. So adjustment was made to obtain thermal resistance of fabric covers. The parameter of all selected fabric covers is presented from low to high in the following table.

Fabric Cover	**Thermal Resistance ($°C/W$)**	**Fabric Cover**	**Thermal Resistance ($°C/W$)**
No.1	0.545	**No.7**	1.905
No.2	0.807	**No.8**	2.699
No.3	0.874	**No.9**	3.175
No.4	1.014	**No.10**	4.396
No.5	1.126	**No.11**	6.537
No.6	1.150		

Table 4.6. Measured thermal resistance of 11 fabric covers by THERMOLABO II. (The thermal resistance here scales the thermal property of a 5*5 area fabric regardless of its thickness, which is different from the standard and well known thermal resistance of a material)

The thermal resistances of the heating fabric before and after applying the fabric cover were measured and calculated in the same way in Part I. According to Equation (4.58), the growth in thermal resistance after applying fabric cover is the thermal resistance of fabric. The measured thermal resistance by THERMOLABO II and actual thermal resistance during heating for all the 11 fabric covers are shown in Figure 4.34. The result shows that the two thermal resistances are very near when the thermal resistance is low enough. With thermal resistance increases, the gap between them increase. It means that when the thermal resistance of a cover fabric is too big, the actual warm-keeping ability is not as good as indicated by tester machine. The reason is the heat flow during heating is not exactly the same as that during test under THERMOLABO II. It is because THERMOLABO II only measures an area of $5 * 5 \ cm^2$, which ensures the heat flow can be ideally vertical to the fabric surface. However, in actual heating process, there exits other kinds of heat flow. When the fabric cover is too good at warm-keeping, other heat flow paths start to contribute more in heat dissipation, which makes the actual thermal resistance of the fabric cover smaller. Therefore, when we estimate the thermal parameters of a fabric in heating process only by using thermal conductivity/resistance tester machine, it should be ensured that the thermal resistance of the fabric should be small enough. This result can speed up selecting fabrics in application of thermal cover and makes the process more efficient for factories.

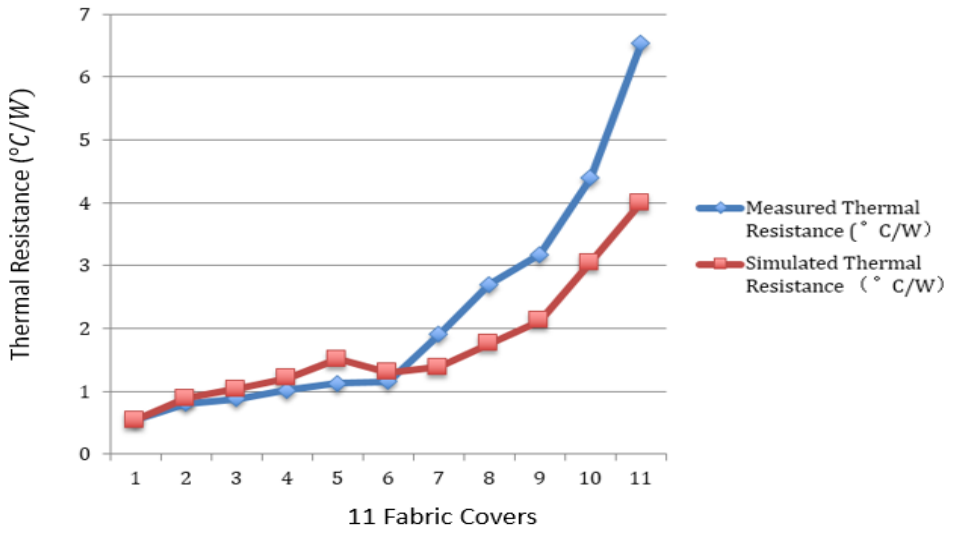

Figure 4.34. The measured thermal resistance by THERMOLABO II and the simulated thermal resistance during heating for 11 different fabric covers.

4.6.6 Summary

In conclusion, the effect of applying cover layers on the temperature control of thermal fabrics has been fully explored. It was found that there is a very good linear relationship between the thermal resistance of the system and the number of cover layers. The linear relationship between the thermal resistance of the system and the thermal resistance of every part in the system was proven. The thermal resistance of the system can be obtained by simply adding up the thermal resistance of every single part in the system. Further, the temperature control of a thermal fabric with multiple-cover layers can be achieved. When thermal textiles are applied in some extreme environments, simply increasing the power input may not be sufficient to resist cold. However, the material of the cover and the number of cover layers can be chosen to adjust the temperature and further reach the temperature requirement. Applying cover layers to adjust the temperature not only provides a new way to control temperature but also contributes to energy savings. Moreover, it was found that the thermal resistance of a fabric cover measured by a thermal conductivity meter can be directly applied to predict the actual resistance

during the heating process when the thermal resistance of the fabric cover is not too large. This result can help the factory managers save time when selecting fabrics.

CHAPTER FIVE
CONCLUSION AND FUTURE WORK

5.1 Conclusion and limitation

In conclusion, thermal fabric, which achieves heat retention through embedded silver-coated yarns, has been fully investigated, and its internal parameters, including electrical resistance and thermal conductivity, have been explored.

The study of the electrical resistance shows that not only the length-related conducting resistance of the conducting yarns but also the contact resistance between conducting yarns play essential roles in the total electrical resistance of conductive knitted fabric. Both types of resistance decrease with increasing temperature. In conclusion, the total resistance of a conductive knitted fabric will change dramatically when the fabric is heated, and we must pay more attention to this characteristic of conductive knitted fabrics in future applications. A linear relationship exists between the stable-state resistance of a fabric and the voltage applied, and a theoretical model was established to precisely predict the stable-state temperature of a conductive knitted fabric.

Based on the observed pattern of resistance variation, a generalized theoretical model, which takes the initial static resistance of the fabric, thermal conductivity, course number and wale number as the input parameters, was proposed to simulate the thermal behaviour of conductive knitted fabrics of various sizes. Verification of the generalized theoretical model for conductive knitted fabrics of different sizes and identification of the parameters of the fabrics were conducted. The satisfactory simulation results indicated that the theoretical model can be used for the temperature prediction or temperature control of conductive knitted fabrics in future applications. However, the deviation existed

in simulation and it was mainly attributed to two reasons: limitation of quality control in textile industry and morphologic change of textile materials.

Then, external environmental factors, including airflow and cover layers over thermal fabric, were explored, and their influence on temperature control was investigated.

The study of the airflow influence shows that airflow greatly influences thermal fabric. The influence of airflow on the heating process was explored for thermal fabric, and the relationship between the heat dissipation capacity (thermal conductivity) and the airflow was determined. A proportional relationship between the thermal conductivity and the airflow rate was found when the airflow was sufficiently strong. The direction of the airflow has a very limited influence on the heat dissipation by a thermal fabric during heating. Moreover, when the airflow rate is zero, the thermal conductivity of the fabric will not be zero due to self-generated convective heat transfer. Based on the above research results, we can adjust the parameters of thermal fabric for applications in windy environments. Furthermore, the $\lambda - v$ curve of a thermal fabric makes conductive textiles promising candidates as wind anemometers.

The study of the effect of cover layers on thermal fabrics shows that a cover on a thermal fabric greatly influences its heating function. The effect of applying cover layers on the temperature control of a thermal fabric was fully explored. It was found that there is a very good linear relationship between the thermal resistance of the system and the number of cover layers. The linear relationship between the thermal resistance of the system and the thermal resistance of every part in the system was proven. The thermal resistance of the system can be obtained by simply adding up the thermal resistance of every single part in the system. Further, temperature control of a thermal fabric with multiple-cover layers can be achieved. When thermal textiles are applied in some extreme

environments, simply increasing the power input may not be sufficient to resist cold. However, the material of the cover and the number of cover layers can be chosen to adjust the temperature and further reach the temperature requirement. Applying cover layers to adjust the temperature not only provides a new way to control the temperature but also contributes to energy savings. Moreover, it was found that the thermal resistance of a fabric cover directly measured by a thermal conductivity metre is different from the implied thermal resistance during actual heating, especially when the thermal resistance is not small. However, the directly measured thermal resistance can still be applied to predict the actual resistance during the heating process when the thermal resistance of the fabric cover is not too large. This result can help factory managers save time when selecting fabrics.

This research is anticipated to complement the research on various factors that can affect the thermal control of thermal textiles and offers a broader range of methods for temperature adjustment to enhance the performance of thermal textiles. However, there are some limitations of the research results.

First, in Section 4.4.6, the thermal conductivities of the samples are regarded as the same. However, the relationship between the thermal conductivity of the fabric and the size of the fabric is still unclear. The correctness of Equation (4.27) is doubtful. Second, the theoretical model in Section 4.4 can only address thermal fabrics with the same loop density. The application of the model is limited when the loop density of the thermal fabric changes. Third, the conducting material used in this study was silver-coated yarn, and all the research was based on thermal fabric embedded with this type of yarn. Thus, the research results and conclusions are based on this type of silver-coated yarn. Although silver-coated yarns are one of the most selected conducting materials for thermal textiles, other conducting yarns or conducting materials, such as copper wires, are still good candidates for conducting materials. Therefore,

when other kinds of conducting yarns are selected to fabricate thermal textiles, the research results obtained in this study may not be applicable. The properties of thermal textiles based on other conducting materials remain to be studied. Finally, in the textile industry, high consistency is difficult to achieve, especially when the fabric is embedded with conducting materials. Error is inevitable between textile products, and the thermal function of products should be adjusted one-by-one.

5.2 Future work

First, the relationship between the thermal conductivity of the fabric and the size of the fabric presented in Section 4.4.6 is still unclear. Equation (4.27) remains to be verified and adjusted in future research. The quantitative relationship between the thermal diffusivity, area and perimeter of the fabric remains to be determined. Moreover, as presented in Section 4.4, the generalized model can simulate thermal fabrics of different sizes. However, the application of this model is limited when the loop density of the thermal fabric changes. Thus, a more generalized theory that can predict the temperature of fabrics with different loop densities needs to be established in future work.

Second, as mentioned previously, the research results of this study are based on thermal fabric embedded with silver-coated yarns. Thermal fabrics combined with other conducting yarns or materials may have different properties and undergo different heating processes. Thus, thermal fabrics fabricated with other conducting materials will be investigated in the future.

Third, as heating garments always consume high levels of electrical power, the ideal candidate power supply for such garments should be able to continuously operate and be conveniently recharged. Considering the rapid improvement in

power conversion efficiency, organic solar cells, especially perovskite solar cells, have attracted our attention. Perovskite solar cells have a number of advantages as a candidate power supply for heating garments. Firstly, perovskite solar cells achieved higher power conversion efficiency than other kinds of organic solar cells. Secondly, compared with the conventional silicon solar cells, the fabrication of perovskite solar cells is convenient and consequently is more cost-effective. What's more, the perovskite solar cells are flexible mechanically due to their extremely thin films. It is precisely because of these advantages mentioned above, perovskite solar cells are qualified for the power supply for the heating garments. In future work, integrating solar cell layer on the conductive yarns in thermal fabrics to make it re-chargeable is a promising research work.

REFFERENCE

Abidi, N., Cabrales, L., & Hequet, E. (2009). Functionalization of a cotton fabric surface with titania nanosols: applications for self-cleaning and UV-protection properties. *ACS applied materials & interfaces, 1*(10), 2141-2146.

Ajayi, J. O. (1992a). Effects of fabric structure on frictional properties. *Textile Research Journal, 62*(2), 87-93.

Ajayi, J. O. (1992b). Fabric smoothness, friction, and handle. *Textile Research Journal, 62*(1), 52-59.

Bashir T, Fast L, Skrifvars M, etc. Electrical resistance measurement methods and electrical characterization of poly(3,4-ethylenedioxythiophene) coated conductive fibers. *Journal of Applied Polymer Science* 2012, 124: 2954-2961.

Brabec, CJ, Sariciftci, NS, Hummelen, JC. *Adv. Mater*. 2001, 11,15.

Braddock, SE and Mahony, MO, "Techno Textiles: Revolutionary Fabrics for Fashion and Design", Thames & Hudson, London, 1998.

Braddock, SE and Mahony, MO, "Techno Textiles 2", Thames & Hudson, London, 2005.

Braddock, SE and Mahony, MO, "SportsTech: Revolutionary Fabrics, Garment and Design", Thames & Hudson, New York, 2002

Bradley, Q. “Techno Fashion”, Oxford University Press, New York, 2002.

Cai, Y., Cui, X., Rodgers, J., Thibodeaux, D., Martin, V., Watson, M., & Pang, S.-S. (2013). A comparative study of the effects of cotton fiber length parameters on modeling yarn properties. *Textile Research Journal*, 0040517512468821.

Cherenack KH, Kinkeldei T, Zysset C, etc. Woven thin-film metal interconnects. *IEEE Electron Device Letters*2010, 31: 740-742.

Chiavazzo Eliodoro, Ventola Luigi, Calignao Flaviana, Manfredi Diego, Asinari Pietro, A sensor for direct measure of small convective heat fluxes: Validation and application to micro-structured surface. *Experimental Thermal and Fluid Science*, doi:10.1016/j. expthermflusci.2014.02.010

Collins GE, Buckley LJ, Conductive Polymer-coated Fabrics for Chemical Sensing, *synth. Metals* 7893-101(1996)

Cooper, H. M. (1998). *Synthesizing research: A guide for literature reviews* (Vol. 2): Sage.

De Rossi D, Carpi F, Lorussi F, Tognetti A, Scilingo EP, Mazzoldi A, Electroactive Fabrics for Distributed, Conformable and Interactive Systems. In “Proc. Of IEEE Sensors 2002, IEEE International Conference on Sensors,”pp.1608-1613,2002.

De Rossi D, Santa A, Mazzoldi A, Dressware: Wearable Hardware, *Mater. Sci. Engng C* 7 pp. 31-35, 1999

De Rossi D, Santa A, Mazzoldi A, Dressware: Wearable Piezo-and Thermoresistive Fabrics for Ergonomics and Rehabiliation, in "XIX International Conference of IEEE & EMBS," Chicago, p. 30 1997

Deloire R, Durand J, Mans L. Heating garment. U.S. Patent No. 3 729 613 .1973

Edmison J, Jones M, Nakad Z, etc. Using piezoelectric material for wearable electronic textiles. *Proceeding of the 6th international symposium on wearable computers (ISWC'02)* 2002; 41-48.

Gregory RV, Kimbrell WC, Kuhn HH, Conductive Textiles, *Synth Metals*, 28(1-2),823-835 (1989)

Griffiths, David. Introduction to Electrodynamics (3rd ed.) *Prentice Hall..* 1999.

Gunes, S, Neugebauer, H, Sariciftci, NS. *Chem. Rev*. 2007, 107,1324.

Haykin, S. S., "Active Network Theory", Addison-Wesley. 1970.

Hearle WS, Morton WE. *Physical properties of textile fibres.* Woodhead Publishing, 2008.

Henock HD. *Literature overview of smart textiles*. Master's Thesis, University of Boras, Sweden, 2010.

Hepworth B, Leaf GAV, Shape of the Loops in an Undeformed plain weft knit fabric, Studies in Modern Fabrics: A Report on the 1970 Diamond Jubilee Conference of the Textile Institute, Part 2, 1970, *Text. Inst*. Ind 8, 209-213 (1970)

Holm R, Electric Contacts (4th Edition), Springer-Verlag, berlin, New York, pp. 7-19 (1967)

Kim, JY, Lee, K, Coates, NE, Moses, D, Nguyen, TQ, Dante, M, Heeger, AJ. *Science* 2007, 317, 222.

Kincal D, Kumar A, Child AD, Reynolds JR, Conductivity Switching in Polypyrrole-Coated Textile Fabrics As Gas Sensors, *Synth. Metals* 92(1), 53-56 (1998).

Krebs, FC, Gevorgyan, SA, Alstrup, JJ. *Mater. Chem*. 2009, 19, 5442.

Kuhn HH, Kimbrell WC, Worrell G, Chen CS, Properties of polypyrrole Treated Textile for Adcanced Applications, proceedings of the Society of Plastics Enginners' 49th Annual Tehnical Conference, Montreal, p. 760-764(1991)

Langenhove, L. V., Smart Textiles for Medicine and Health-care: Materials, Systems and Applications. Woodhead *Pub* .2007

Leung MY, Tao XM, Yuen MCW, Kwok WY, Strain Sensitivity of Polypyrrole-coated woven fabrics under unidirectional deformation. *Text. Res. J*. (2004)

Li L, Au WM, Ding F, Tao H, Wong KS, Wearable electronic design: Electrothermal properties of conductive knitted fabrics. Vol84, Issue5, 2014

Li L, Au WM, Li Y, Wan KM, etc. Electromechanical analysis of conductive yarn knitted in plain knitting stitch under unidirectional extension. *Textile Res*

J , *Proc TBIS*; 1:793-797. 2008.

Li L, Au WM, Tao H, Wong KS. Design of a conductive fabric network by the sheet resistance method. *Textile Res J*, 81: 1568-1577. 2011

Li L, Au WM, Wan KM, etc. A resistive network model for conductive knitting stitches. *Textile Res J* , 80: 935-947 .2010.

Li L, Au WM, Li Y, et al. A novel deisgn method for an intelligent clothing based on garment design and knitting technology. *Textile Res J*, 79: 1670-1679. 2009.

Li L, Au WM, Li Y, et al. Deign of intelligent garment with transcutaneous electrical nerve stimulation function based on the intarsia knitting technique. *Textile Res J*, 80: 279-286. 2010

Liu, MZ, Johnston M, Snaith HJ. *Nature*. 2013, 501, 395-398.

Locher L and Troster G. Enable technologies for electrical circuits on a woven monofilament hybrid fabric. *Textil Res J* 2008, 78:583-594.

Lymberis, A., and Rossi. D. D., Wearable eHealth Systems for Personalized Health Management: State of the Art and Future Challenges. *Woodhead Pub* .2004

Maddox DE, Mudawar I. Single- and Two- phase Convective Heat Transfer From Smooth and Enhanced Microelectronic Heat Sources in a Rectangular Channel. *J Heat Transfer*. 111.

MoShe R. Electric heating/warming fabric articles. U.S. Patent No.

20050127057A1.

Munden DL, The Geometry and Dimensional property of Plain-knit Fabrics, *J. Text. Inst.* 50,448-471(1959)

Nakad Z, Jones M, Martin T, etc. Networking in E-textiles. *Computer Communications*2010; 33: 655-666.

Narendra VB, Devender TS, Mandar MN, etc. Development of conductive cotton fabrics for heating devices. *Journal of Applied Polymer Science* 102:4690-4695. 2006.

Oh, K. W., Park, H. H., and Kim, S. H. Stretchable Conductive Fabric for Electrotherapy, *J. Appl. Polymer Sci*., 88, 1225-1229 .2003.

Paradiso, R., Belloc, C., Loriga, G., and Taccini, N., Wearable Healthcare Systems, New Frontiers of e-Textile, Stud. *Health Technol. Inform*., 117, 9-16 .2005

Paradiso, R., Belloc, C., Loriga, G., and Taccini, N., A Wearable Health Care System Based on Knitted Integrated Sensors, *IEEE Trans. TITB,* 9(3), 337-344. 2005

Postle R, Munden DL, Analysis of the Dry-Relaxed Knitted Loop Configuration, *J. Text. Inst.* 58,329-365 (1967).

Pu X, Li LX., Song HQ, Du, CH, Zhao ZF, Jiang CY, CAO GZ, Hu WG, Wang ZL, A Self-Charging Power Unit by Integration of a Textile Triboelectric Nanogenerator and a Flexible Lithium-Ion Battery for Wearable Electronics. *Advanced Materials*, doi:10.1002/adma.201500311.

Robert F. *Science*. 2014, 344, 6183.

Roell F. Electric heating element in knitted fabric. U.S. Patent No.5 484 983. 1996.

Scott RA. The technology of electrically heated clothing. *Ergonomics* 1988; 31: 1065-1081

Serway, Raymond A. Principles of Physics (2nd ed.). *Saunders Colledge Pub.* 1998

Shanahan WJ, Postle R, A Theoreticla Analysis of the Plain Knitted Structure, *Text Res. J*. 40, 656-665(1970)

Shanahan WJ, Postle R, A theoretical Analysis the Tensile properties of Plain-Knitted Fabrics. Part I: The Load-Extension Curve for Fabric Extension Parallel to the Course. *J. Text. Inst.*65, 200-212(1974)

Shishoo, R. “Textiles in Sport”, Woodhead Pub. Ltd, Cambridge, 2005.

Tao, XM. “Wearable Electronics and Photonics”, Woodhead Pub. Ltd, Cambridge, 2005.

Tao, XM. “Smart Fibers, Fabrics and Clothing”, Woodhead Pub. Ltd, Cambridge, 2005.

Tsang, H. Y., Design and Development of Electrically Conducting Textile Sensor for Smart Textiles and Apparel. PhD thesis. *The Hong Kong Polytechnic University* .2006.

Tong JH, Ding F, Tao XM, et al. Temperature effect on the conductivity of knitted fabrics embedded with conducting yarns. *Textile Research Journal* 2014; 84:1849-1857.

Tong JH, Liu S, Yang CX, et al. Modelling of package-free flexible conductive fabric with thermal regulation where temperature can be customized. *Textile Research Journal* 2015; 85:590-600.

Tong JH, Zhao YF, Yang CX, et al. Comparison of airflow environmental effects on thermal fabrics. *Textile Research Journal* 2016;

Welty JR, Wicks CE, Wilson RE, Rorrer GL. *Fundamental of Momentum, Heat and Mass transfer (5th edition)*. John Wiley and Sons. ISBN 978-0470128688.

Xue P, Tao XM, Kwok WY, et al. Electromechanical behavior of fibers coated with an electrically conductive polymer. *Textle Res J* 2004; 74: 924-937.

Zhang H., Tao, X. M., Wang, S. Y., etc. Electro-Mechanical Properties of Knitted Fabric Made From Conductive Multi-Filament Yarn Under Unidirectional Extension. *Textile Res J* ,75;598. 2005.